# Biochemical and Biophysical Investigations on the Ligand Binding and Chaperone-like Activities of PDC-109
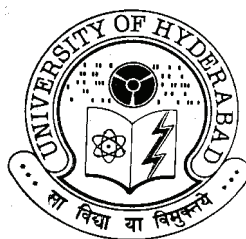
*A thesis*
*submitted for the degree of*
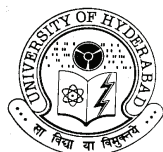**DOCTOR OF PHILOSOPHY**

*By*
**Rajeshwer Singh Sankhala**

**School of Chemistry**
**University of Hyderabad**
**Hyderabad – 500 046**
**INDIA**
**February 2011**

*Dedicated to*
*my beloved family, who taught me*
*to be optimistic and patient about*
*everything in life…*

# Contents

# STATEMENT

I hereby declare that the matter embodied in this thesis is the result of investigations carried out by me in the School of Chemistry, University of Hyderabad, Hyderabad, under the supervision of **Prof. Musti J. Swamy**.

In keeping with the general practice of reporting scientific observations, due acknowledgements have been made whenever the work described is based on the finding of other investigators. Any omission which might have occurred by oversight or error is regretted.

**Hyderabad**

**February 2011**                                    **Rajeshwer Singh Sankhala**
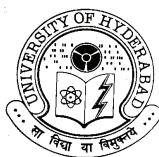
**School of Chemistry**
**University of Hyderabad**
**Hyderabad – 500 046**

# CERTIFICATE

Certified that the work embodied in this thesis entitled **"Biochemical and Biophysical Investigations on the Ligand Binding and Chaperone-like Activities of PDC-109"** has been carried out by **Mr. Rajeshwer Singh Sankhala** under my supervision and the same has not been submitted elsewhere for any degree.

**Hyderabad**
**February 2011**

**Prof. Musti J. Swamy**
**(Thesis Supervisor)**

**Dean**
**School of Chemistry**

# Acknowledgement

First and foremost I wish to thank Prof. Musti J. Swamy, my doctoral thesis supervisor. His discussions have been a great source of learning for me. I appreciate all his critics, comments and suggestions which have been very fruitful in improving my scientific as well as personal skills. He always has been very supportive and optimistic about my scientific ideas, which developed a sense of confidence in me. Apart from scientific life he has been kind, understanding and supportive in personal affairs as well.

I thank Prof. D. Basavaiah, Dean, School of Chemistry and former Dean, Prof. M. Periasamy for providing excellent research facilities and supporting environment. I extend my sincere thanks to all faculty members of the School for their cooperation on various occasions. My special thanks to my doctoral committee members Prof. A. Samanta and Prof. T. P. Radhakrishnan, who have been supportive throughout the course. I express my sincere gratitude to Dr. Ch. Mohan Rao (Director, *Centre for Cellular & Molecular Biology*) and Dr. T. Ramakrishna Murti for the fruitful collaboration, which provided me opportunity to learn various molecular biological tools. The support from Abhishek Asthana and other members of Dr. Mohan Rao's research group is appreciable. I am also grateful to Dr. Bhanuprakash Reddy (*National Institute of Nutrition*, Hyderabad) and Dr. PNBS Srinivas for fruitful discussions, which improved my understanding about molecular chaperones.

I would like to thank all the non-teaching staff of the School of Chemistry for providing me their valuable services at the appropriate time. I am also grateful to the *Central Instrumental Laboratory*, University of Hyderabad for providing an excellent instrumentation facility and my special thanks to Mr. C. S. Murthy and Mr. Suresh for their kind co-operation.

I am grateful to Dr. K. Babu Rao of the Lam, Guntur, ANGR University of Agricultural Science; Dr. Sadasiva Rao, Dr. Salmon Raju of the Department of Gynecology & Animal Reproduction, ANGR University of Agricultural Science, Hyderabad for providing bovine semen samples used in the studies reported in this thesis.

It is a pleasure to thank my colleagues and seniors Dr. Mahesh Panwar, Gopal Singh, Kuldeep Wadhwa and Krishna from Institute of Genomics & Integrative Biology (*IGIB*, Delhi), who have been always supportive in personal and professional life.

I am extremely grateful to my colleagues Dr. Ravikanth, Dr. Kavitha, Dr. Rajani, Dr. Narahari, Dr. Pradip, Kishore B., Thirupathi, Pavan, Siva Rama Krishna, Bhanu and Sudhir for maintaining a jovial and helpful atmosphere in the Lab.

A company of my friends Saurabh, Hema, Moumita, Vikas, Deepshikha, Shashank and Rupesh from Jiwaji University (Gwalior) has been fruitful in many ways. I thank all of them for those wonderful moments we shared together.

This acknowledgement will be definitely incomplete if I forget to thank Chetan, Satpal, Tejpal, Rajesh Bhai, Tejender Thakur, Sanjeev Bhai, Prashant Bhatt, Sanjib, Ranjit, Tridib, Bipul Rabha, Gaurango, Narendra Pati, Rishi, Shiva, Anand, Shyam, Sidhu, Mayank, Abhishek Rajput, Lucky, Tapan, Anshuman, Naveen, kamlesh, Prashant, Shishu, Ratinder Nath, Sarkar and all the members of Prof. D. Basavaiah research group with whom I spent my memorable time at University of Hyderabad.

Finally I want to thank my family. My father (Shri Badal Singh) always has been a source of inspiration and energy. My mother (Smt. Santosh Sankhala), brother (Ravinder Singh), bhabhi (Poonam Sankhala), my fiancee (Sonika) and joyful nieces Nishka, Shriya, Sejal have been very supportive and encouraging all the time. A special thought is devoted to my all the family members for a never-ending support.

"Above all, I thank God Almighty for his eternal love and blessings in every moment of my life."

Rajeshwer Singh Sankhala

# Abbreviations

| | | |
|---|---|---|
| AD | - | Alzheimer's disease |
| ADH | - | Alcohol dehydrogenase |
| ADP | - | Adenosine di phosphate |
| AFM | - | Atomic force microscopy |
| ANS | - | 8-anilino-1-naphthlene-sulfonic acid |
| ATP | - | Adenosine tri phosphate |
| AR | - | Acrosome reaction |
| Asp | - | Aspartate |
| bis-ANS | - | 4,4'-dianilino-1,1'-binaphthyl-5,5'-disulphonic acid |
| BSP | - | Bovine seminal plasma |
| C | - | Carbon |
| $\Delta C_p$ | - | Change in heat capacity |
| CA | - | Carbonic anhydrase |
| cAMP | - | cyclic Adenosine mono phosphate |
| CD | - | Circular dichroism |
| CDNB | - | 1-chloro-2, 4-dinitrobenzene |
| CF | - | Cystic fibrosis |
| CFTR | - | Cystic fibrosis transmembrane receptor |
| Chol. | - | Cholesterol |
| CJD | - | Creutzfeldt–Jakob disease |

| | | |
|---|---|---|
| CLA | - | Chaperone-like activity |
| CRAC | - | Cholesterol recognition amino acid consensus |
| Da | - | Dalton |
| DNA | - | Deoxyribonucleicacid |
| DEAE | - | Diethylaminoethyl |
| DMPC | - | 1,2-dimyristoyl –*sn*-glycero-3-phosphocholine |
| DMPG | - | 1,2-dimyristoyl –*sn*-glycero-3-phosphoglycerol |
| DSC | - | Differential scanning calorimetry |
| EDTA | - | Ethylenediamine tetra acetic acid |
| ESR | - | Electron spin resonance |
| FFT | - | Fast fourier transform |
| Fn | - | Fibronectin |
| $\Delta G$ | - | Change in free energy |
| GAG | - | Glycosaminoglycans |
| G6PD | - | Glucose-6-phosphate dehydrogenase |
| GST | - | Glutathione-S-transferase |
| $\Delta H$ | - | Change in enthalpy |
| HB-GAM | - | Heparin binding growth-associated molecule |
| HCl | - | Hydrochloric acid |
| HD | - | Huntington's disease |
| His | - | Histidine |
| HIV | - | Human immunodeficiency virus |

| | | |
|---|---|---|
| HPD | - | His-Pro-Asp |
| HPLC | - | High performance liquid chromatography |
| Hsps | - | Heat shock proteins |
| ITC | - | Isothermal titration calorimetry |
| $K_a$ | - | Association constant |
| LDH | - | Lactate dehydrogenase |
| MOPS | - | 3-($N$-morpholino)propanesulfonic acid |
| MRE | - | Mean residual ellipticity |
| NaCl | - | Sodium chloride |
| NADP | - | Nicotinamide adenine dinucleotide phosphate |
| NMR | - | Nuclear magnetic resonance |
| OD | - | Optical density |
| PC | - | Phosphatidylcholine |
| PD | - | Parkinson's disease |
| PDB | - | Protein data bank |
| pI | - | Isoelectric point |
| POPC | - | Palmitoleoylphosphatidylcholine |
| PrC | - | Phosphorylcholine |
| $PrP^C$ | - | Cellular prion protein |
| $PrP^{SC}$ | - | Abnormal prion protein |
| Pro | - | Proline |
| PDC-109 | - | BSP-$A_1$/-$A_2$ |

| | | |
|---|---|---|
| PolyQ | - | Polyglutamine |
| RBC | - | Red blood cells |
| $\Delta S$ | - | Change in entropy |
| SCA1 | - | Spinocerebellar ataxin1 |
| SDS | - | Sodium dodecyl sulphate |
| SPR | - | Surface plasmon resonance |
| SUV | - | Small unilamellar vesicles |
| TBS I | - | Tris buffer containing, 50 mM Tris, 0.15 M NaCl, 5 mM EDTA, 0.025% $NaN_3$, pH = 7.4 |
| TBS II | - | Tris buffer containing, 25 mM Tris, 1 M NaCl, 0.025% $NaN_3$, pH = 6.4 |
| ThT | - | Thioflavin T |
| TRA1 | - | Tumor rejection antigen1 |
| Trp (W) | - | Tryptophan |
| TS | - | Transverse section |
| Tyr (Y) | - | Tyrosine |
| UPS | - | Ubiquitin proteasome system |
| ZP | - | Zona pellucida |

# Chapter 1

# Introduction
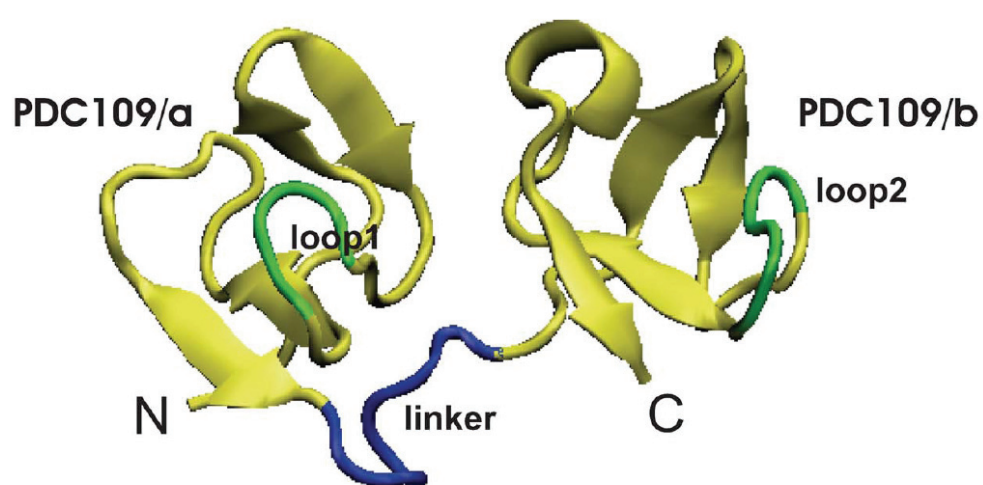
Reproduction is the biological process by which new individuals are produced from their parents. The known methods of reproduction can be grouped into two main types: sexual and asexual. Organisms with asexual means of reproduction can generate new offspring on their own, without involvement of another individual from the same species, whereas in sexual reproduction the male germ cell (sperm cell or spermatozoon) coalesces with female germ cell (ovum), and the fused cell develops to form a new individual. Sperm cells are suspended in a fluid (seminal plasma) during their journey from the male testes to the female uterus. The mixture of sperm cells and seminal plasma is jointly termed as "**semen**". Semen thus consists of a cellular component, the sperm and a non-cellular component, the seminal plasma.

## 1.1. Sperm

The term **sperm** is derived from the Greek word *sperma* (meaning "seed") and refers to the male reproductive cells. Sperm cells were discovered by Leeuwenhoek and he termed them seeds from which future embryo is developed (von Leeuwenhoek, 1679). Prevost and Dumas showed for the first time that fertilizing capacity of semen lies in the sperm (Prevost and Dumas, 1842a, b). Spermatozoa are produced by a process known as ***spermatogenesis***, which occurs in the male gonad, the testes (Clermont *et al.*, 1993; de Krester and Kerr, 1994). The testes are composed of numerous thin, tightly coiled tubules known as the seminiferous tubules; the immature sperm cells (spermatogonia) are produced within the walls of the tubules. Spermatogonia undergo a series of changes, in order to develop into a mature spermatozoon. The spermatogonia cells are composed almost entirely of nuclear material. Spermatogonia destined to develop into mature sperm cells are known as primary sperm cells. The primary sperm cells then develop somewhat by

increasing the amount of cytoplasm and other organelles within the cytoplasm. Primary cells undergo cell division to form secondary sperm cells. During this cell division there is a division of the nuclear material. The nucleus of the primary sperm cells contains 46 chromosomes, whereas in each of the secondary sperm cells there are only 23 chromosomes. The female germ cells (ovum) are also haploid. When the ovum and sperm combine and their chromosomes unite, the characteristics of both individuals merge to form a new organism. The secondary sperm cell needs to mature before it can fertilize an egg and this process is termed as ***spermiogenesis*** (Fig. 1.1). Maturation entails certain changes in the shape and form of the sperm cell as described below:

- o **Nuclear condensation**

   All unnecessary cytoplasm is eliminated and the nuclear material becomes more condensed and oval in shape; this area develops as the head of the sperm. The head is covered partially by a cap, called the acrosome.

- o **Acrosome formation**

   The Golgi complex increases in size and settles close to the cell nucleus and finally inverts itself like a cap over the largest part of the nucleus to form acrosome, which helps in sperm/ovum fusion.

- o **Development of the flagellum**

   The future axonemal structure grows out into a long tail and lies on the opposite side of the acrosome.

### 1.1.1. Sperm Structure

Mammalian sperm is a microscopic structure which can be differentiated into three major parts i.e., head, midpiece and tail (Fig. 1.1).
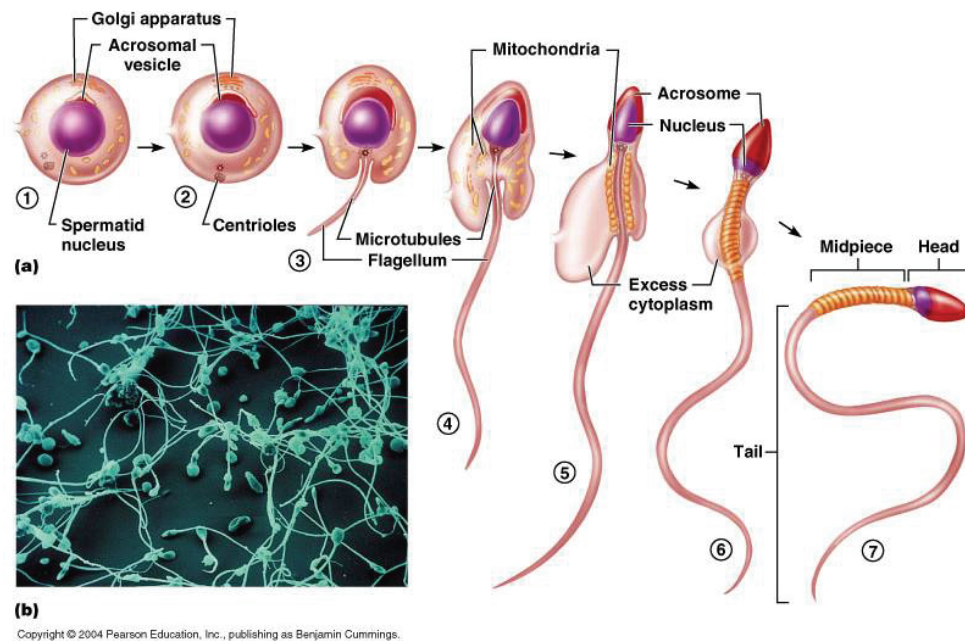


**Fig. 1.1:  Spermiogenesis and spermatozoon structure:** In spermatid, Golgi vesicles cluster at the top of the nucleus and transform into acrosome (**1**,**2**). Unnecessary cytoplasm is discarded, nucleus becomes more condensed, oval shaped and a small flagellum originates at the bottom of the nucleus (**3**,**4**). Most of the cytoplasm is discarded, flagellum is transformed into a long tail and nucleus along with acrosome differentiates as head (**5**,**6**), which finally results in a mature spermatozoon (**7**). *Copyright © 2004 Pearson Education, Inc., publishing as Benjamin Cummings*.

o **Head:** The head is a flattened almond-shaped structure which contains a large nucleus and acrosome in front of the nucleus (Guraya, 1965; Phillips, 1975). The nucleus is haploid (carries half of the genetic information to create a new life) and consists of highly compact chromatin material. Acrosome occupies the anterior end of the nucleus and is covered by its

own acrosomal membrane. The acrosome is formed from Golgi apparatus and carries several hydrolytic enzymes, which help in sperm-egg fusion. There is only very thin layer of cytoplasm around the nucleus. The whole head including the acrosome is covered by a plasma membrane, which is continuous with the membrane covering the remaining parts of the sperm.

o **Midpiece:** It carries a large number of mitochondria which are arranged in the form of a spiral around axial filament and this sheath is termed ***nebenkern***. It supplies energy to sperm for the movement and other metabolic processes (Premkumar and Bhargava, 1972 and 1973). It is surrounded by a thin sheath of cytoplasm called manchette. Midpiece is connected to head through a small neck, which carries two centrioles, proximal and distal. The proximal centriole initiates zygotic division after fertilization while the distal centriole gives rise to axial complex of the tail.

o **Tail:** The tail is a long and cylindrical structure which helps in sperm movement (propel) towards ovum. It consists of an axial filament arising from distal centriole and is surrounded by the plasma membrane. It is made up of two central filaments surrounded by nine filaments.

## 1.1.2. Sperm Capacitation

Freshly ejaculated mammalian spermatozoa are unable or poorly able to fertilize the egg. They must undergo a series of biochemical changes in order to gain this competence and this process is known as ***capacitation*** (Visconti *et al.,* 1995; Fraser, 1995). The sperm cells are capacitated during their stay in the female reproductive tract. The molecular events involved in sperm capacitation are not well understood but ultra-structural and biochemical studies suggest that sperm

undergoing capacitation exhibit a membrane remodeling process (Yanagamachi, 1994; Visconti *et al.*, 1995; Patrat *et al.*, 2000). Capacitation involves removal of adherent seminal plasma proteins and reorganization of plasma membrane lipids. It increases the influx of extracellular calcium, resulting in increased level of intracellular cyclic AMP which in turn yields hyperactivated spermatozoa. Most importantly however, capacitation appears to destabilize the sperm plasma membrane to prepare it for the acrosome reaction, as described below.

### 1.1.3. Acrosome Reaction (AR)

In order to meet a successful fertilization, sperm has to penetrate the zona pellucida. This is attained through ***acrosomal reaction***, in which hydrolytic enzymes are secreted from the acrosome to destabilize the zona pellucida. As the acrosome reaction progresses and the sperm passes through the zona pellucida, more and more of the plasma membrane and acrosomal contents are lost. By the time the sperm traverses zona pellucida, the entire anterior surface of its head, down to the inner acrosomal membrane, is denuded. There could be many different inducers for the AR; the role of ZP3 is most accepted (Yanagamachi, 1994; Bleil and Wassarman, 1983; Ward and Kopf, 1993; Florman *et al.*, 1998). Interaction of zona pellucida with sperm results in sperm membrane depolarization and increase in intracellular $Ca^{+2}$ level (Aranoult, 1996; Lievano, 1996), which triggers the acrosomal reaction.

### 1.1.4. Fertilization

Fertilization is the fusion of gametes to produce a new organism (Fig. 1.2). Depending on the animal species, the process can occur within the body of the female (internal fertilization) or outside (external fertilization). Broadly, fertilization is a combination of two important events. First, propeller movement of

sperm towards oocyte followed by its attachment to the oocyte membrane and incorporation into the cytoplasm. Second, two haploid nuclei of the male (sperm) and female (oocyte) gametes fuse in a process called ***amphimixis*** and a diploid nucleus (***zygote***) is formed, which divides further and develops into the ***embryo***.
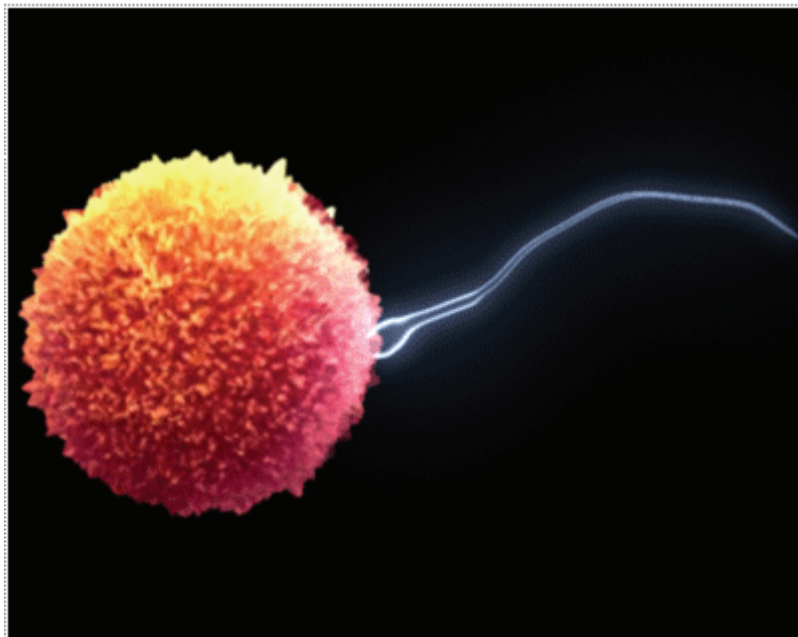


**Fig. 1.2:  Fertilization:** A sperm cell fertilizing the ovum. Adapted from
(http://www.thenervousbreakdown.com)

## 1.2. Seminal Plasma

Seminal plasma constitutes the non-cellular component of semen, which transports the spermatozoa from the male testes to the female uterus. The seminal plasma also provides a nutritive and protective medium for the spermatozoa during their journey through the female reproductive tract. The seminal plasma is a complex fluid and contains organic as well as inorganic molecules of low and high

molecular weight.  While the low molecular weight fraction contains a wide variety of chemical species, proteins are the only high molecular weight constituents found in seminal plasma; other biopolymers such as polysaccharides and nucleic acids are not present in it (Shivaji *et al.*, 1990). Although most of the seminal fluid is produced by accessory genital ducts, the seminal vesicle, prostate glands, bulbourethral glands etc., a major portion (~70%) of this fluid is composed of the secretions from seminal vesicles (Mann, 1954). The normal environment of the vagina is acidic (due to the native microflora producing lactic acid), viscous and rich in immune cells, which is not suitable for sperm survival. Seminal plasma contains a variety of basic amines such as putrescine, spermine, spermidine etc., which counteract the acidic environment of the vagina and protect nuclear DNA of sperm from acidic denaturation.

### 1.2.1. Bovine Seminal Plasma

Among the various mammalian species proteins of bovine seminal plasma have been studied in great detail.  The major protein fraction of bovine seminal plasma is composed of four acidic proteins designated as BSP-A1, BSP-A2, BSP-A3 and BSP-30 kDa, which are collectively referred to as bovine seminal plasma proteins, or as BSP proteins (Manjunath and Sairam, 1987).  The BSP proteins are acidic with pI in the range of 3.6-5.2.  All BSP proteins are made up of single polypeptide chain with an *O*-glycosylated *N*-terminus of variable length, except BSP-A3 which is not glycosylated (Manjunath and Sairam, 1987).  BSP-A1 and BSP-A2 have identical primary structure and differ only in the degree of glycosylation, and a mixture of these two proteins is also referred to as PDC-109 (Esch *et al.*, 1983; Seidah *et al.*, 1987).  BSP-A1/A2 and BSP-A3 bind specifically to choline phospholipids, whereas BSP-30 kDa displays a much broader binding specificity (Desnoyer and Manjunath, 1992).  Homologues of BSP proteins are also present in

the seminal plasma of other mammalian species such as stallion, pig, goat etc. (Calvete *et al.*, 1995; Calvete *et al.*, 1997; Villemure *et al.*, 2003; Boisvert *et al.*, 2004; Bergeron *et al.*, 2005). These observations show that the BSP family of proteins are widely distributed in mammalian seminal plasma, exist in several forms in each species and may play a common biological role. Recent studies show that spermatozoa of several mammals such as bull, pig, rabbit etc. bind with the surface of mucosal epithelium by sperm surface proteins, leading to the formation of oviductal sperm reservoir, which prevents polyspermic fertilization, assists hyperactivated motility and ensures sperm capacitation at the appropriate time (Harper *et al.*, 1994; Suarez *et al.*, 1998).

## 1.2.2. Major Protein of Bovine Seminal Plasma, PDC-109: Structure and Function

PDC-109 is the major protein of bovine seminal plasma and is present at 15-25 mg/mL concentration in it (Scheit *et al.*, 1988). It is a polypeptide with 109 amino acids and contains a 23-residue N-terminal stretch followed by two tandemly repeating fibronectin type-II (Fn-II) domains (Baker, 1985; Esch *et al.*, 1983; Seidah *et al.*, 1987). Upon ejaculation, around 9.5 million PDC-109 molecules bind to each sperm cell (Calvete *et al.*, 1994). This interaction is mediated by the binding of PDC-109 to choline phospholipids such as phosphatidylcholine (PC) and sphingomyelin, present on the outer leaflet of the sperm plasma membrane (Desnoyers and Manjunath, 1992). Each Fn-II domain binds one choline phospholipid on the sperm plasma membrane and stimulates cholesterol and phospholipid efflux (termed as *cholesterol efflux*), which is an important step in sperm capacitation (Thérien *et al.*, 1998; Moreau *et al.*, 1998). Single crystal X-ray diffraction studies have shown that both the choline phospholipid binding sites of

PDC-109 are on the same face of the protein molecule (Fig. 1.3) (Wah *et al.* 2002). A number of biophysical studies have been carried out on the interaction of PDC-109 with phospholipids, in order to understand the mechanism involved in sperm capacitation (Swamy, 2004; Anbazhagan *et al.*, 2008; Lassiseraye *et al.*, 2008; Damai *et al.*, 2009; Scolari *et al.*, 2010; Damai *et al.*, 2010). Spin-label ESR studies indicate that, upon binding to phosphatidylcholine membranes PDC-109 penetrates into the hydrophobic interior of the membrane up to the 14th C-atom of the lipid acyl chains and that cholesterol increases the selectivity of the protein for different phospholipids (Ramakrishnan *et al.*, 2001; Swamy *et al.*, 2002). The higher affinity of PDC-109 for choline phospholipids could be explained in terms of faster association and slower dissociation rate constants for phosphatidylcholine as compared to other phospholipids (Thomas *et al.*, 2003). Biophysical studies have shown that although PDC-109 exhibits high specificity for choline phospholipids, it also recognizes other phospholipids such as phosphatidylglycerol and phosphatidylserine, albeit with considerably lower specificity (Ramakrishnan *et al.*, 2001; Swamy *et al.*, 2002; Thomas *et al.*, 2003; Greube *et al.*, 2001). The intrinsic fluorescence emission spectrum of PDC-109 was blue shifted upon binding to phosphatidylcholine whith increase in intensity, which indicates that the environment of Tryptophan residues becomes more hydrophobic (Fig. 1.3) (Müller *et al.*, 1998; Anbazhagan *et al.*, 2008). Very recently the presence of a cholesterol recognition amino acid consensus (CRAC) sequence in PDC-109 has been identified (Scolari *et al.*, 2010).

PDC-109 appears to be a multi-functional protein as it binds – besides choline phospholipids – to a variety of other, structurally unrelated molecules. Interaction of this protein with Le$^a$ trisaccharide, present on the surface of the oviductal epithelium in the cow, has been suggested to help in the formation of sperm reservoir in the oviduct (Revah *et al.*, 2000; Ignotz *et al.*, 2001). Heparin and other

glycosaminoglycans (GAGs) are also components of follicular and oviductal fluids, which play an important role in sperm capacitation processes (Parrish *et al.*, 1989; Lane *et al.*, 1999). Binding of PDC-109 and the other BSP proteins to heparin forms the basis of an affinity chromatographic method for their purification (Manjunath *et al.*, 1987; Chandonnet *et al.*, 1990).
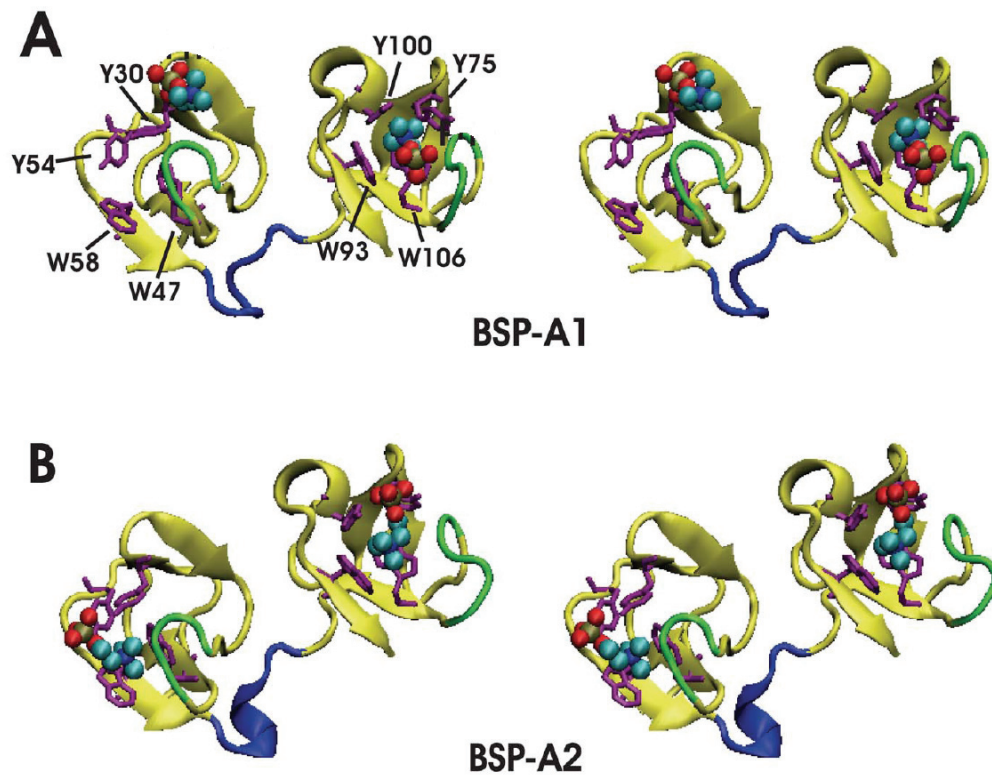


**Fig. 1.3: Stereoviews of the homodimer crystal structure of PDC109 complexed with PrCs** (PDB ID: 1h8p) (*Wah et al., 2002*). (**A**) BSP-A1 protomer and (**B**) BSP-A2 protomer. Bound PrC molecules are shown as spheres, aromatic sidechains at the PrC binding sites are shown in orange, and loops 1 and 2 that neighbor the binding sites and interact with PrC ligand are denoted in green. Adapted from (*Kim et al., 2010*).

Affinity chromatographic experiments have shown that while polydisperse PDC-109 binds heparin, the monomeric form does not display heparin binding ability (Calvete *et al.*, 1999). It has been reported earlier that bovine sperm incubated in-vitro with heparin display higher fertilizing capacity than sperm incubated without heparin (Parrish *et al.*, 1985; Parrish *et al.*, 1986a; Thérien *et al.*, 1995). The above studies establish the importance of heparin/BSP interactions for the sperm capacitation process but a molecular understanding of the role of heparin in BSP induced sperm capacitation is not clear. In addition, PDC-109 recognizes a number of other biomolecules such as D-fructose, different types of collagen, fibrinogen and apolipoprotein A-1 (Liberda *et al.*, 2001; Manjunath *et al.*, 1989; 2002). Very recently PDC-109 has been shown to exhibit chaperone-like activity against a variety of target proteins *in vitro*, suggesting that it may function in a similar capacity *in vivo* and help to maintain other seminal plasma proteins in a functionally active folded form (Sankhala and Swamy, 2010).

## 1.3. Molecular Chaperones

Chaperones are molecules that assist the non-covalent folding/unfolding and the assembly/disassembly of other macromolecular structures (proteins), but do not occur in these structures when the latter are performing their normal biological functions. The term ''molecular chaperone'' was first coined in the late 1970's when referring to the ability of nucleoplasmin to inhibit inappropriate interactions between histones and DNA (Laskey *et al.*, 1978). In biological systems generally proteins function as molecular chaperones, which play a crucial role in cell physiology both under normal and stressful conditions by protecting newly synthesized as well as non-native polypeptides from misfolding and aggregation (Ellis, 1987; Gething and Sambrook, 1992; Horwitz, 1992; Hartl, 1996; Rajaraman

*et al.*, 1996; Kumar *et al.*, 2005; Qu *et al.*, 2009). They do not necessarily convey steric information required for proteins to fold, which is already encoded in its amino acid sequence (Dobson and Karplus, 1999). The key issues needed to understand in such protein/protein interactions are: i) the factors responsible for protein aggregation and ii) how chaperones prevent the aggregation.

o   ***Protein aggregation***: Under in-vitro conditions small/single domain proteins that bury exposed hydrophobic amino acid residues rapidly tend to refold more efficiently as compared to large/multi domain proteins (Dobson and Karplus, 1999). In the folding process of large proteins, regions of the native protein which are generally spaced apart may interact leading to the formation of non-native states with exposed hydrophobic surfaces. These hydrophobic segments readily self-associate to form aggregated structures (Dobson and Karplus, 1999; Radford, 2000). On the other hand, during protein translation (*in vivo*), an average domain can completely fold only when its entire sequence has emerged from the ribosome; hence for larger polypeptide domains newly synthesized non-native structures could be exposed to surrounding environment which may lead to their aggregation. Compared to refolding in dilute solution, the tendency of non-native states to aggregate in the cell is expected to be higher because of the high local density of nascent chains in polyribosomes (macromolecular crowding). Factors which may expose the interior hydrophobic residues of proteins or provide nonspecific force (molecular crowding) leading to macromolecular compaction and association, are known to induce protein aggregation (Fig. 1.4) (Minton, 2000).

o   ***How Chaperones Prevent Aggregation***: Newly synthesized proteins (client) with exposed interior hydrophobic residues are prone to aggregation. Multi-

protein complexes containing various chaperones, co-chaperones and accessory molecules associate with the client proteins through hydrophobic interactions and prevent their aggregation (Fig. 1.5). Despite the presence of chaperones, a certain level of protein aggregation does occur in cells. In some instances these aggregates could be transformed into fibrillar structures (amyloid fibrils), that are associated with diseases such as Alzheimer's, Huntington's and Parkinson's disease (Dobson, 1999; Radford, 2000). Additionally, depending upon the nature and state of the client proteins, chaperones can direct them towards various pathways such as membrane translocation, degradation etc. (Fig. 1.5).
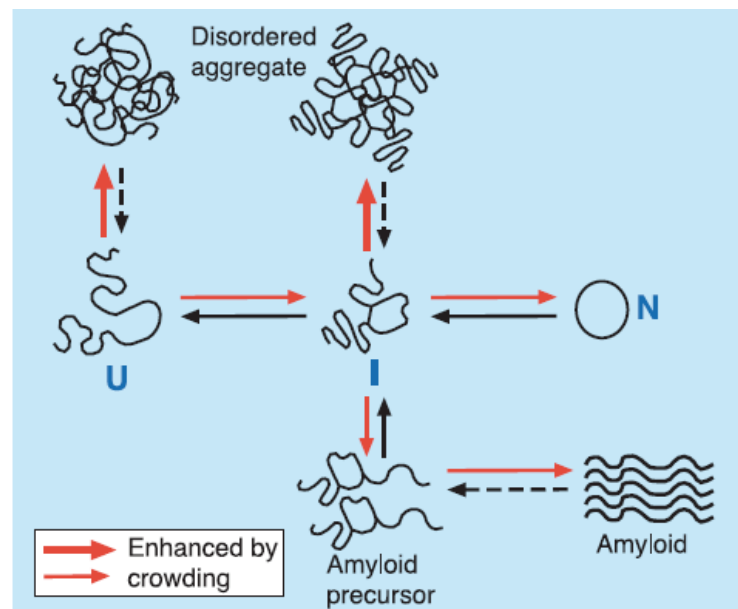


**Fig. 1.4: Aggregation of non-native protein chains**. Nascent polypeptide chains which are released from ribosomes do not fold spontaneously, but remain unfolded (**U**) for a small duration. Information for their perfect folding is normally encoded in their primary structure but sometimes they need assistance from chaperones for productive folding. In the folding process unfolded polypeptides first form partially folded intermediates (**I**), which then give rise to native protein (**N**). Overcrowding of **U** or **I** results in the formation of aggregated structures through hydrophobic interaction. The effects of molecular crowding are represented by red arrows. Adapted from (*Dobson and Karplus, 1999; Hartl and Hayer-Hartl, 2002*).
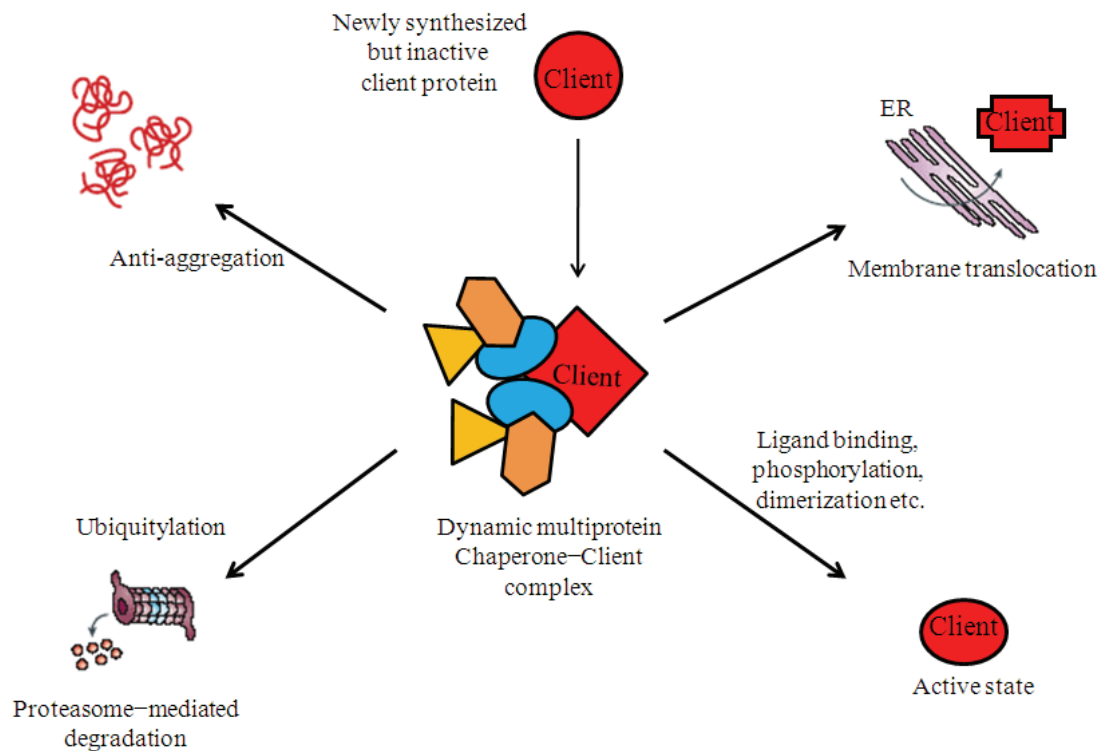
**Fig. 1.5:**  Participation of molecular chaperones in regulating many aspects of post-translational protein homeostasis. Adapted from (*Whitesell and Lindquist, 2005*).

The expression of many chaperones is increased significantly under stress conditions; hence they are classified as stress proteins or heat-shock proteins (Hsps) (Tissieres *et al.*, 1974; Gething and Sambrook, 1992).  Stress proteins belong to multigene families that range in molecular size from 10 to 150 kDa and are found in all major cellular compartments. Conventionally stress proteins of various molecular sizes are designated, for example, as Hsp27, Hsp70, and Hsp90, whereas

the corresponding heat shock protein genes are referred to as hsp27, hsp70, and hsp90 (Hightower and Hendershot, 1997).

## 1.3.1. Major Families of Molecular Chaperones

The major classes of general chaperones are the Hsp40, Hsp60, Hsp70, Hsp90, 100-kDa heat shock protein (Hsp100), and the small heat shock proteins.

### 1.3.1.1. Small Heat Shock Proteins and α-Crystallins

The small heat shock protein (Hsp) and α-crystallin family consists of 12- to 43-kDa proteins and contain a conserved C-terminal region termed the α-crystallin domain. They assemble into large oligomeric structures of 300–1000 kDa, which appear to be essential for their chaperone-like activity (Laufen *et al.*, 1998; Sun and MacRae, 2005). Many of the small Hsps are produced only under stress conditions. They have been shown to function *in vitro* as chaperones by preventing protein aggregation in an ATP independent manner (Horwitz, 1992; Wang and Spector, 1994; Fink, 1999). The small Hsps exhibit high affinity for partially folded intermediates but show no apparent substrate specificity (Laufen *et al.*, 1998). Under stress conditions they form stable complexes with non-native structures and prevent their aggregation. Subsequently, upon removal of stress, these complexes may provide a reservoir for the Hsp70 or other chaperone machinaries to renature the bound proteins (Ehrnsperger, 1998). The mechanism of action of the small Hsps is not very well characterized. It was proposed that under stress conditions substrate proteins coat the outside of the large oligomeric chaperones through hydrophobic interactions and form stable complexes which can resist the unfavorable environment (Lee *et al.*, 1997).

**1.3.1.2. Hsp40**

The Hsp40 family consists of more than 100 members, defined by the presence of a highly conserved domain of ~78 residues (J domain) (Laufen *et al.*, 1998). These are multi-domain proteins which interact with Hsp70 in the presence of ATP to suppress protein aggregation, and thus function as cochaperones for Hsp70 (Cyr, 1995). It has been proposed that Hsp40 is required for the efficient binding of substrate proteins to Hsp70 through the stimulation of its ATPase activity (Minami *et al.*, 1996). However, some of the proteins of this family such as DnaJ have been reported to function as molecular chaperones on their own (Hendershot *et al.*, 1996). The three-dimensional structure of the J domain in DnaJ has been determined using nuclear magnetic resonance spectroscopy (NMR), which suggests the presence of two long helices and a highly conserved hydrophobic core (Fig. 1.6) (Hill *et al.*, 1995; Qian *et al.*, 1996).

A small conserved segment of His-Pro-Asp sequence is believed to be responsible for the specific interaction of DnaJ and its homologs with their corresponding Hsp70 partners (Pellecchia *et al.*, 1996; Qian *et al.*, 1996). Other than functioning as chaperones, in yeast DnaJ and its homologs have been reported to induce ubiquitin-dependent degradation of abnormally folded proteins (Lee *et al.*, 1996). It has also been suggested that DnaJ possesses an active dithiol/disulfide group and may catalyze protein disulfide formation, reduction, and isomerization. Hence it may participate in protein folding processes more efficiently (De Crouy-Chanel *et al.*, 1995).

**Fig. 1.6:  Ribbon representation of Hsp40 (HDJ-1) J-domain (residues 0 to 76)**. The chain termini are identified by the letters N and C. Helices I to IV are shown in cyan, the loop and turns connecting the helices are shown in orange. The HPD tripeptide is indicated by the residues in red (His31), green (Pro32) and blue (Asp33). Adapted from (*Qian et al., 1996*).

### 1.3.1.3. Hsp60

Hsp60 proteins are encoded by heat-inducible hsp60 gene.  These proteins are abundant in all bacteria, mitochondria and plastids of eucaryotic cells.  The members of the Hsp60 family have been shown to mediate the folding of many different proteins *in vivo* and *in vitro*. Because of this activity these proteins have been called chaperonins (Ellis and van der Vies, 1991).  Chaperonins have a characteristic oligomeric structure usually consisting of 14 subunits of approximately 60 kDa each arranged in two heptameric rings stacked on top of each other (Hendrix, 1979; Hohn *et al.*, 1979; Pushkin *et al.*, 1982).  GroEL is the bacterial Hsp60 which is required for the assembly of bacteriophages (Georgopoulos *et al.*, 1973). It is also essential for growth of *E. coli* under normal

conditions (Fayet *et al.*, 1989).  GroEL is an ATP dependent chaperone which binds and stabilizes the substrate proteins in the absence of ATP. Upon ATP binding and hydrolysis the polypeptide is released in a stepwise manner, thus causing the controlled folding of the substrate proteins (Fig. 1.7) (Langer *et al.*, 1992a; Martin *et al.*, 1991; van der Vies *et al.*, 1992).
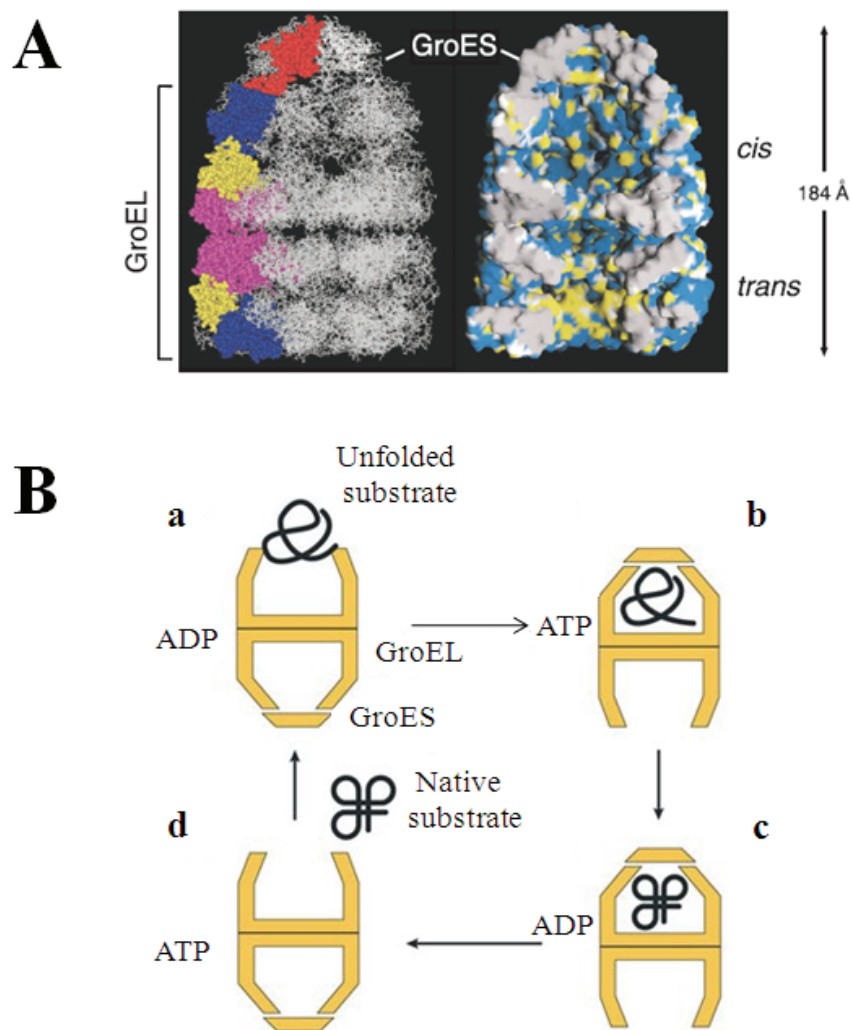
GroEL needs to interact with another chaperonin, GroES, in order to be fully functional. In the absence of GroES the binding of GroEL to substrate proteins results in the release but not in productive folding of the substrate (Martin *et al.*, 1991; Mendoza *et al.*, 1991). Although the mechanism of GroEL/GroES mediated protein folding is not well understood, it is believed that the binding of GroES couples the ATP hydrolysis by GroEL, yielding properly folded proteins (Bochkareva *et al.*, 1992; Gray and Fersht, 1991; Langer *et al.*, 1992b). Similar to GroEL, other Hsp60 proteins are also ATP dependent chaperones.

### 1.3.1.4. Hsp70

Proteins of this family are found in most, if not all, cellular compartments of eukaryotes including nuclei, mitochondria, chloroplasts, endoplasmic reticulum and cytosol, as well as in all bacteria. The structure of Hsp70 can be differentiated into two major functionally active domains, which cooperate in protein folding. The N-terminal domain is highly conserved and exhibits weak ATPase activity, whereas the C-terminal domain is required for polypeptide binding. Hsp70 can participate in the folding process by exhibiting three different activities: prevention of aggregation, promotion of folding to the native state and degradation of misfolded proteins (Fig. 1.8). Mostly Hsp70 requires assistance from cochaperones (J-domain proteins), in order to participate efficiently in the folding process. Hsp70 proteins together with their cochaperones coat the hydrophobic segments of non-native proteins and reduce the intermolecular interactions which results in a decrease

**Fig. 1.7: GroEL-GroES chaperonin system**. (**A**) Crystal structure of the asymmetric GroEL–GroES–(ADP)$_7$ chaperonin complex. GroEL consists of two homo-heptameric rings, which form a barrel-shaped structure. Adapted from (*Xu et al., 1997*). (**B**) GroEL/GroES complex in cooperation with ATP/ADP binding is required for protein folding. Upon substrate binding to one ring (**a**), ATP and GroES also bind to the same ring and displace the substrate into a closed cavity (**b**). Substrate is folded into native conformation at the expense of ATP (**c**). ATP binding results in GroES dissociation and release of natively folded substrate protein (**d**). Adapted from (*Young et al., 2004*).

in the rate of aggregation. Some members of the Hsp70 family can solubilize and subsequently refold the protein aggregates by cooperating with proteins of other chaperone families (e.g., Hsp100) (Goloubinoff *et al.*, 1999). The *E. coli* Hsp70, DnaK has been studied in great detail. Substrate proteins bind to DnaK-ATP complex more rapidly than to DnaK alone, indicating that the ATP-bound form is crucial to initiate DnaK/substrate interaction for chaperone activity (Schmid *et al.*, 1994). The resulting DnaK-ATP-substrate complexes, however, are also characterized by rapid dissociation of bound substrate. ATP binding induces
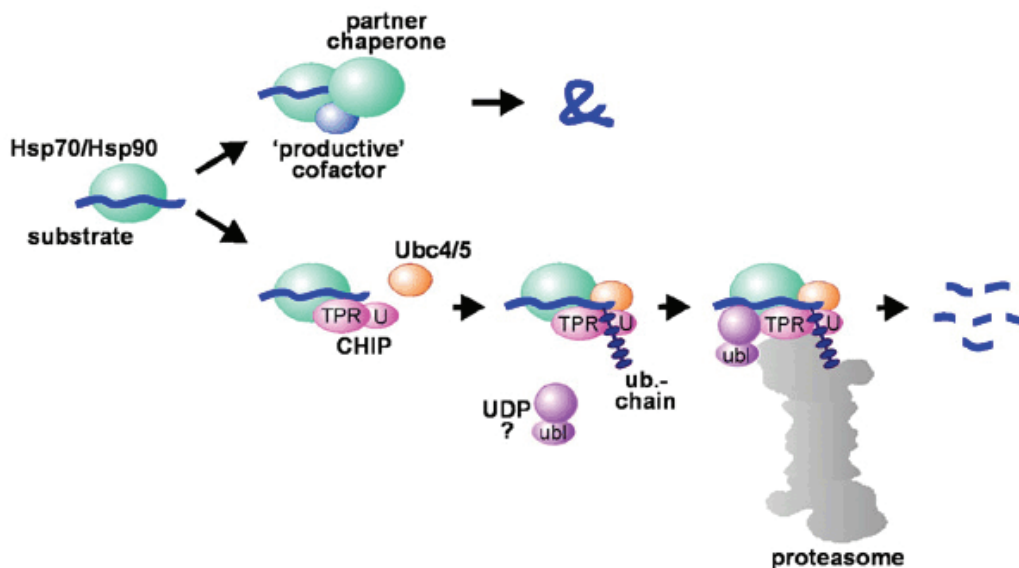


**Fig. 1.8: Hsp70/Hsp90 mediated protein folding and degradation**. Initial decision to fold or degrade a substrate protein depends on competing cofactors. When the substrate protein is in a favorable state, cochaperones and productive cofactors are recruited by Hsp70/Hsp90, which direct the protein towards functionally active conformation. If the substrate protein is recognized in an unfavorable state, Hsp70/Hsp90 shifts towards factors which direct the substrate towards ubiquitin mediated degradation. Adapted from (*Höhfeld et al., 2001*).

conformational changes in the Hsp70 structure, which in turn decrease the affinity of Hsp70 for non-native substrate proteins and leads to their dissociation (Palleros *et al.*, 1993). Because the binding of ATP occurs in the N-terminal domain and substrate binds at the C-terminal domain, it is clear that strong coupling occurs between the two domains.

### 1.3.1.5. Hsp90

Members of this family of heat shock proteins are present in almost all organisms from bacteria to humans. Mammalian Hsp90 proteins exist as dimers (Prodromou *et al.*, 1997) and function in cooperation with a wide variety of cochaperones. There has been a long-standing controversy as to whether Hsp90 binds or hydrolyzes ATP. The crystal structures of N-terminal domain of the yeast Hsp90 complexed with ADP/ATP revealed the presence of a specific adenine nucleotide binding site (Prodromou *et al.*, 1997). In vitro studies suggest that in the absence of the nucleotide, Hsp90 creates a reservoir of folding intermediates of the substrate proteins that refold upon addition of Hsp70, DnaJ and nucleotide (Freeman and Morimoto, 1996). Hsp90 complex mediated refolding of substrate proteins depends on which co-factors are collaborating with Hsp90 and what is the folding state of the substrate protein. If the substrate protein is in a state which is recognized by Hsp90 as favorable, respective co-factors are recruited and the substrate is directed towards perfectly folded conformations; otherwise Hsp90 shifts towards factors which direct the substrate towards degradation (Fig. 1.8) (Wang *et al.*, 2006). Among various chaperones, members of the Hsp90 family, Hsp90α and Hsp90β have the best characterized *in vivo* function. Hsp90 along with its chaperone partners (Hsp70 and Hsp56) binds with steroid aporeceptor and maintains it in an inactive state. Ligand binding (e.g., estrogen) to the aporeceptor complex triggers ATP hydrolysis by Hsp90, which dissociates from an "activated"

receptor that can now induce downstream signaling for the transcription of the target gene (Denis and Gustafsson, 1989).   Finally, Hsp90 chaperones of *Saccharomyces cerevisiae* are essential for survival under all conditions, supporting their important physiological roles in lower eukaryotes (Borkovich *et al.*, 1989).

### 1.3.1.6. Hsp100/Clp

The members of this family of heat shock proteins are highly conserved and present in almost all organisms.   They exist as large hexameric structures and possess unfoldase activity in the presence of ATP. The diameter of the interior of the rings is smaller than proteins of Hsp60 family (e.g. GroEL), indicating that the mode of action of these proteins is quite different from that of Hsp60 proteins. Hsp100 proteins are believed to function as chaperones by threading substrate proteins through their narrow cavities.   The mechanism of their action is not well understood, although it has been suggested that they may function in concert with other well known chaperones such as proteins of Hsp60 and Hsp70 family, to increase the yields of perfectly folded proteins (Glover *et al.*, 1998).   Some of the members of this family (e.g. ClpA, ClpX etc.) associate with serine proteases and instead of catalyzing protein refolding, these complexes target the misfolded proteins towards degradation pathway.   Interestingly, Hsp100 proteins have also been reported to solubilize thermally aggregated proteins both *in vivo* and *in vitro* (Parsell *et al.*, 1994).   Overall it appears that Hsp100 proteins are unique, which perform a diverse set of functions that are not very common among heat shock proteins.

**1.3.1.7. Chaperones Associated with Spermatozoa**

Several somatic and germline specific molecular chaperones such as HspE1, DnaJB1, HspD1, HspA1A, HspCA, HspH1, HspA5, Tra1 etc. have been identified in the male germline (Mitchell *et al.*, 2007). Among these chaperones HspE1, DnaJB1, HspD1 and HspA1A have been localized to be present in the midpiece and principal piece of the sperm tail. Interestingly, HspA1A was also detected within the equatorial region of the sperm head, as was HspCA. Tra1 was identified to be present at the base of the sperm head, whereas the location of HspA5 and HspH1 are not clear so far. Although the actual role of spermatozoal chaperones is not well characterized, the fact that incubation of sperm with anti-HspA1A antiserum impaired fertilization indicates their significance in the fertilization process (Spinaci *et al.*, 2005). Although the presence of chaperones has been established in germ line cells, reports of their presence in mammalian seminal plasma are scarce. The major protein of bovine seminal plasma, PDC-109, is the only chaperone, which has been identified so far in the seminal plasma (Sankhala and Swamy, 2010).

**1.3.2. Protein Conformational Disorders and Chaperone-based Therapeutics**

Proteins need to acquire a unique 3-dimensional conformation in order to be functionally active. Proteins which cannot acquire such conformation are recognized as misfolded and are directed towards a functionally active state or degradation pathway. This is called quality control system and is composed of two components: *molecular chaperones* and *ubiquitin proteasome system* (UPS) (Berke and Paulson, 2003). A small mutation in the protein or error in the folding process may result in protein-misfolding disorders. A large number of diseases in human such as Alzheimer's disease, Parkinson's disease, Huntington's disease, Creutzfeldt–Jakob disease and many other neurodegenerative disorders result due

to protein misfolding. Misfolded proteins could be harmful because of loss of function, as observed in cystic fibrosis (CF) or formation of nonfunctional amyloidal aggregates, as seen in many neurodegenerative diseases (Cohen and Kelly, 2003). Mutations which result in the formation of thermodynamically stable folding intermediates may also decrease the yield of correctly folded protein. These conformations are referred to as "*dead end*" conformations, which may lead to the occurrence of insoluble aggregated structures followed by neurodegenerative diseases (Kopito, 2000).
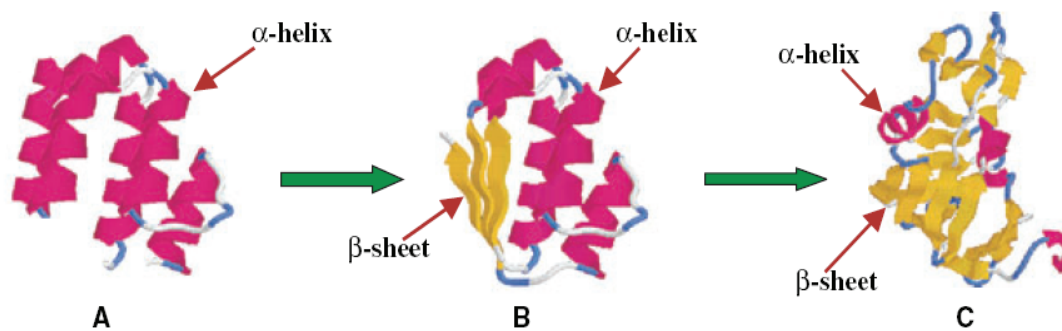


**Fig. 1.9: Conversion of α-Helical Structure to the β-Sheet**. (**A**) Native protein with α-helical secondary structure. (**B**) Appearance of β-sheet secondary structure during misfolding. (**C**) Final misfolded product composed of increased β-sheet and reduced α-helical secondary structure. Adapted from (*Chaudhuri and Paul, 2006*).

In some instances aggregated/misfolded proteins can inhibit the proteasome function (UPS), leading to the occurrence of disordered states such as mad cow disease (Hooper, 2001). Although the initial process of the formation of aggregates may vary from disease to disease, a common trend is that, α-helical structure is converted to a β-sheet dominated secondary structure (Fig. 1.9). Increase in the expression of chaperones followed by prevention or suppression of

neurodegenerative diseases suggest that chaperones could have possible application as therapeutic agents (Barrel *et al.*, 2004).

### 1.3.2.1. Neurodegenerative Disorders

A large number of neurodegenerative disorders such as Alzheimer's disease (AD), Parkinson's disease (PD), Huntington's disease (HD), Creutzfeldt–Jakob disease (CJD) etc. result from intra- or extracellular accumulation of amyloidal aggregates. AD is characterized by the deposition of amyloidal aggregates in the extracellular spaces of brain, which results in a progressive loss of memory and causes impaired behavior (Martin, 1996). In this disease a membrane protein (amyloid precursor protein) is cleaved by β-secretase, to produce β-amyloid precursor peptide, which is further cleaved by another β-secretase, to yield an amyloidogenic peptide fragment, Aβ-42 (Games *et al.*, 1995; Oltersdorf, 1989). Generally Aβ-42 is degraded in the cell by *ubiquitin proteasome system*, however in some instances it accumulates in the extracellular spaces because of failure of UPS and forms amyloidal aggregates (Fig. 1.10) (Dobson, 1999).

**I. Dimerization**          **II. Oligomerization**



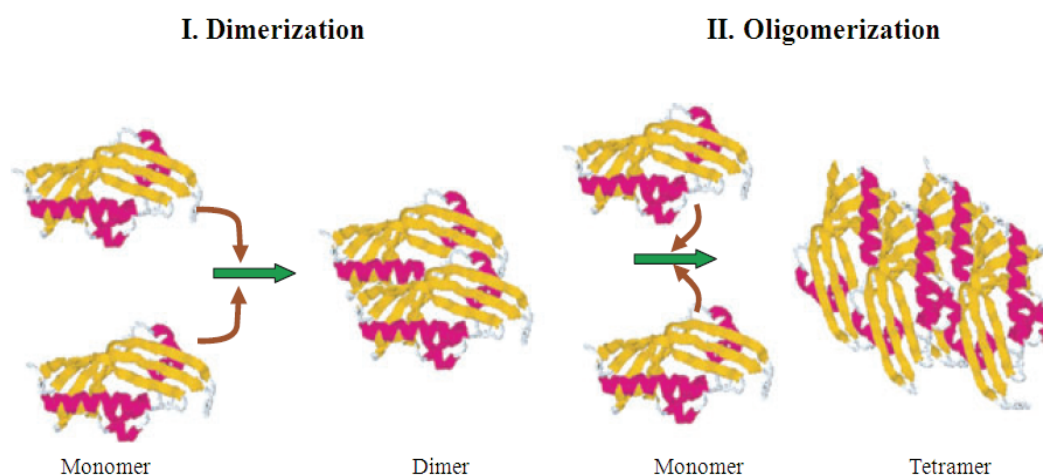Monomer          Dimer          Monomer          Tetramer

**Fig. 1.10: Alzheimer's Disease**. Aβ-42 peptide forming β-sheet rich oligomeric structures. Adapted from (*Chaudhuri and Paul, 2006*).

PD is the second most common neurodegenerative disorder which is characterized by muscular rigidity, postural instability and resting tremor. In PD misfolded aggregates are accumulated in the intracellular spaces, which is in contrast with AD (Forloni *et al.*, 2002). In PD dopaminergic neurons are degenerated with the accumulation of intracytoplasmic inclusion bodies, called as Lewy bodies. Pathologies of PD could be familial (genetic) or sporadic (non-genetic) in nature. To date, three genes encoding α-synuclein, parkin and ubiquitin C-terminal hydrolase L1 protein have been identified to be associated with familial forms of PD (Shastry, 2003). All three proteins also have been identified to be present with Lewy bodies in sporadic PD as well. Prion is another protein which causes mad cow disease in cattle and variant Creutzfeldt–Jakob disease in human (Prusiner, 2001). In these diseases, which are similar to AD and PD, a wild type protein ($PrP^C$) is converted to a β-sheet rich conformation ($PrP^{Pc}$). Pathologies of these diseases include severe sleeping defects (insomania).

### 1.3.2.2. Protein Misfolding and Loss of Function

Cystic fibrosis (CF) is the most suitable example for this class of pathology, which is characterized by thick mucus secretions in the lung and intestines (Muchowski, 2002). CFTR is a membrane protein which contains 12 potential transmembrane domains, two nucleotide-binding domains, and a highly charged hydrophilic domain. Hydrophilic segment appears to perform a regulatory function (Welch, 2003). Although the gene encoding CFTR protein has been identified to carry a range of mutations, the deletion of a nucleotide triad which encodes phenylalanine (at 508 position), appears to be the most common alteration (Kopito, 1999). This mutation develops trafficking defects by blocking the maturation of proteins in ER and directs them towards premature proteolysis (Kerem *et al.*, 1989).

Other diseases associated with this class are α1-antitrypsin deficiency, defective tumor suppressor protein p53, sickle cell anemia, nephrogenic diabetes insipidus, retinitis pigmentosa, Fabry disease etc. and all of them result from a mutation, which impairs the function of the protein associated with the respective disorder.

### 1.3.2.3. Molecular Chaperones as a Therapeutic Agent

Newly synthesized proteins are exposed to a crowded cellular environment during translation; hence they are prone to aggregate more rapidly than under in vitro conditions. Molecular chaperones interact with these nascent polypeptides with hydrophobic interactions (non-covalent) and prevent their aggregation. Under in vitro conditions many chaperones such as DnaK, secB, GroEL, α-crystallin etc. alone or in combination with other chaperones can prevent the aggregation of chemically or thermally denatured substrate proteins (Mogk *et al.*, 1999; Zahn *et al.*, 1996; Horwitz, 1992). Chernoff *et al.* (1995) reported that in yeast a prion-like factor, psi+ is propagated in the presence of moderate amounts of Hsp104 and overproduction or inactivation of Hsp104 causes loss of this factor. These results suggest that chaperones are crucial for the progression of prion disease and a critical level of chaperones can remove the prions from cells, indicating that regulated expression of Hsp104 in the cells may provide a therapy against prion diseases. Additionally, Hsp104/Hsp70 complexes have been reported to solubilize the prion-like aggregates in *Saccharomyces cerevisiae*, which approves their use as potential therapeutic agents (Chernoff *et al.*, 1995; Patino *et al.*, 1996). In an independent research, Muchowski reported that overexpression of human Hsp70 protein in *Drosophila melanogaster* completely suppresses the polyQ neurodegenerative disorder, which otherwise could induce external eye defects (Muchowski, 2002). Hsp70 also increased the lifespan of the fruit fly by twofold. Similar experiments were carried out in a mouse model, where, overexpression of

Hsp70 was found to be protective against type 1 spinocerebellar ataxin (SCA1) disease (Michelin, 2004).  The role of Hsp70 and Hsp40 has also been suggested in some human neurodegerarative disorders like PD, AD etc., where, overexpression of Hsp70 was observed to reduce α-synuclein induced dopaminergic neuronal loss in a Drosophila model (Auluck *et al.*, 2002).  Proteins, which fail to attain a functionally active conformation in the ER, are retrotranslocated to the cytoplasm with the help of Hsp40, Hsp70, Hsp90 etc., where they are degraded by the proteasome (Cohen and Kelly, 2003).  Very recently Welker *et al.* (2010) reported a novel cell survival mechanism, in which it was demonstrated that under stress conditions heat shock protein Hsp12 protects the cell membrane against leaks and ruptures.  Overall, chaperones perform a diverse set of functions in biological systems in order to assist their survival under normal as well as stress conditions.

## 1.4. Motivation and Major Findings of the Present Study

As mentioned above, *capacitation* which involves some sort of membrane remodeling makes spermatozoa fertilization competent (Visconti *et al.*, 1995; Fraser, 1995).  Proteinaceous factors present in the seminal plasma have been implicated in this process (Chang, 1951; Austin, 1952).  Among various mammalian species proteins from bovine seminal plasma have been studied extensively.  PDC-109 constitutes the major portion of BSP and has been reported to induce the efflux of cholesterol and phospholipids from outer membrane of the spermatozoa, which is an important step in the capacitation process (Thérien *et al.*, 1998; Moreau *et al.*, 1998).  Although PDC-109 has been the subject of a number of biochemical and biophysical studies aimed at investigating its involvement in sperm capacitation and its interaction with lipid membranes, a molecular level

understanding of the role of this protein in sperm capacitation is not clear.  It is expected that such an understanding can be achieved by investigating the interaction of PDC-109 with other macromolecules or macromolecular assemblies with which it is likely to interact during fertilization.  In view of this in the present studies a few questions related to the involvement of PDC-109 in fertilization have been addressed.  The major objectives of these studies are as follows:

* Although the interaction of PDC-109 with phospholipids has been investigated by various research groups, the direct evidences showing PDC-109-induced membrane disruption are scarce.  In view of this atomic force microscopic (AFM) experiments were carried out to directly probe the interaction of PDC-109 with supported membranes.  Since biological membranes are predominantly in the liquid crystalline phase, the experiments were performed with phospholipid membranes in both gel and liquid crystalline states.  Since PDC-109 exhibits differential affinity for different phospholipids depending upon their head groups (Ramakrishnan *et al.*, 2001), studies with carried out with membranes containing different phospholipids or phospholipid/cholesterol mixtures.  Experiments were also carried out with intact erythrocytes using confocal microscopy.  In order to understand the thermodynamic forces governing the PDC-109/phospholipid interaction isothermal titration calorimetric studies were carried out at different pH.

* PDC-109 is a multifunctional protein which participates in sperm capacitation either alone or in combination with other macromolecules such as apolipoproteins, heparin etc. (Manjunath *et al.*, 1989; Chandonnet *et al.*, 1990).  Some of the characteristics exhibited by PDC-109 such as polydispersity, high abundance and reversibility of thermal unfolding are similar to those displayed by well-characterized stress proteins with chaperone-like activity such as

spectrin, α-crystallin and α-synuclein.   Therefore, in order to investigate whether PDC-109 can function as a molecular chaperone studies were carried out employing a variety of biochemical and biophysical techniques with different substrate proteins.   Since phosphorylcholine binding and high salt concentrations are known to dissociate the oligomeric states of PDC-109 (Gasset *et al.*, 1997), these conditions were used to probe the importance of polydispersity for the chaperone-like activity of this protein.   Several studies suggest the involvement of surface exposed hydrophobic residues in the chaperone like activity of various proteins.   Binding of PDC-109 to phospholipid membranes and partial insertion of protein segments into hydrophobic interior of the membranes indicate the presence of hydrophobic stretches in this protein (Ramakrishnan *et al.*, 2001; Greube *et al.*, 2001).   In view of this, hydrophobic nature of PDC-109 has been investigated using isothermal titration calorimetry and fluorescence spectroscopy.   Since, as mentioned above, PDC-109 is a membrane binding protein, it was considered interesting to study that how phospholipid and phospholipid/cholesterol binding modulates the chaperone-like activity of PDC-109, which was investigated using various biochemical and biophysical methods.
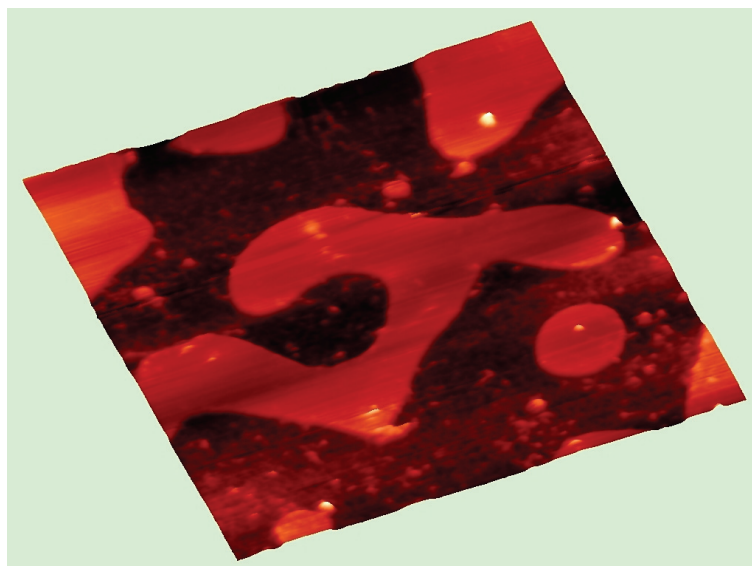
∗   Besides binding to phospholipid membranes, PDC-109 also interacts with a variety of other ligands including apolipoproteins A1 and A2, several types of collagens, heparin etc. (Manjunath *et al.*, 1987;   Chandonnet *et al.*, 1990; Manjunath *et al.*, 2002; Majunath *et al.*, 1989).   Heparin and other glycosaminoglycans (GAGs) are components of follicular and oviductal fluids, which have been reported to enhance the BSP protein-induced sperm capacitation but the exact role of heparin in this process is not clear (Thérien *et*

*al.*, 1995).　In view of this, the thermodynamic forces governing PDC-109/heparin interaction were investigated using isothermal titration calorimetry and differential scanning calorimetry.　Since PDC-109/heparin interaction has been reported to be driven by electrostatic forces (Calvete *et al.*, 1999), the effect of charge modulation on the PDC-109/heparin interaction was investigated by varying the pH and ionic strength of the medium using ITC.

The results obtained from the above studies have been discussed in the following chapters.

# Chapter 2

# Interaction of PDC-109 with Cell and Model Membranes. Isothermal Titration Calorimetric and AFM Studies

## 2.1. Abstract

The interaction of the major bovine seminal plasma protein, PDC-109 with phospholipid membranes was investigated by isothermal titration calorimetry (ITC) and atomic force microscopy (AFM). Binding of the protein to both dimyristoylphosphatidylcholine (DMPC) and dimyristoylphosphatidylglycerol (DMPG) multi-lamellar vesicles (MLVs) was found to be endothermic and could be analyzed in terms of a single type of binding sites on the protein. The positive values of entropy ($\Delta S$) for the binding of PDC-109 to phospholipid vesicles indicates that during the binding process water molecules are expelled from the interface of PDC-109 – phospholipid complex. PDC-109 exhibited stronger affinity for DMPC than DMPG which is consistent with previous reports. The interaction of PDC-109 with phospholipids was observed to be sensitive to the pH of the medium. The affinity of PDC-109 increases slightly for DMPC with pH, whereas a significant decrease was observed for binding to DMPG. AFM results show that addition of PDC-109 leads to a complete disruption of phosphatidylcholine membranes, whereas DMPG membranes are partially fragmented, consistent with the higher affinity of PDC-109 for choline phospholipids. Incorporation of cholesterol into DMPC multilamellar vesicles afforded a partial stabilization of the lamellar structure, which is in agreement with previous reports of membrane stabilization by cholesterol. Confocal microscopic studies show that addition of PDC-109 to human erythrocytes results in disruption of the plasma membrane in a concentration dependent manner.

## 2.2. Introduction

The seminal plasma in mammals serves as a carrier of freshly ejaculated spermatozoa through the female genital tract to their final destination, the uterus. During this passage spermatozoa undergo a series of biochemical and ultrastructural changes – collectively referred to as capacitation – a necessary event before they attain the ability to fertilize the egg (Shivaji *et al.*, 1990; Yanagamachi, 1994). It has been established that certain seminal plasma proteins inhibit inappropriate acrosomal reaction whereas others bind to the surface of spermatozoa and induce their capacitation (Harrison, 1996; Visconti *et al.*, 1998). Among the various mammalian species, proteins of bovine seminal plasma have been studied in great detail. The major protein fraction of bovine seminal plasma is composed of PDC-109, which helps in priming the spermatozoa through a membrane remodeling process (Desnoyers and Manjunath, 1992). The interaction of PDC-109 with membranes made up of different phospholipids has been investigated in great detail using different biophysical techniques (Swamy, 2004; Anbazhagan *et al.*, 2008; Lassiseraye *et al.*, 2008; Scolari *et al.*, 2010). However, a knowledge of the thermodynamic forces governing this interaction is scarce. In view of this, in the present study key information on the energetics of PDC-109/phospholipid interaction have been derived using ITC. In addition, studies in which the pH of the medium was altered suggest that PDC-109 exhibits a higher affinity for choline phospholipids at higher pH, which could be of physiological significance because the pH of seminal plasma is basic. Although the interaction of PDC-109 with phospholipids has been investigated by many research groups, reports showing direct evidence for PDC-109 induced membrane disruption are scarce. In the present study atomic force microscopy has been used to probe the effect of PDC-109 binding to different phospholipid vesicles and supported bilayers. The effect of

cholesterol incorporation into phospholipid membrane on PDC-109/phospholipid interaction has also been investigated using AFM.  In another set of experiments, the effect of PDC-109 interaction with human erythrocytes was investigated by confocal microscopy, which demonstrate that PDC-109 disrupts the membrane in a concentration dependent manner.  Overall, results of the studies reported here present a clear and direct view about the action of PDC-109 on membranes made up of different phospholipids, which are consistent with the earlier observations that this protein disrupts membrane integrity (Swamy, 2004).  These observations are of considerable interest in view of the crucial role played by the interaction of PDC-109 with sperm plasma membranes in sperm capacitation.

## 2.3. Materials and Methods

### 2.3.1. Materials

Choline chloride, acrylamide, bis-acrylamide and TEMED were obtained form Sigma (St. Louis, MO, USA).  Sephadex G-50 (superfine) and DEAE Sephadex A-25 were purchased from Pharmacia Biotech (Uppsala, Sweden).  Dimyristoylphosphatidylcholine (DMPC), dipalmitoylphosphatidylcholine (DPPC), dimyristoylphosphatidylglycerol (DMPG) and cholesterol were from Avanti Polar Lipids (Alabster, AL, USA).  Tris(hydroxymethyl)aminomethane (Tris base), sodium chloride, dichloromethane, EDTA and sodium azide were obtained from local suppliers and were of the highest purity available.

### 2.3.2. Purification of PDC-109

PDC-109 was purified from bovine seminal plasma from healthy and reproductively active Ongole bulls by gel filtration on Sephadex G-50 followed by affinity chromatography on DEAE Sephadex A-25 in buffer containing 1 M NaCl

(Calvete *et al.*, 1996) and eluted with 100 mM choline chloride (Ramakrishnan *et al.*, 2001) and its purity was assessed by SDS-PAGE on 10% or 12% gels (Laemmli, 1970).  The purified protein was dialyzed extensively against 50 mM Tris-HCl buffer, pH 7.4, containing 0.15 M NaCl, 5 mM EDTA and 0.025% sodium azide (TBS-I) to remove the choline chloride used for elution. Concentration of PDC-109 was estimated from its extinction coefficient of 2.5 for 1 mg/mL concentration at 280 nm for 1.0 cm path length (Calvete *et al.*, 1996).

### 2.3.3. Isothermal Titration Calorimetry

The interaction of PDC-109 with different phospholipids was investigated by isothermal titration calorimetry using a MicroCal VP-ITC instrument (MicroCal LLC, Northampton, MA, USA).  Samples were prepared by taking a small, weighed quantity of the lipid (DMPC or DMPG) in a glass test tube, dissolving it in ca. 50-100 μL of dichloromethane (or dichloromethane/methanol mixture), followed by removing the solvent under a stream of nitrogen gas.  The resulting thin lipid film was vacuum desiccated for 3–4 hours to completely remove the solvent and then hydrated with an appropriate buffer to yield the desired final concentration of the phospholipid.  This suspension was then subjected to bath sonication until a clear solution was obtained, indicating the formation of unilamellar vesicles in the solution.  PDC-109 was taken in sufficiently high concentration and dialyzed against tris buffer (50 mM) containing 150 mM NaCl and 5 mM EDTA, at different pH (7.4-9.0).  This stock solution was diluted to a final working concentration of 250 μM.  All the solutions were degassed under vacuum prior to use.  ITC experiments were performed by injecting protein from the syringe into the calorimeter cell containing ca. 90 μM of the phospholipid vesicles (DMPC and DMPG).  Typically, 25 consecutive injections of 5 μL aliquots of the protein were added to the calorimeter cell containing the phospholipid

vesicles.  Injections were made at intervals of 180 sec, and to ensure proper mixing after each injection, a constant stirring speed of 300 rpm was maintained during the experiment.  Control titrations were performed by injecting the protein into the buffer of appropriate pH.  The data were analysed by fitting the experimental values to the '*one set of sites*' binding model.

## 2.3.4. Confocal Microscopy

The effect of PDC-109 binding to the plasma membrane on the shape and integrity of erythrocytes was investigated by confocal microscopy.  Imaging was done in the transmission mode using a Leica TCS SP2 confocal microscope (Heidelberg, Germany).  Human erythrocytes (0.04 %) in TBS-I buffer were used for control experiments whereas to monitor the interaction of PDC-109 with erythrocyte membranes, a 0.04% suspension of erythrocytes was incubated with different concentrations of PDC-109 (0.25 and 0.5 mg/mL) for one hour prior to imaging.  Erythrocyte suspensions were directly spotted on a clean glass slide and then transferred to confocal stage for imaging.

## 2.3.5. Atomic Force Microscopy

Supported membranes of DPPC, DMPC and DMPG were prepared in the following manner.  About 0.2 mg of the lipid was taken in a glass test tube and dissolved in ca. 200 μL of dichloromethane or dichloromethane/methanol mixture. The solvent was dried under a stream of nitrogen gas followed by vacuum desiccation for a minimum of 3 hours.  The lipid film thus obtained was hydrated with 1 mL of TBS-I buffer and subjected to bath sonication for 30 minutes. Sonicated vesicles were deposited gently upon freshly cleaved mica sheets (1 cm × 1 cm) and kept for 30-40 minutes.  Samples were then rinsed with HPLC grade water, dried and transferred to the AFM stage for imaging.  Experiments with

DPPC membranes and studies on the interaction of PDC-109 with them were carried out in a liquid cell where DPPC membranes, supported on mica were fixed and then 1 mL of TBS-I buffer was added.  The cell was kept at room temperature for ~20 minutes in order to allow the membrane to attain complete hydration and then imaging was performed in contact mode by using silicon nitride cantilevers (0.6 N/m spring constant).  To monitor the interaction of PDC-109 with the membrane, about 1.5 mg of PDC-109 in TBS-I buffer was added to the same liquid cell (having membrane) and imaging was performed at different time intervals.

Experiments to investigate the interaction of PDC-109 with membranes made up of DMPC, DMPG or DPPC/cholesterol (3:2; mol/mol) were carried out in air. Here PDC-109 (0.5 mg/mL) was added to the sonicated lipid vesicles, before their deposition on mica and imaging was performed in semi-contact mode by using NSG10 cantilevers with Au reflective coating and a nominal spring constant of 11.8 N/m.  All the experiments were carried out with the help of a SOLVER PRO-M atomic force microscope (NT-MDT, Moscow, Russia), equipped with a 3/10 μm bottom scanner and operating with a NTEGRA controller.  Force was kept at the lowest possible value by continuously adjusting the set-point and feed-back gain during imaging.

## 2.4. Results and Discussion

Binding of PDC-109 to spermatozoa results in a membrane reorganization which is a necessary event before the sperm can undergo acrosome reaction and finally fertilize the egg.  Hence considerable attention has been focused on investigating the interaction of this protein with sperm plasma membranes and model membranes (Swamy, 2004).  In the present study, the interaction of PDC-109 with model membranes containing DMPC, DPPC and DMPG as well as with

intact cell membranes was investigated by using ITC, AFM and confocal microscopy.  The results obtained are discussed below.

## 2.4.1.  Effect of pH on the Interaction of PDC-109 with Phospholipid Membranes

Thermodynamic parameters characterizing the interaction of PDC-109 with DMPC and DMPG were determined using ITC at temperatures below the gel-liquid crystalline phase transition.  The effect of pH on the thermodynamic parameters associated with the interaction of PDC-109 with DMPC and DMPG vesicles was studied at 15 and 20 ºC, respectively.  Measurements could be performed only in the pH range of 7.4 and 9.0 since the protein tended to precipitate at low pH and ITC profiles above pH 9.0 were not consistent.  Fig. 2.1 shows typical ITC profiles for the binding of PDC-109 to DMPC unilamellar vesicles in TBS-I buffer (pH 7.4).  The ITC profile in Fig. 2.1 shows that injection of 5 μL aliquiots of PDC-109 into DMPC suspension gives large endothermic heats of binding, which decrease in magnitude with subsequent injections, showing saturation behaviour.  The data could be best fitted by a nonlinear least squares approach to '*one set of sites*' binding model.  Similar titrations were carried out with DMPG and the profile obtained is presented in Fig. 2.2.  Stoichiometry ($n$) and thermodynamic parameters [changes in free energy ($\Delta G$), enthalpy ($\Delta H$) and entropy ($\Delta S$)] obtained from an analysis of the ITC data for the binding of DMPC and DMPG to PDC-109 at different pH are listed in Table 2.1.
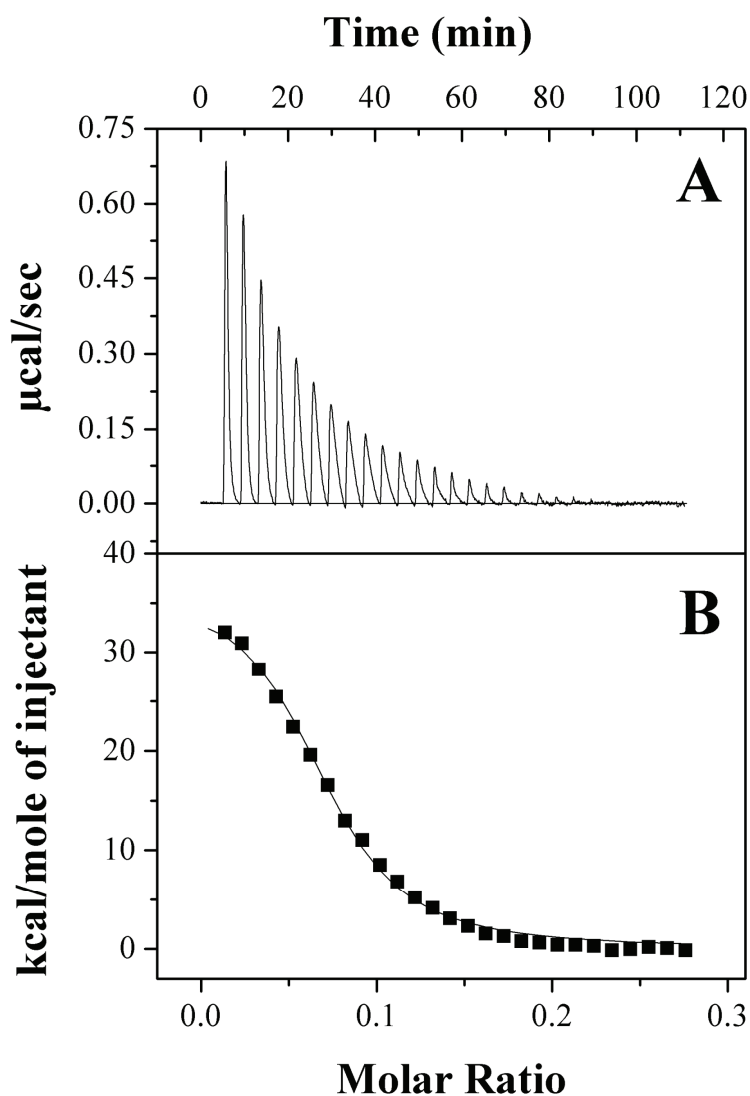
**Fig. 2.1: Calorimetric titrations for the binding of PDC-109 to DMPC vesicles**. An ITC profile for the binding of PDC-109 to unilamellar vesicles of DMPC is shown. The upper panel (**A**) shows the raw data for the titration of DMPC vesicles (90 µM) with protein (250 µM) and the lower panel (**B**) shows the integrated heats of binding obtained from the raw data, after subtracting the heat of dilution. The solid line in the bottom panel represents the best curve fit to the experimental data, using the *one set of sites* model from MicroCal Origin. See text for further details.

The thermodynamic parameters obtained for the interaction of DMPC and DMPG to PDC-109 indicate that the binding is stabilized by entropy of binding,

with negative contribution from binding enthalpy. The observed binding constant for the interaction of PDC-109 with DMPG was smaller than that of the choline phospholipid (DMPC), reflecting a lower affinity of PDC-109 for this lipid.



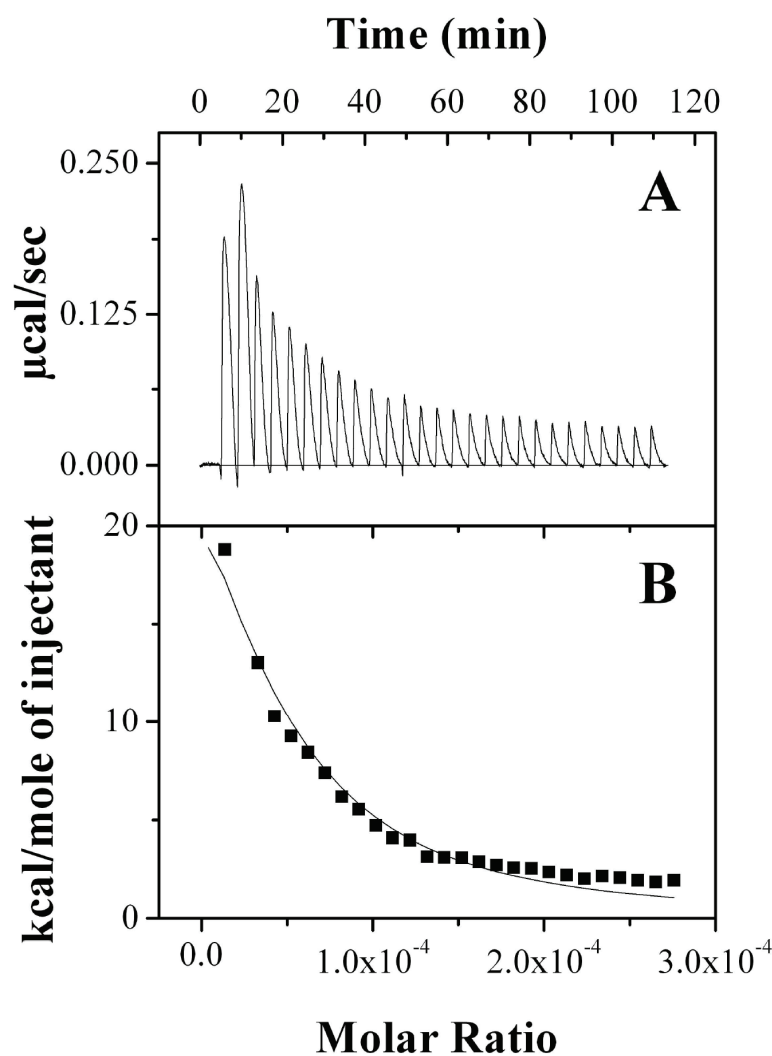**Fig. 2.2: Titration calorimetry for PDC-109 binding to DMPG vesicles**. Injection of PDC-109 (250 µM) to DMPG vesicles (~90 µM) at 20 ºC, yielded an endothermic binding isotherm (**A**). Lower panel (**B**) shows the integrated data obtained from the raw data, after subtracting the heat of dilution. Experimental data were fitted by using the *one set of sites* model from MicroCal Origin.

**Table 2.1:** Effect of pH on the thermodynamic parameters obtained by isothermal titration calorimetry for PDC-109 binding to DMPC and DMPG unilamellar vesicles.

| pH | $n$ | $K_a$ $\times 10^{-5}$ (M$^{-1}$) | $\Delta G$ (kcal.mol$^{-1}$) | $\Delta H$ (kcal.mol$^{-1}$) | $\Delta S$ (cal.mol$^{-1}$.K$^{-1}$) |
|---|---|---|---|---|---|
| DMPC at 15 ºC | | | | | |
| 7.4 | 12.7 ± 0.32 | 2.22 ± 0.17 | 6.98 ± 0.03 | 2.86 ± 0.03 | 34.2 |
| 8.0 | 11.1 ± 0.10 | 2.90 ± 0.25 | 7.20 ± 0.03 | 2.96 ± 0.03 | 35.3 |
| 9.0 | 8.7 ± 0.08 | 5.10 ± 0.86 | 7.51 ± 0.47 | 3.20 ± 0.47 | 37.2 |
| DMPG at 20 ºC | | | | | |
| 7.4 | 24.0 ± 0 | 0.3 ± 0.02 | 5.90 ± 0.10 | 1.6 ± 0.10 | 25.6 |
| 8.0 | 24.0 ± 0 | 0.05 ± 0.007 | 4.96 ± 0.10 | 1.8 ± 0.10 | 23.1 |

Interestingly, the interaction between PDC-109 and both the phospholipids was found to be sensitive to the pH of the medium.  In the case of DMPC association constant increases slightly at higher pH, whereas the stoichiometry of binding decreases.  On the contrary for DMPG stoichiometry remains nearly unaltered, whereas binding constant decreases significantly (Table 2.1).  This decrease of affinity of PDC-109 to DMPG could be attributed to the increase in the net negative charge on the protein, resulting in electrostatic repulsion between the protein and the lipid membrane which is also negatively charged.  These results also indicate that the binding strength of DMPC for PDC-109 is higher than that of DMPG, which is consistent with earlier reports (Thomas *et al.*, 2003).

## 2.4.2. Confocal Microscopic Studies on the Destabilization of Erythrocyte Plasma Membrane by PDC-109

Morphological changes in intact human erythrocytes induced by the binding of PDC-109 were monitored by confocal microscopy. The outer leaflet of the erythrocyte membranes is rich in choline phospholipids and hence provides an excellent model system to investigate the interaction of PDC-109 with cell membranes.
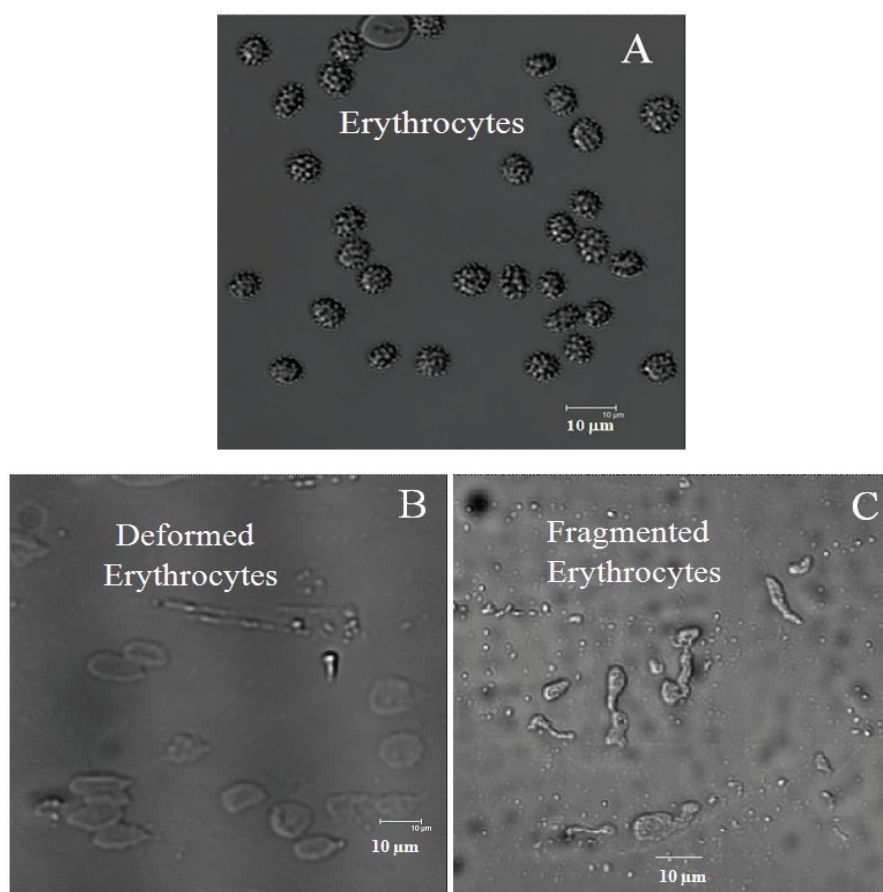


**Fig. 2.3: Effect of PDC-109 on human erythrocyte membrane**. Confocal image of (**A**) human erythrocytes in TBS-1 buffer, (**B**) in the presence of 0.25 mg/mL of PDC-109 at room temperature and (**C**) after incubation with 0.5 mg/mL PDC-109 at room temperature.

As shown in Fig. 2.3A, intact human erythrocytes are 5-6 μm in size (diameter) and show a well defined morphology, whereas erythrocytes that were incubated with 0.25 mg/mL PDC-109 for one hour show a distorted morphology (Fig. 2.3B). Interestingly, incubation of erythrocytes with higher concentrations of PDC-109 (≥0.5 mg/mL) resulted in their fragmentation (Fig. 2.3C). The above studies thus demonstrate that PDC-109 can destabilize the cell membrane in a concentration dependent manner.

### 2.4.3. AFM Studies on the Destabilization of Model Membranes by PDC-109 Binding

Atomic force microscopy is a powerful method to study the interaction of proteins with supported membranes (Grandbois *et al.*, 1998; Milhiet *et al.*, 2006). Here the effect of PDC-109 binding on the morphology of supported membranes made up of DMPC, DPPC, DMPG as well as DPPC containing 40 mol% cholesterol was studied by AFM. Upon deposition on mica, sonicated vesicles of DPPC, DMPC and DMPG yielded well-ordered supported membranes (bilayers or multilayers) (Fig. 2.4, panels A, G and I). In order to investigate the effect of PDC-109 binding on the structural integrity of the supported membranes, experiments were carried out both in the liquid cell and in air.

**Fig. 2.4: Atomic force microscopic studies to investigate the effect of PDC-109 on model membranes**. (**A**) AFM image of DPPC bilayer in liquid cell (3 × 3 μm). (**B**) DPPC incubated with 1.5 mg/mL of PDC-109 for 10 minutes (3 × 3 μm). (**C**) DPPC incubated with the same concentration of PDC-109 for 25-30 minutes (3 × 3 μm). (**D**, **E**, **F**) Height profiles of the regions corresponding to the white bars marked in **A**, **B**, and **C**, respectively. (**G**) DMPC multi-layers in air (1.5 × 1.5 μm). (**H**) DMPC in the presence of 0.5 mg/mL of PDC-109 (5 × 5 μm). (**I**) DMPG bilayer in air (3.5 × 3.5 μm). (**J**) DMPG in the presence of 0.5 mg/mL of PDC-109 (10 × 10 μm).
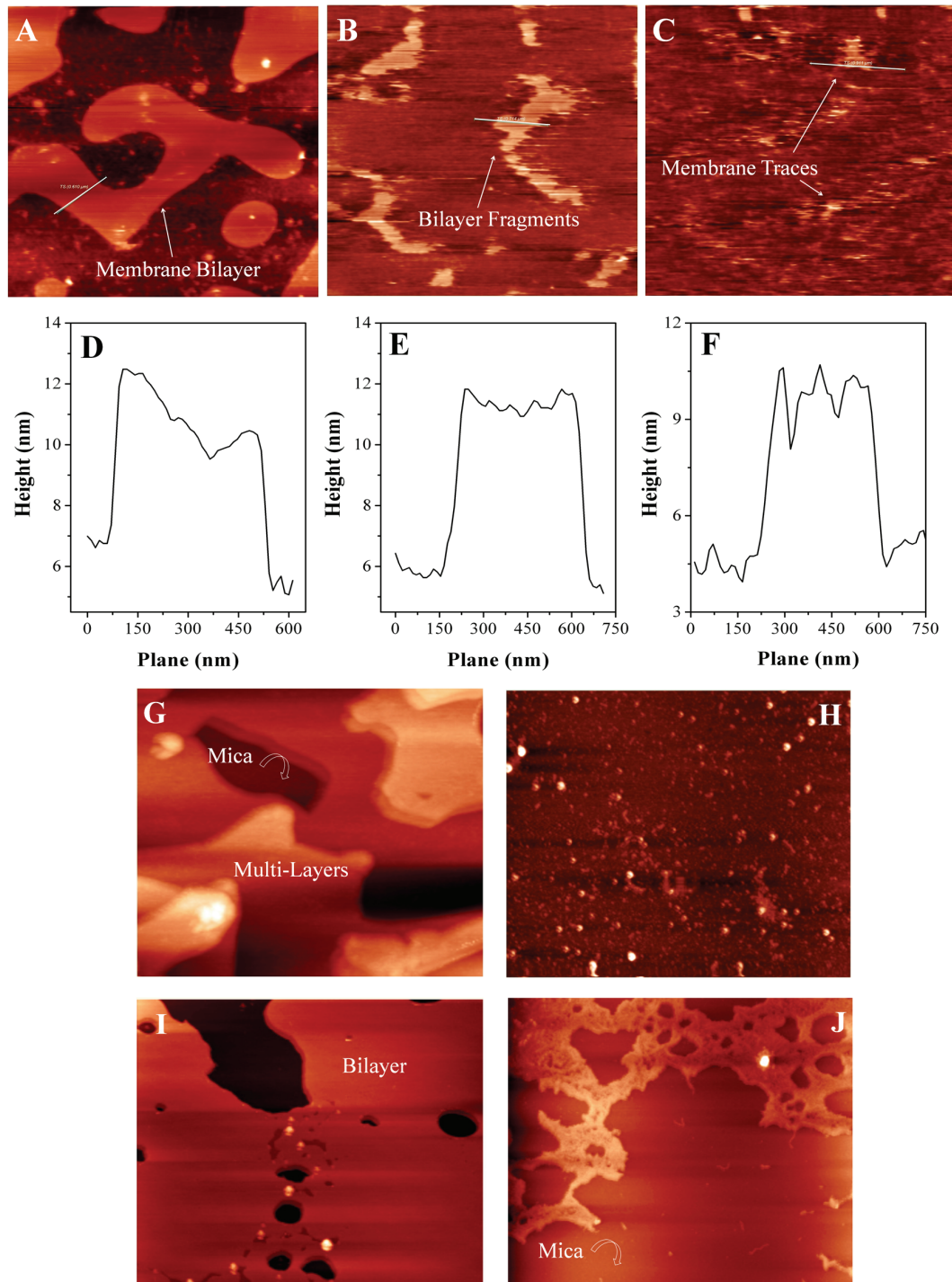
Fig. 2.4A shows the AFM image of a DPPC membrane supported on mica, obtained in a liquid cell at 25 $^o$C, where the phospholipid is in the gel-phase. Panels A, B and C of Fig. 2.4 present a typical time sequence of DPPC monolayer degradation due to removal of the phospholipid by PDC-109, whereas panels D, E and F show the height profiles, corresponding to the white bars in panels A, B and C, respectively. The measured height of the lipid film was found to be 6.0 ± 0.3 nm, which is in agreement with the thickness of 6.15 ± 0.93 nm reported for hydrated DPPC bilayer in the gel phase (Milhiet *et al.*, 2006). Incubation of the supported DPPC membrane for 10 minutes after the addition of PDC-109 resulted in a partial degradation of the phospholipid bilayer (Fig. 2.4B), whereas incubation for ca. 30 minutes led to a significant disintegration of the membrane structure (Fig. 2.4C). These observations support the above confocal microscopic findings that PDC-109 destabilizes cell and model membranes in a concentration dependent manner. Further, they demonstrate that the destabilization is also dependent on the incubation time.

Sonicated vesicles of DMPC and DMPG, which were pre-incubated with PDC-109, failed to form intact membrane layers. After incubation with PDC-109, no significant membranous structure of DMPC could be observed by AFM (Fig. 2.4H). Instead, small, nearly spherical particles, which most likely correspond to lipoprotein aggregates, were observed. The average diameter of these particles was measured to be 89 ± 7 nm, which correlates very well with the diameter of efflux particles (>80 nm) released from fibroblasts upon incubation with PDC-109 (Moreau and Manjunath, 1999). Interestingly, electron microscopic studies by Gasset *et al.* (2000) indicated that incubation of DOPC (dioleoyl-sn-glycero-3-phosphocholine) large unilamellar vesicles with PDC-109 led to the formation of particles of 10 to 40 nm in size. Although the exact reason for the difference in the particle size observed in the two studies is not clear, it is possible that it may be

due, at least in part, to the use of the saturated phospholipid DMPC in the present study and the unsaturated DOPC by Gasset *et al.* (2000).

Binding of PDC-109 to DMPG model membranes could not induce complete disintegration of the membrane, but yielded fragmented membrane layers and small membrane fragments (Fig 2.4J), which is consistent with the relatively lower affinity of PDC-109 for DMPG as compared to the choline containing phospholipids (Thomas *et al.*, 2003).

## 2.4.4. Effect of Cholesterol on PDC-109/Phospholipid Interaction

The presence of cholesterol at high mol fractions has been reported to provide a significant stabilization to the lamellar structure of phosphatidylcholine membranes (Swamy, 2004; Ramakrishnan *et al.*, 2001; Thomas *et al.*, 2003; Gasset *et al.*, 2000). In order to investigate this further AFM studies on membranes made up of DPPC/cholesterol (3:2; mol/mol) were carried out. Fig. 2.5A shows that in the absence of PDC-109 intact multilayer structures are formed by this lipid mixture. Height profiles of these multilayers at two regions marked TS-1 (transverse section − 1) and TS-2 (transverse section − 2) are shown in Fig. 2.5B and Fig. 2.5C, respectively. Although the height profile of TS-1 shown in Fig. 2.5B corresponds to several layers as can be judged from the appearance of the image as well as the overall height measured (ca. 50 − 55 nm), the height of individual layers is not clearly discernible. On the other hand, the height profile of TS-2, shown in Fig. 2.5C displays a zig-zag pattern and each vertical edge of the pattern, measuring ca. 5.0 − 5.5 nm most likely corresponds to the height of the bilayer as this value is comparable to the thickness of the DPPC bilayer (4.55 nm), determined by X-ray diffraction measurements (Lis *et al.*, 1982). Addition of PDC-109 to the DPPC/cholesterol multilayers results in a significant break down of the membranous structures. However, unlike in the case of membranes containing only
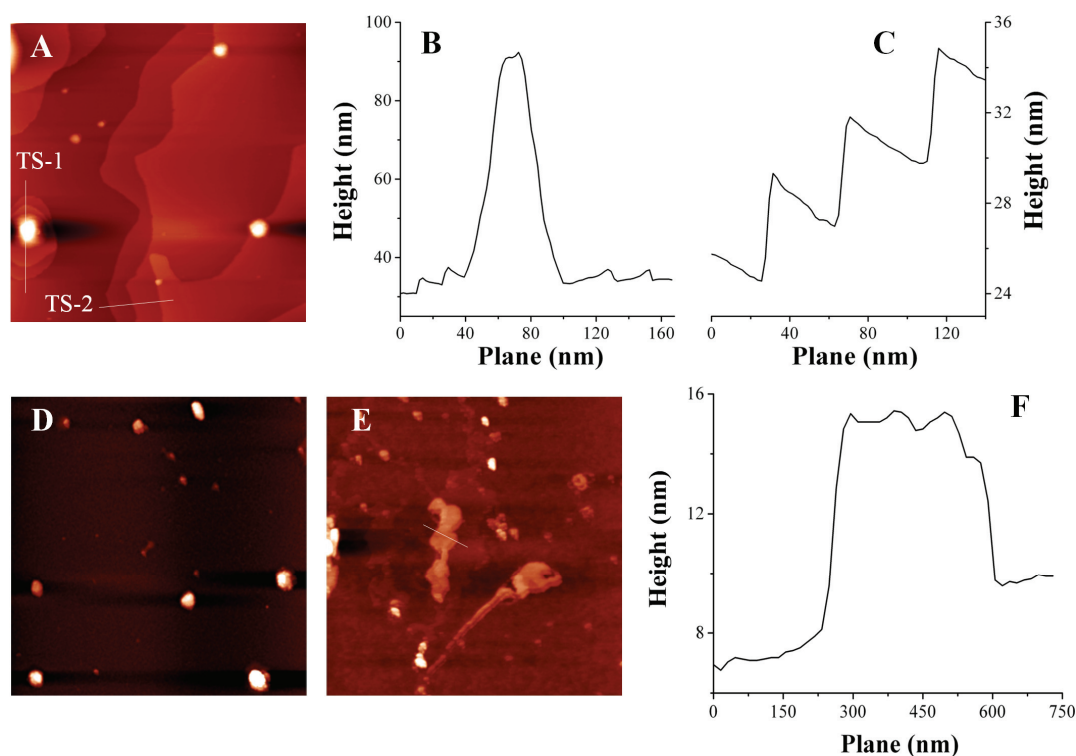
**Fig. 2.5:  Cholesterol induced stabilization of DPPC model membranes**.  (**A**) AFM image of DPPC multi-layers, containing cholesterol at a ratio of 1:1 (mol/mol).  Image size is 5 × 5 μm.  (**B**) Height profile for transverse section 1 (TS-1), shown in panel **A**.  (**C**) Height profile for transverse section 2 (TS-2), shown in panel **A**.  (**D**) Small DPPC model membrane fragments and aggregated structures composed of PDC-109 and model membrane (5 × 5 μm).  (**E**) Image of intact membrane fragments, observed after the action of PDC-109 on DPPC model membranes containing 40 mol% cholesterol (5 × 5 μm).  (**F**) Height profile for transverse section, shown in panel **E**.

DPPC (Fig. 2.5D), membrane fragments of moderate size are observed in some regions (Fig. 2.5E), suggesting that presence of cholesterol afforded a partial stabilization of lipid membranes.  A height profile corresponding to the region marked with a white bar in Fig. 2.5E is shown in Fig. 2.5F.  The height of the membrane, measured from this profile is ca. 5 – 7 nm, which is consistent with a bilayer architecture.

In summary, in the work reported in this chapter, the energetics of interaction of PDC-109 with phospholipids has been investigated by isothermal titration

calorimetry.  It has been found that the binding of PDC-109 to gel phase lipids is endothermic in nature and is governed by a positive entropic contribution.  Further, the interaction of PDC-109 with DMPG vesicles was observed to be more sensitive to the pH of the environment as compared to DMPC.  AFM studies demonstrate that the binding of PDC-109 to different cell membranes, model membranes (multilamellar vesicles) as well as supported membrane layers leads to the extraction of lipids and cholesterol which ultimately results in membrane destabilization.  Presence of cholesterol provides a partial stabilization to the membrane.  AFM and ITC studies further confirm the higher selectivity of PDC-109 towards choline phospholipids as compared to other phospholipids such as phosphatidylglycerol.  Overall, the present study leads to a better understanding of the interaction of PDC-109 with phospholipid membranes at the molecular level and provide direct and conclusive evidence for the earlier reports.

# Chapter 3

## Exploration of Chaperone-like Activity of PDC-109
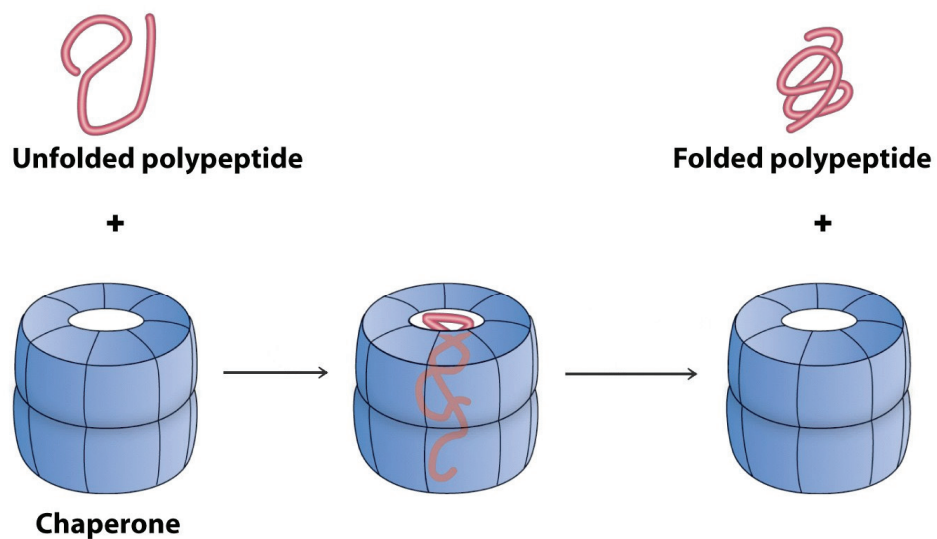
## 3.1. Abstract

The major protein of bovine seminal plasma, PDC-109 binds to choline phospholipids on the sperm plasma membrane and induces the efflux of cholesterol and choline phospholipids, which is an important step in sperm capacitation. The high abundance, polydisperse nature and reversibility of thermal unfolding of PDC-109 suggest significant similarities to chaperone-like proteins such as spectrin, α-crystallin, α-synuclein etc. In the present study, biochemical and biophysical approaches were employed to investigate the chaperone-like activity of PDC-109. The effect of various stress factors such as high temperature, chemical denaturant (urea) and acidic pH on target proteins such as lactate dehydrogenase, alcohol dehydrogenase, insulin etc. were studied both in the presence and absence of PDC-109. The results obtained indicate that PDC-109 exhibits chaperone-like activity, as evidenced by its ability to suppress the nonspecific aggregation of target proteins and direct them into productive folding. Atomic force microscopic studies demonstrate that PDC-109 effectively prevents the fibrillation of insulin, which is of considerable significance since amyloidogenesis has been reported to be a serious problem during sperm maturation in certain species. Binding of phosphorylcholine or high ionic strength in the medium inhibited the chaperone-like activity of PDC-109, suggesting that most likely the aggregation state of the protein is important for the chaperone function. These observations show that PDC-109 functions as a molecular chaperone in vitro, suggesting that it may assist the proper folding of proteins involved in bovine sperm capacitation pathway.

## 3.2. Introduction

As discussed in Chapter 1, binding of PDC-109 to spermatozoa leads to the extraction of lipids and cholesterol from the plasma membrane, a process referred to as cholesterol efflux, which appears to be a critical step in sperm capacitation (Thérien *et al.*, 1998; Moreau *et al.*, 1998). Some of the characteristics exhibited by PDC-109 such as polydispersity, high abundance and reversibility of thermal unfolding are quite similar to those displayed by well-characterized stress proteins with chaperone-like activity such as spectrin, α-crystallin etc. In view of this, investigations were carried out to find out if PDC-109 exhibits chaperone-like activity. Stress proteins are part of the anti-stress mechanism that all cells possess to deal with stress (Lindquist and Craig, 1988). Some stress proteins are molecular chaperones, which constitute the cellular chaperoning system. These systems play a central role in cell physiology under both normal and stress conditions, by assisting in the folding of newly synthesized polypeptides. Molecular chaperones also assist in the refolding of proteins that are partially denatured due to stress and in the dissolution of pathological protein aggregates etc (Horwitz, 1992; Das and Surewicz, 1995; Datta and Rao, 1999; Reddy *et al.*, 2000). The first step in the protective action of a molecular chaperone is its interaction with denatured or unfolded proteins to provide a suitable environment to facilitate their normal folding or prevent the formation of large protein aggregates (Wang and Spector, 1994; Rao *et al.*, 1995; Rajaraman *et al.*, 1996; Qu *et al.*, 2009).

In the studies reported in this chapter, biochemical assays aimed at investigating the chaperone-like activity of PDC-109 have been performed, which demonstrated that this protein is able to effectively prevent the unfolding and aggregation of target proteins such as insulin, lactate dehydrogenase (LDH), alcohol dehydrogenase (ADH) and $\beta_L$-crystallin. It has been also shown that PDC-109 protects enzymes such as glucose-6-phosphate dehydrogenase (G6PD) and glutathione-S-transferase (GST) against thermal

and chaotrope-induced inactivation, respectively.  The aggregation and chaperone-induced disaggregation processes have been characterized in detail by atomic force microscopy and image processing of the AFM data.  Refolding of taget proteins was arrested by PDC-109 in a concentration dependent manner, similar to some other heat-shock proteins such as spectrin and Hsp90 (Yonehara *et al.*, 1996; Chakrabarti *et al.*, 2001).   Binding of PrC and choline to PDC-109 as well as presence of high concentration of sodium chloride in the medium resulted in an inhibition of the chaperone-like activity of the protein, suggesting that aggregation state of the protein is likely to be important for the chaperone-like activity of PDC-109.  The results obtained clearly demonstrate that PDC-109 exhibits chaperone-like activity which is likely to be physiologically significant.

## 3.3. Materials and Methods

### 3.3.1. Materials

Choline chloride, phosphorylcholine chloride, insulin, G6PD (from *Leuconostoc mesenteroides*), glucose-6-phosphate (G6P), GST, Thioflavin T (ThT), 1-chloro-2, 4-dinitrobenzene (CDNB) and MOPS were from Sigma (St.  Louis, MO).  Sephadex G-50 (superfine) and DEAE Sephadex A-25 were obtained from Pharmacia (Uppsala, Sweden).  LDH, ADH, nicotinamide adenine dinucleotide phosphate (NADP), tris base, glutathione and other chemicals were purchased from local suppliers and were of the highest purity available.  $\beta_L$-Crystallin from bovine eye lens was a kind gift from Dr. G. B. Reddy (National Institute of Nutrition, Hyderabad, India).  PDC-109 was purified as described in Chapter 2.  The purified protein was dialyzed extensively against 50 mM tris buffer, 0.15 M NaCl, 5 mM EDTA, pH 7.4 (TBS-I) and stored at 4 ºC.

### 3.3.2. PDC-109 Assisted Reactivation of Heat Denatured G6PD

G6PD activity was assayed by a spectrophotometric method (Kumar *et al.*, 2005). In this assay G6P is oxidized to 6-phospho-D-gluconate by G6PD with simultaneous reduction of NADP to NADPH. The assay medium contained G6PD (0.25 μM), NADP (0.1 mM), G6P (5 mM) and 12 mM each of $MgCl_2$ and KCl. The reaction was initiated by the addition of NADP and increase in absorbance at 340 nm due to the reduction of NADP was monitored using a Cary 100 UV/Vis Bio spectrophotometer, which was also used for all other spectrophotometric measurements. To investigate the effect of PDC-109 on the thermal inactivation of the enzyme, G6PD was incubated for 30 minutes in the absence or presence of 0.5 μM PDC-109 at 45 ºC. Relative activity of various treated samples was normalized with respect to the activity of native G6PD.

### 3.3.3. Aggregation-inhibition Assay of Thermally Aggregated Enzymes

Chaperone activity was assayed as described previously (Horwitz, 1992) by monitoring the ability of PDC-109 to prevent heat-induced aggregation of ADH at 48 ºC. Aggregation was monitored by recording light scattering at 360 nm as a function of time. Concentration of ADH was 0.1 mg/mL in all the samples and PDC-109:ADH (w/w) ratios of 1:2, 1:1.4 and 1:1 were used. Aggregation profile for the native enzyme was taken as 100% and percent aggregation of other samples was calculated with respect to the native enzyme.

### 3.3.4. Reactivation of Urea Denatured GST

Glutathione-S-transferase activity was assayed by the CDNB-GST spectrophotometric assay (Habig *et al.*, 1974) with a slight modification. The reaction mixture consisted of 4 mM reduced glutathione (GSH), 0.4 mM CDNB and 5 μg of GST in TBS-I buffer in a final volume of 1.0 mL. Reaction was initiated with the addition of GST. Unfolding of GST was performed by mixing the stock solutions of

GST and urea in TBS-I buffer (pH 7.4) to give the desired concentration of protein (25 μg/mL) and denaturant (2 M).  The solution was incubated at room temperature for one hour in the presence or absence of PDC-109 (0.5 mg/mL), followed by dialysis against TBS-I at 4 ℃ for two hours to remove the denaturant.  The dialyzed samples were then assayed for GST activity.

### 3.3.5. Circular Dichroism Measurements on G6PD

CD studies were performed on a Jasco J-810 spectropolarimeter fitted with a thermostatted cell holder and interfaced to a thermostatic waterbath.  Spectra were recorded with native and heat-treated G6PD at 25 °C at a scan rate of 50 nm/min.  A 2 mm pathlength quartz cell and a slit width of 2 nm were used in all measurements.  To investigate the ability of PDC-109 to prevent thermal unfolding of the target protein, samples of G6PD (0.05 mg/mL) in TBS-I buffer were incubated for 60 minutes at 50 °C, in the presence and in the absence of PDC-109 (0.025 mg/mL) and cooled to 25 before recording the CD spectra.  All spectra were corrected with respective blanks and data are expressed as mean residual ellipticities.  CD experiments were also carried out with G6PD (0.1 mg/mL) by monitoring the spectral intensity of the protein at 221 nm as a function of temperature when scanned from 25 to 90 °C at a rate of 1 °/min.  In order to investigate the stabilization induced by PDC-109 on the structure of this enzyme, experiments were also carried out at PDC-109:G6PD ratios of 1:2 and 1:4.

### 3.3.6. Calorimetric Studies on PDC-109-induced Stabilization of Target Proteins

Thermal unfolding studies on LDH were carried out using a VP-DSC differential scanning calorimeter from MicroCal (Nothampton, MA).  Protein solutions in TBS-I were heated from 10 to 75 ℃, at a scan rate of 40°/h under a constant pressure of 22.9 psi.  PDC-109:target protein (w/w) ratios were 1:1 and 1:1.6 for LDH.  Buffer scans were subtracted from all thermograms to eliminate the contribution from buffer and the

temperature dependence of excess heat capacity was further analyzed using the Origin software supplied by MicroCal.

### 3.3.7. Inhibition of Insulin Fibrillation by PDC-109

Insulin was dissolved in water at 0.5 mg/mL concentration and its pH was adjusted to 1.6 with HCl. Incubation of this sample at 45 °C for 5 days yielded a turbid solution, indicating the formation of amyloidal fibrils. The sample was then centrifuged at 12,000g for 12 hours at 15 °C in an Eppendorf 5810 R centrifuge. The supernatant was discarded and the pellet was suspended in TBS-I. To investigate the effect of PDC-109 on insulin fibrillation, samples were prepared in the same way in the presence of 1 mg/mL PDC-109. Protein samples were diluted and used for AFM imaging as follows. A 50-80 μL aliquot of the protein solution was carefully deposited on a freshly cleaved mica sheet (1 cm × 1 cm) and allowed to dry for 20-30 minutes, rinsed with HPLC grade water, dried and transferred to the AFM stage. Imaging was performed in Semi-Contact mode using a SOLVER PRO-M atomic force microscope (NT-MDT, Moscow, Russia), equipped with a 3.0 μm bottom scanner. NSG10 cantilevers with Au reflective coating and a nominal spring constant of 11.8 N/m were used for the scanning. Force was kept at the lowest possible value by continuously adjusting the set-point and feed-back gain during imaging.

### 3.3.8. Fluorometric Assay for Thioflavin T Binding to Insulin Fibrils

The presence of amyloidal fibrils can be detected by ThT binding assay (Wang *et al.*, 2008). Binding of ThT to insulin fibrils was studied by titrating a fixed concentration of ThT (0.1 mM) with increasing concentrations of insulin (in fibrillar form) ranging from 0.43 μM to 6.45 μM. Steady state fluorescence measurements were performed on a Jobin-Yvon Spex Fluoromax-4 spectrofluorometer at 25 °C. ThT in

TBS-I buffer (pH 7.4) was excited at 440 nm and emission spectra were recorded between 450 and 550 nm. All fluorescence spectra were corrected for dilution effects.

### 3.3.9. Inhibition of Thermal Aggregation of ADH by PDC-109

ADH samples at a concentration of 40 μg/mL in TBS-I were incubated in the presence and absence of 20 μg/mL of PDC-109 at 48 ºC in a water bath for 30-40 minutes and then transferred to an ice bath. AFM samples were prepared as described above. An AFM image of native enzyme (kept at 4 ºC) was used as a control. Images were analyzed using the NOVA software, supplied by NTMDT.

**i) Average Fast Fourier Transform (FFT) Analysis:** Average FFT profiles of individual images, which indicate the periodicity of surface topography in X and Y directions, have been calculated. Fourier transformation transforms the data from time domain to frequency domain. Briefly, it shows how often which amplitudes are met on the image. FFT is used to calculate the average frequency components of a signal. Since we have used magnitude of surface topography as a signal or FFT scaling parameter, average FFT profile shows the average magnitude of surface topography in each frequency domain and plots it against the frequency (El. Feninat *et al.*, 2001). Small values of averaged FFT traces and equal distribution in all frequency regions indicate homogeneity of the samples, whereas, vice-versa is indicative of less homogenous sample or aggregated proteins.

**ii) Roughness Analysis:** This analysis yields several statistical parameters and a distribution density histogram. The distribution density histogram indicates values of Z-function in X-direction, whereas, Y-direction shows the corresponding number of points where the function value exists.

**iii) Bearing Ratio Analysis:** Abbot and Fireman (1933) proposed the notion of bearing area to characterize surface quality. This is defined as the area lying above a given depth (bearing depth). Bearing ratio is defined as the ratio of the bearing area to the whole sampled area. The bearing ratio forms a curve for the distribution of the 2D function values (i.e. Z-function values), of the source image. Z-function values are set in the X-direction, whereas, the Y-direction indicates a relation of the number of points, where the function value is less than X to the total number of points.

Here, statistical parameters were calculated for all the images. And finally parameters for ADH, which was incubated at 4 °C and 48 °C, prior to imaging were compared with the statistical parameters of the same target proteins in the presence of PDC-109 at 48 °C.

### 3.3.10. Refolding of Denatured Enzymes

Porcine muscle LDH (14.28 µM) was incubated in 6M GdnHCl at room temperature overnight, in order to achieve complete denaturation. Refolding was initiated by a 200-fold dilution of the denatured enzyme with renaturation buffer (TBS-1, pH 7.4) in the absence and presence of different concentrations of PDC-109. Recovery of enzyme activity was taken as a measure of refolding. In this assay lactate is converted to pyruvate by LDH with simultaneous reduction of $NAD^+$ to NADH which absorbs at 340 nm. The assay mixture contained LDH (0.07 µM), $NAD^+$ (0.2 mM) and sodium lactate (100 mM) in TBS-1 buffer. Reaction was initiated by addition of the enzyme and increase in absorbance at 340 nm due to the reduction of $NAD^+$ was monitored at room temperature.

### 3.3.11. Effect of Phosphorylcholine Binding on the Chaperone-like Activity of PDC-109

Chaperone activity was assayed as described above by monitoring the ability of PDC-109 to prevent heat-induced aggregation of ADH at 48 ºC.  To probe the effect of ligand binding on the chaperone activity, PDC-109 was incubated for 10 minutes with different concentrations of PrC before the assay was performed.  The reaction mixture contained 60 μg/mL ADH and 40 μg/mL PDC-109 in TBS-1.  Aggregation was monitored by recording light scattering at 360 nm in a UV/Vis Bio spectrophotometer.

### 3.3.12. Effect of Salts on Chaperone like Activity of PDC-109

Increase in ionic strength of the medium results in a dissociation of higher oligomers of PDC-109 and yields smaller oligomers (Gasset *et al.*, 1997).  Maximal dissociation occurs in high ionic strength buffer containing 50 mM EDTA and 0.5 M NaCl.  PDC-109 in 10 mM MOPS buffer (pH 7.4) containing 50 mM EDTA and 0.5 M NaCl was used to check the effect of high ionic strength on the chaperone activity.  PDC-109 in the same buffer without salt and EDTA was used as the control.  Chaperone activity was studied by ADH aggregation assay as described above.

### 3.3.13. Sequence Alignment

To compare the sequence homology and analogy of PDC-109 with other well known chaperone proteins, *pairwise alignment* was performed using the Needleman and Wunsch method (1970) of global alignment as implemented in the EMBOSS suite of software.  Eblosum40 was used as the scoring matrix.  The sequence of PDC-109 was aligned with two well known chaperone-like proteins, namely α-synuclein and α-crystallin, in order to identify the conserved regions that PDC-109 may share with them. Sequence similarity of PDC-109 with other seminal plasma proteins was analyzed using

multiple sequence alignment tool, ClustalW2 of European Bioinformatics Institute (http://www.ebi.ac.uk).

## 3.4. Results

PDC-109, the major protein of bovine seminal plasma, appears to be a multifunctional protein as it binds to a variety of other molecules including choline phospholipids, apolipoproteins A1 and A2, heparin etc (Chandonnet *et al.*, 1990; Desnoyers and Manjunath, 1992; Manjunath *et al.*, 2002). However, the precise functional roles played by this protein are not fully clear. Since several characteristics of PDC-109 are akin to the properties exhibited by proteins that act as molecular chaperones such as small heat shock proteins, spectrin, α-crystallin etc., in the present study chaperone-like activity of PDC-109 has been investigated. Results from different biophysical studies and biochemical assays, presented below, indicate that PDC-109 assists in the proper refolding of several other proteins and keeps them active, strongly suggesting that it functions as a molecular chaperone.

### 3.4.1. G6PD Activity Assay to Probe Chaperone-like Function of PDC-109

To investigate whether PDC-109 can prevent the thermal denaturation of G6PD, the activity of this enzyme was assayed in the absence and presence of PDC-109 (Fig. 3.1A). When incubated at 45 °C for 30 minutes, G6PD lost about 60% of its activity in

---

**Fig. 3.1:  PDC-109 exhibits chaperone-like activity against different target proteins.  A)** PDC-109 assisted reactivation of G6PD.  Activity of the enzyme at room temperature under native conditions (1), after incubation at 45 °C (2), upon incubation at 45 °C in the presence of PDC-109 (3) and after incubation at 4 °C in the presence of PDC-109 (4) is shown. **B)** Bar diagram representing the activity of G6PD at 300 seconds (from panel **A**).  **C)** Prevention of aggregation of ADH (0.1 mg/mL) by PDC-109. Aggregation profiles of (1) ADH at 48 °C, (2) ADH + 0.048 mg/mL PDC-109, (3) ADH + 0.072 mg/mL PDC-109, and (4) ADH + 0.096 mg/mL PDC-109 are shown.  **D)** Bar diagram representing percent aggregation (black bars) and protection (gray bars) of ADH with PDC-109 at different concentrations.  **E)** Reactivation of urea-denatured GST.  Activity of native enzyme at room temperature (1), urea-denatured enzyme (2), and urea-treated GST in presence of PDC-109 (3). **F)** Bar diagram representing the activity of GST at 900 seconds (from panel **E**).

the absence of PDC-109 (curve 2), while activity in the presence of PDC-109 was comparable to that of the native enzyme (curve 3). In control experiments, activity of G6PD alone and G6PD in the presence of PDC-109, incubated at 4 ºC, was assayed.
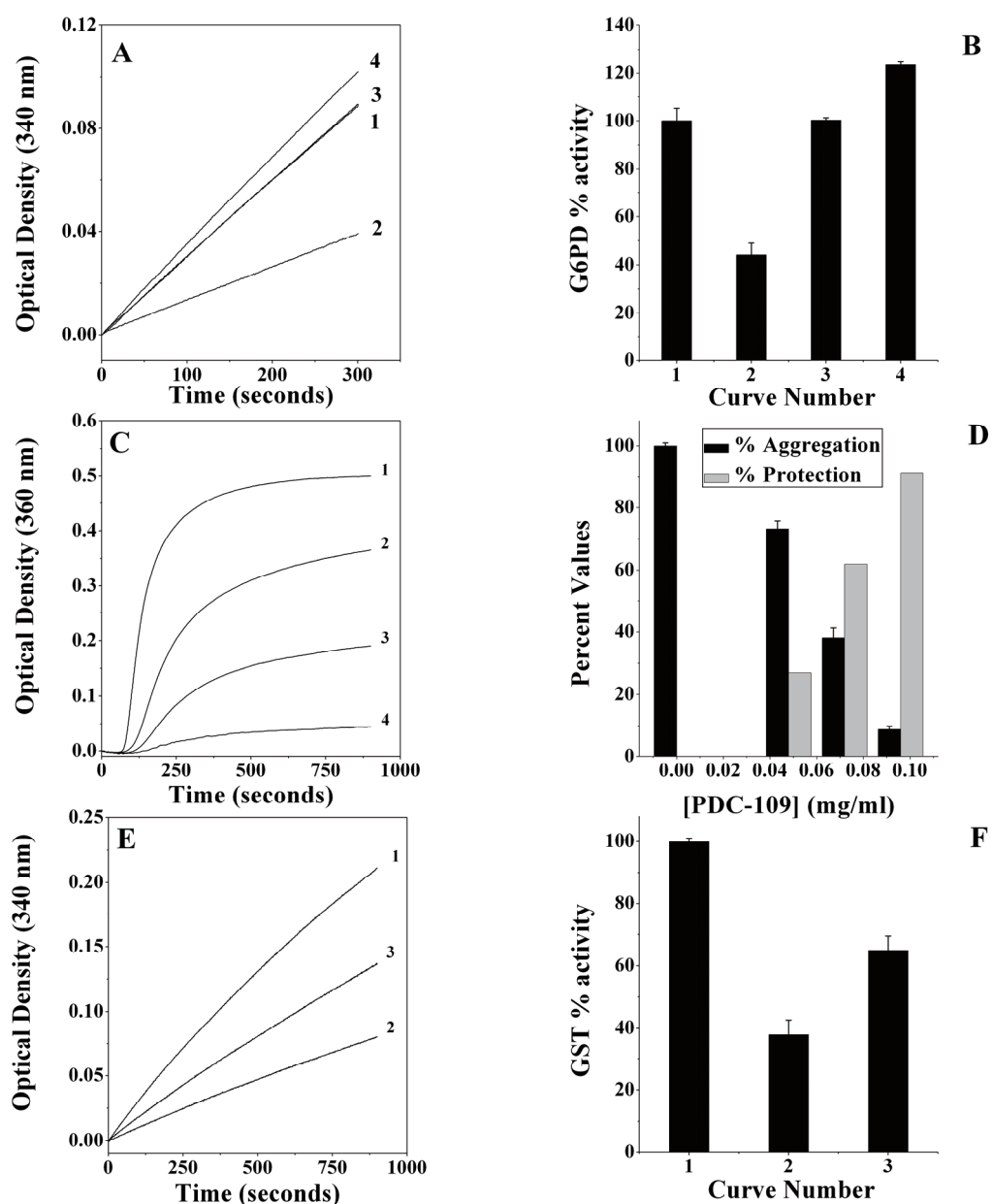
Activity of the enzyme solution which was incubated in the presence of PDC-109 at 4 ºC was found to be 23% higher than that of the native enzyme (curve 4).  Percent activity of different samples is shown in the form of a bar diagram in Fig. 3.1B.

### 3.4.2. Chaperone-like Function of PDC-109 Investigated by Aggregation Assay

Results of turbidimetric studies aimed at investigating the effect of PDC-109 on the thermal aggregation of ADH are shown in Fig. 3.1C.  When ADH was incubated at 48 °C, it is seen that turbidity of the sample increases rapidly with time, reaches a maximum and then levels off (curve 1).  Presence of PDC-109 reduced the rate of this aggregation significantly in a concentration-dependent manner.  A PDC-109 to ADH (w/w) ratio of 1:2 led to a considerable reduction in the rate of aggregation (curve 2). The aggregation decreased further when the PDC-109 to ADH ratio was increased to 1:1.4 (curve 3), whereas very little aggregation was observed at a ratio of 1:1 (curve 4). A bar diagram showing percent aggregation versus concentration of PDC-109 is given in Fig. 3.1D.  PDC-109 exhibited similar chaperone-like activity on other proteins such as aldolase, LDH and $\beta_L$-crystallin (see Figures S3.1, S3.2 and S3.3)*.

### 3.4.3. PDC-109 Assisted Reactivation of Urea Denatured GST

Urea induced unfolding of GST, which results in a loss of its activity, was monitored by GST-CDNB spectrophotometric assay (Fig. 3.1E).  It was observed that urea treatment results in more than 60% loss in the activity of GST (curve 2), whereas in the presence of PDC-109 considerable protection was observed and its activity was found to be ca.  65% of that observed in its native state (curve 3).  A bar diagram indicating percent activity of different samples with respect to the activity of native GST (taken as 100%) is shown in Fig. 3.1F.

---

* *Supporting Information is given in electronic format in a CD enclosed with the thesis.*

### 3.4.4. Conformational Stabilization of G6PD by PDC-109

To probe the ability of PDC-109 to stabilize the conformation of G6PD, changes in the secondary structure of this enzyme (at 50 °C) were investigated in the absence and presence of PDC-109 by CD spectroscopy. Room temperature far-UV CD spectrum of G6PD was used as a control to compare the loss of secondary structure at elevated temperature. The CD spectrum of native G6PD shown in Fig. 3.2A indicates a well defined secondary structure (curve 1), whereas the spectrum of the enzyme that was incubated at 50 °C has a significantly reduced intensity in the far UV region, indicating considerable loss of secondary structure (curve 2). At a PDC-109 to target protein ratio of 1:2 (w/w), most of the conformational features of the enzyme are retained (curve 3).
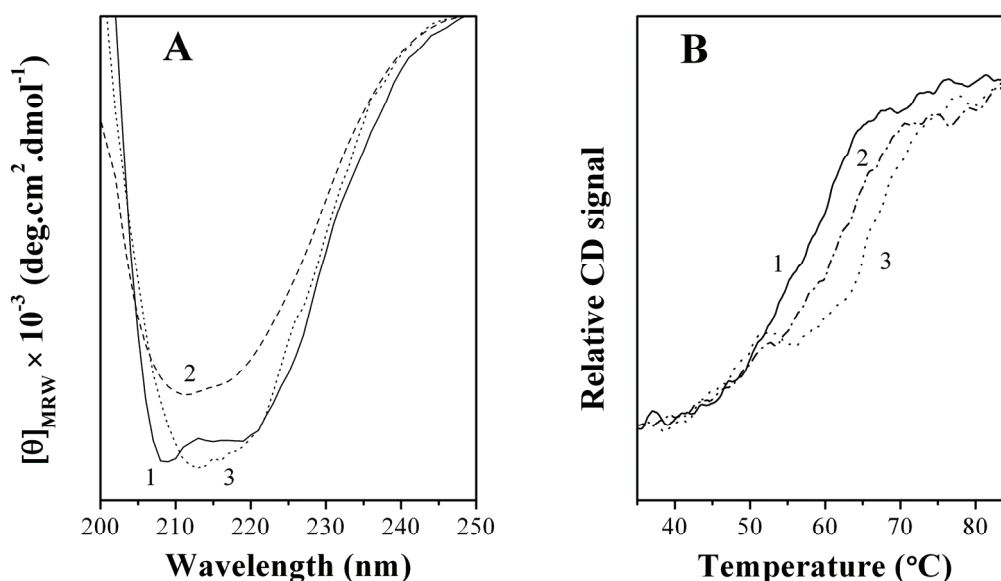


**Fig. 3.2: Circular dichroism studies on the stabilization of G6PD structure by PDC-109. A)** Far-UV CD spectra of G6PD. Spectra of G6PD (0.05 mg/mL) under native conditions at 25 °C (1), upon incubation at 50 ºC (2), and upon incubation at 50 °C in the presence of 0.025 mg/mL PDC-109 (3) are shown. **(B)** Variation of far-UV CD signal at 221 nm as a function of temperature. (1) G6PD alone (0.1 mg/mL), (2) G6PD (0.1 mg/mL) + 0.05 mg/mL of PDC-109, (3) G6PD (0.1 mg/mL) + 0.1 mg/mL of PDC-109.

In order to investigate the thermally-induced changes in the conformation of G6PD CD thermal scans were carried out at a fixed wavelength (221 nm). It is evident from Fig. 3.2B that native G6PD undergoes a transition centered at 52.8 °C (curve 1). In the presence of increasing concentrations of PDC-109, it was observed that the transition shifts to higher temperatures. At a PDC-109 to G6PD ratio of 1:4, the transition midpoint shifts to 56.4 °C (curve 2), whereas, increasing the PDC-109 to G6PD ratio to 1:2 results in a further shift of the transition midpoint to 63.8 °C (curve 3).

### 3.4.5. Prevention of Thermal Aggregation of LDH by PDC-109

DSC thermograms corresponding to the unfolding of LDH alone and in the presence of different concentrations of PDC-109 are shown in Fig. 3.3.
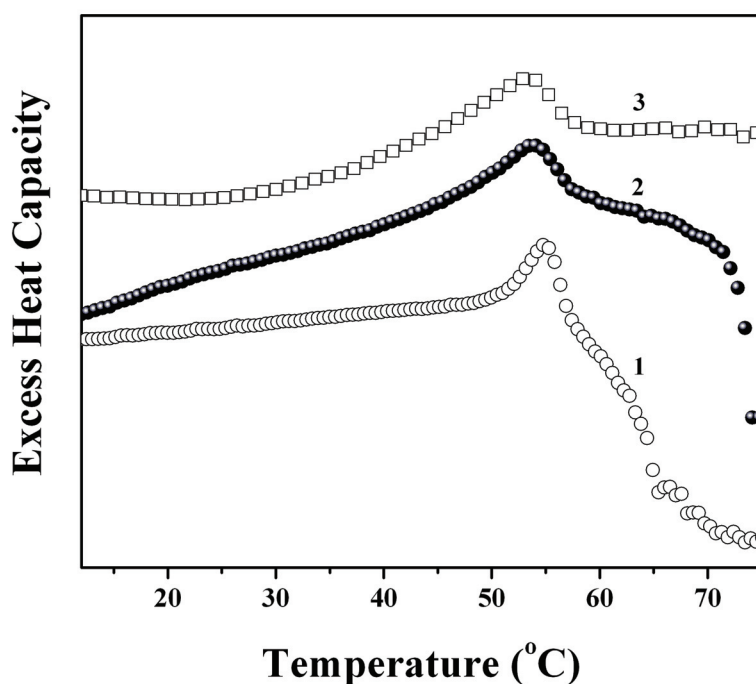


**Fig. 3.3: Calorimetric studies on PDC-109 induced stabilization of LDH**. DSC thermograms of 0.4 mg/mL LDH alone (○), and in the presence of 0.25 mg/mL (●) and 0.4 mg/mL (□) PDC-109. See text for details.

Under native conditions LDH shows an unfolding transition centered at ~54.7 ℃, and a steep decline is seen in the baseline above 60 °C.  Such a steep decrease of the baseline is normally associated with precipitation of the protein and examination of the sample after completion of the thermal scan confirmed that LDH precipitated during the DSC scan (○).  When a mixture of LDH and PDC-109 (1:0.625, w/w) was subjected to DSC analysis, the thermal transition peak of LDH was nearly unaltered, whereas the steeply declining region in the thermogram shifted towards higher temperatures (>70 °C) (●).  However, when the LDH to PDC-109 weight ratio was increased to 1:1, no precipitation of LDH was observed up to 75 ℃ (□).

### 3.4.6. PDC-109 Assisted Protection of Insulin Under Amyloidogenic Conditions

Under amyloidogenic conditions (e.g., acidic pH and high temperature) insulin molecules unfold partially and interact with each other to form linear aggregates or fibrils (Fig. 3.4A).  However, insulin samples which were subjected to similar conditions in the presence of PDC-109 failed to form such linear aggregates and showed native like homogenous distribution (Fig. 3.4B).  Inhibition of insulin fibrillation by PDC-109 was also confirmed by fluorometric assay of Thioflavin T binding to insulin fibrils (see below).

### 3.4.7. Inhibition of Insulin Fibrillation by PDC-109

Thioflavin T (ThT) is known to bind to amyloid fibrils.  Fluorescence emission spectra for the binding of ThT to insulin fibrils both in the absence and presence of PDC-109 are shown in Fig. 3.4.  ThT binding to insulin fibrils resulted in an increase in the intensity of fluorescence maximum of the probe (Fig. 3.4C), whereas in the presence of PDC-109 increase in the fluorescence intensity of ThT was found to be negligible (Fig. 3.4D), which is consistent with the ability of PDC-109 to prevent fibrillation of insulin, as suggested above.
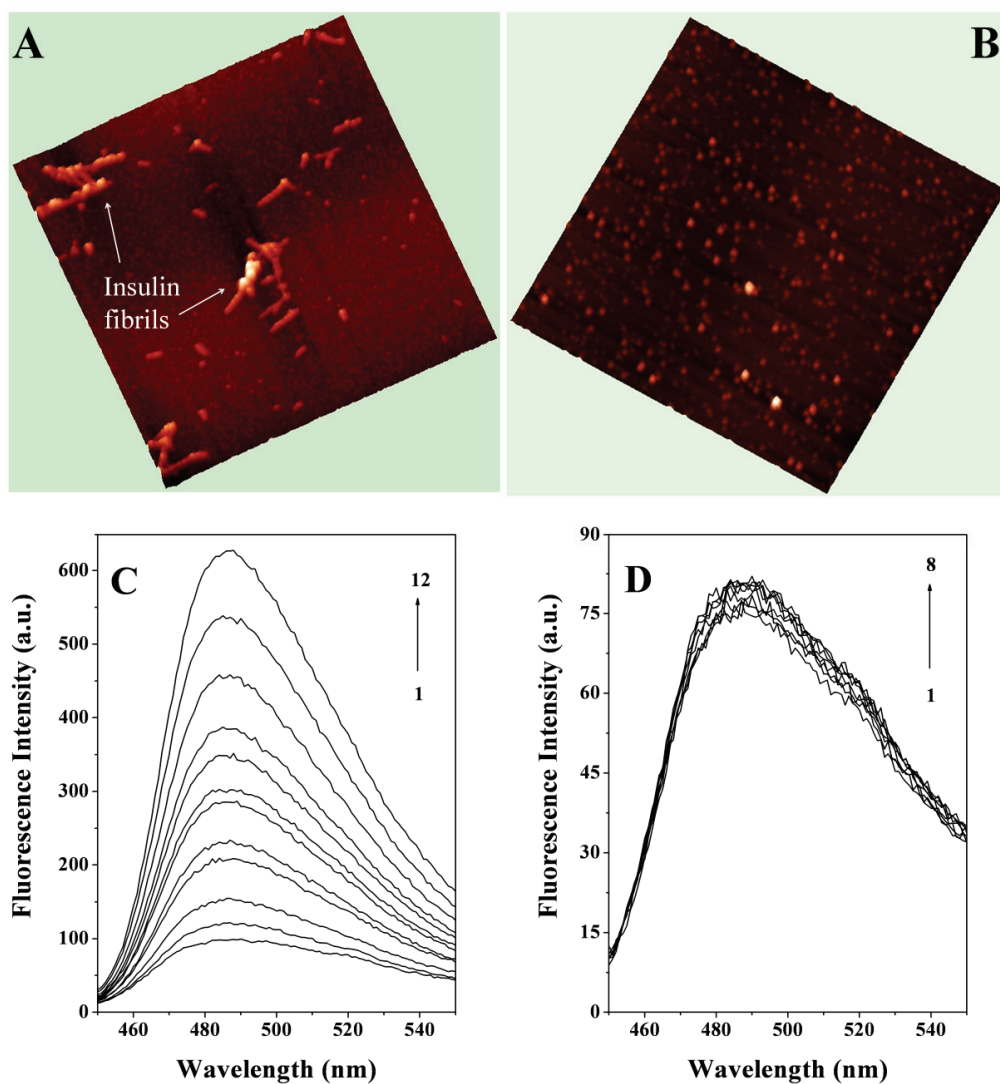
**Fig. 3.4: Inhibition of insulin fibrillization by PDC-109.** **A)** AFM image of insulin fibrils (0.5 mg/mL, pH 1.6) after incubation at 45 °C for 5 days (5 × 5 µm scale). **B)** Insulin subjected to similar treatment in the presence of 1.0 mg/mL PDC-109 (5 × 5 µm scale). **C)** Fluorometric assay for ThT binding to insulin fibrils. Spectrum 1 corresponds to ThT alone (0.1 mM) and spectra 2-12 correspond to those recorded in the presence of increasing concentrations of insulin. The highest insulin concentration was 6.45 µM (spectrum 12). **D)** ThT binding to insulin in the presence of PDC-109. Spectrum 1 corresponds to ThT alone (0.1 mM) and spectra 2-8 correspond to those recorded in the presence of increasing concentrations of insulin, which was preincubated with 1.0 mg/mL PDC-109. The highest concentration of insulin was 4.54 µM (spectrum 8).

### 3.4.8. PDC-109 Mediated Protection of Target Proteins Studied by AFM and Image Analysis

AFM images obtained at room temperature indicate that ADH shows a uniform size distribution and does not form large aggregates (Fig. 3.5A). Upon incubation at 48 °C fairly large aggregates are formed (Fig. 3.5B). However, when incubated at the same temperature in the presence of PDC-109, ADH did not form aggregated structures but remained homogeneous similar to the native protein (Fig. 3.5C).

In order to get more quantitative information from the AFM images, average FFT analysis was performed (Fig. 3.5E). Average FFT trace values for the native target proteins were observed to be very low. The maximum value obtained for native ADH was 0.75 nm (curve 1) which increased to 6.6 nm upon heat treatment because of the formation of large clumps (curve 2). The presence of PDC-109 significantly reduced the aggregation of ADH, resulting in reduced values of average FFT traces (curve 3). Similarly, distribution density histogram shows a size distribution in the range of 2-7 nm for native ADH (Fig. 3.5F, curve 1). Thermally induced aggregation resulted in an increase in the size distribution to 80-120 nm (curve 2). The size distribution again shifted towards lower values, viz., 4-10 nm (curve 3) in the presence of PDC-109, suggesting that this protein prevents the aggregation of the target proteins. Statistical parameters for the native enzyme, and enzyme subjected to heat treatment in the absence and presence of PDC-109 are presented in Table 3.1. Bearing ratio analysis also yielded similar interpretations (Fig. 3.6). Bearing ratio profile for native ADH reaches its maximum at ~10 nm and then gets saturated (curve 1). This suggests that maximum protein molecules in the sampled area have a size distribution lesser than 10 nm, which is in good agreement with distribution density histogram (Fig. 3.5F, curve 1). Heat-induced aggregation of target proteins resulted in a shift in the bearing ratio profile of these aggregates towards higher values. Bearing ratio profile for aggregated ADH was found to be saturated at about 140 nm (curve 2), which shifted towards lower
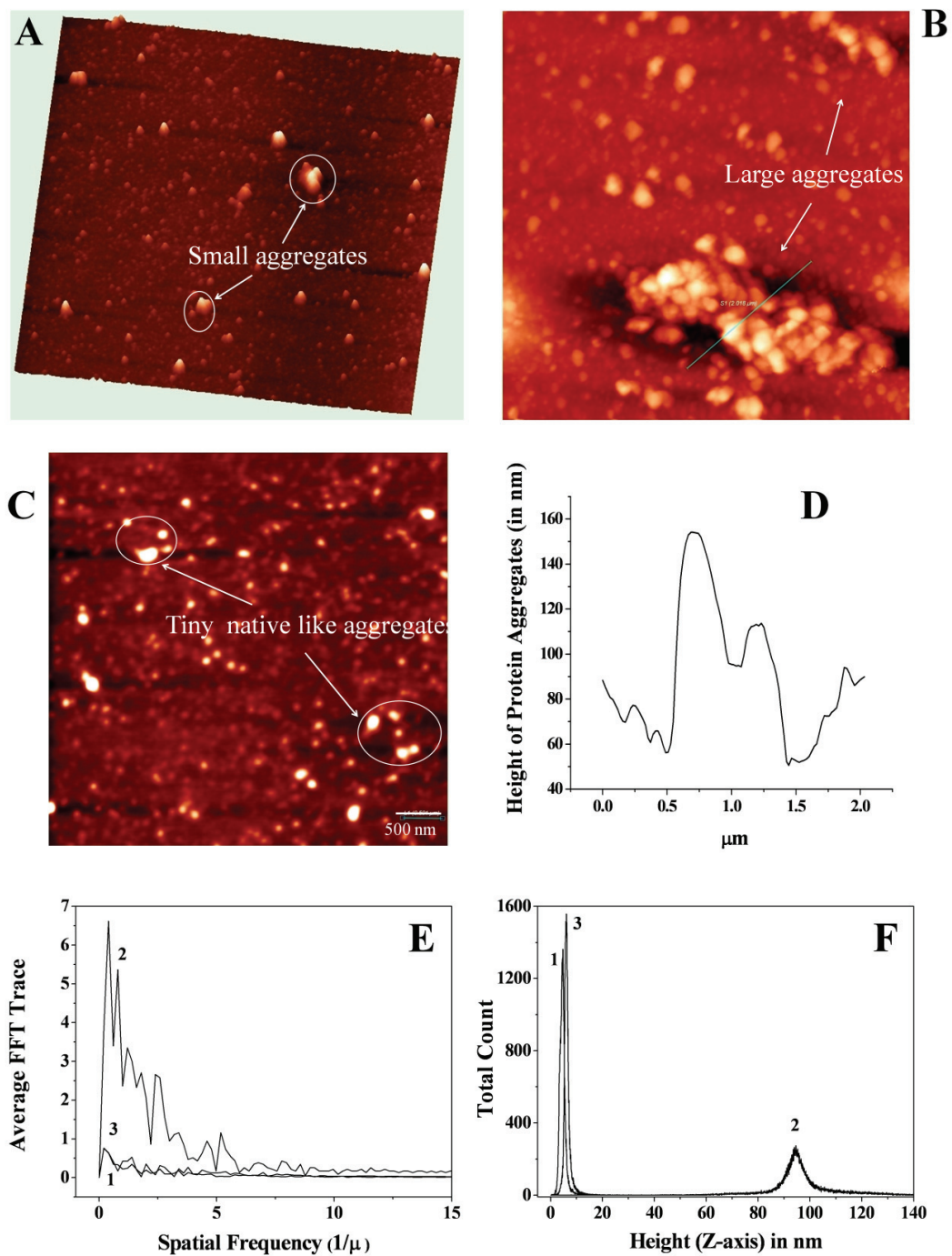
**Fig. 3.5: Prevention of thermal aggregation of ADH by PDC-109.**

**Table 3.1:** Parameters obtained from statistical analysis of AFM images of alcohol dehydrogenase under different experimental conditions.

| Sample | Amount of Sampling (pixels) | Maximum height (nm) | Mean height (nm) | Entropy |
|---|---|---|---|---|
| Native Enzyme | 65536 | 20.6 | 4.68 | 6.66 |
| Enzyme at 48 ºC | 65536 | 163.00 | 96.5 | 9.86 |
| Enzyme + PDC-109 (2:1; w/w) at 48 ºC | 65536 | 33.2 | 6.4 | 6.62 |
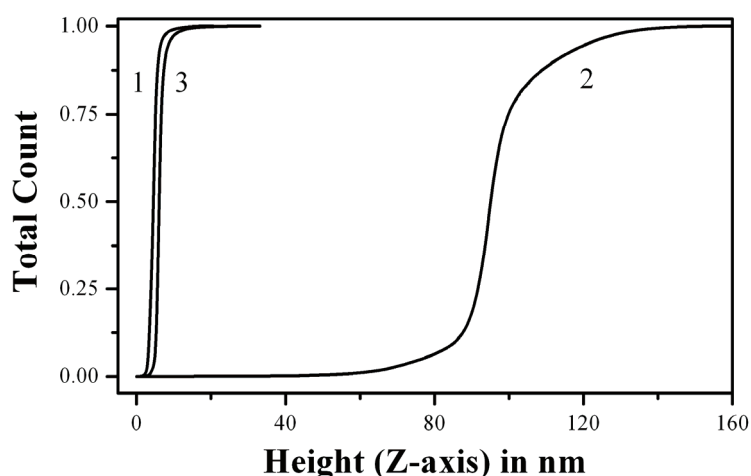


**Fig. 3.6: Bearing ratio profile for alcohol dehydrogenase (ADH).** (1) native enzyme, (2) ADH incubated at 48 ºC, (3) ADH incubated at 48 ºC in the presence of PDC-109 (2:1; w/w ratio).

**Fig. 3.5:** AFM images of 0.04 mg/mL ADH under native condition (**A**), upon heat treatment (**B**) and upon heat treatment in the presence of 0.02 mg/mL PDC-109 (**C**) are shown. Each image is 5 × 5 μM in size. **D)** Height profile of aggregated structure (marked in panel **B**). **E)** Average FFT analysis of AFM images of ADH: (1) native enzyme, (2) upon incubation at 48 ºC, (3) upon incubation at 48 ºC in the presence of PDC-109. **F)** Distribution density histogram analysis for ADH: (1) native enzyme, (2) upon incubation at 48 ºC, (3) upon incubation at 48 ºC in the presence of PDC-109. See text for details.

limit in the presence of PDC-109 and was found to be saturated at about 10 nm (curve 3), indicating that PDC-109 stabilizes ADH against thermal stress, thus exhibiting chaperone-like activity. Similar results were obtained when LDH was used as a target protein (Figs. S3.4 and S3.5).

### 3.4.9. PDC-109 Assisted Folding Arrest of Target Proteins

Results of studies aimed at investigating the effect of PDC-109 on the refolding of LDH are shown in Fig. 3.7A. Dilution resulted in the spontaneous refolding of completely denatured enzyme, whose activity reaches a maximum level and remains steady afterwards (curve 1). Inclusion of increasing concentrations of PDC-109 in the renaturation buffer resulted in folding arrest and it was observed to be concentration dependent, i.e., higher the concentration of PDC-109, more the arrest (curve 2-4). Extent of refolding at different concentrations of PDC-109 is shown in the form of a bar diagram in Fig. 3.7B. PDC-109 exhibited a similar effect on the refolding of G6PD (see Fig. S3.6).
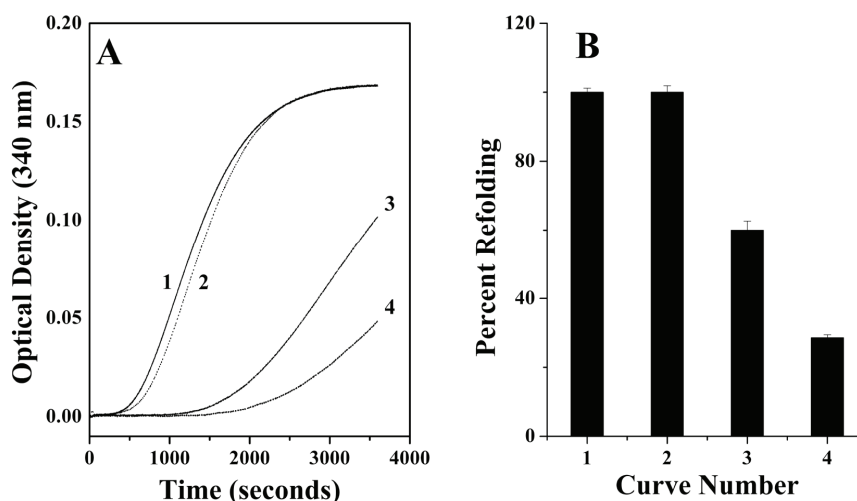


**Fig. 3.7: Refolding of LDH in the absence and presence of PDC-109.** **A**) LDH was refolded from completely unfolded state in the absence (curve 1) as well as presence different concentrations of PDC-109 in TBS-I buffer as indicated: 0.35 μM (curve 2), 3.5 μM (curve 3) and 5.36 μM (curve 4). **B)** Bar diagram showing extent of refolding under different conditions.

### 3.4.10. Inhibition of Chaperone Activity of PDC-109 by Phosphorylcholine and Choline

The effect of PrC binding on the chaperone-like activity of PDC-109 was assessed by turbidimetry and the results obtained are presented in Fig. 3.8A. Incubation of ADH at 48 °C resulted in a rapid increase in the turbidity of the solution, which reached a maximum and remained steady thereafter (curve 1). Presence of PDC-109 resulted in a significant reduction in the aggregation, which was observed to be less than 50% as compared to that of the native enzyme (curve 2). However, addition of increasing concentrations of PrC along with PDC-109 yielded a proportional increase in the extent of aggregation (curve 3-5). A bar diagram representing percent aggregation of ADH under different conditions is shown in Fig. 3.8B. LDH also showed similar behavior in the presence of PrC (see Fig. S3.7). Choline binding also had a similar effect on the chaperone activity of PDC-109 (see Fig. S3.8).
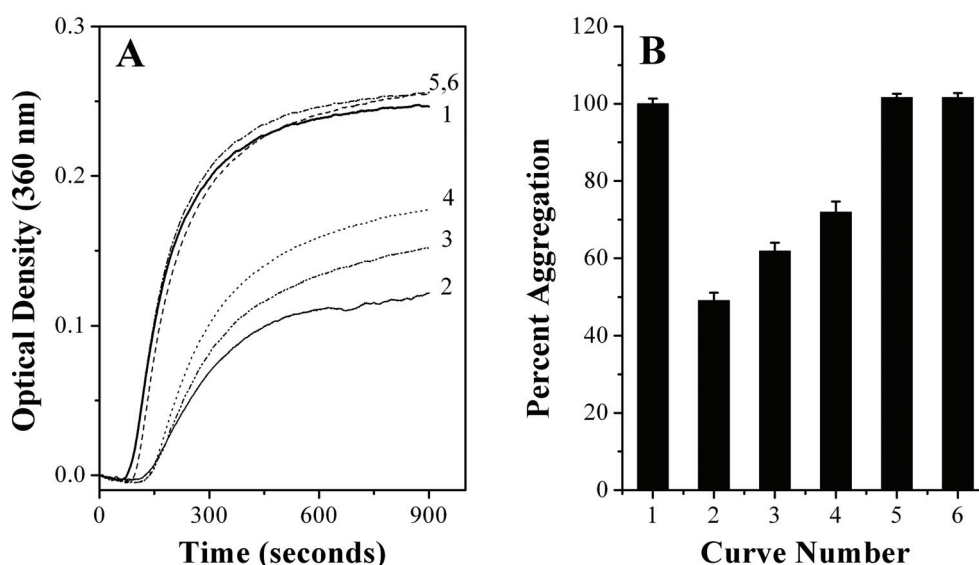


**Fig. 3.8: Effect of phosphorylcholine binding on the chaperone-like activity of PDC-109. A**) Aggregation profiles of ADH in the absence and presence of PDC-109 and phosphorylcholine. The samples are: (1) ADH at 48 °C, (2) ADH + PDC-109, (3) ADH + PDC-109 + 0.01 mM PrC, (4) ADH + PDC-109 + 0.05 mM PrC, (5) ADH + PDC-109 + 0.1 mM PrC and (6) ADH + 0.05 mM PrC. Concentrations of ADH and PDC-109 were 0.06 mg/mL and 0.04 mg/mL, respectively. **B**) Bar diagram representing the aggregation of ADH in the different samples.

### 3.4.11. Inhibition of Chaperone Activity of PDC-109 in High Ionic Strength Buffer

Incubation of ADH at 48 ºC resulted in an increase in the turbidity of the solution, which reached a maximum and then remained constant (Fig 3.9A, curve 1). However, incubation of ADH with PDC-109 prior to assay resulted in a significant decrease in the turbidity and it was observed to be less than 20% of the turbidity observed with the sample in the absence of PDC-109 (curve 2). A bar diagram indicating the relative aggregation of the different samples is given in Fig. 3.9B.
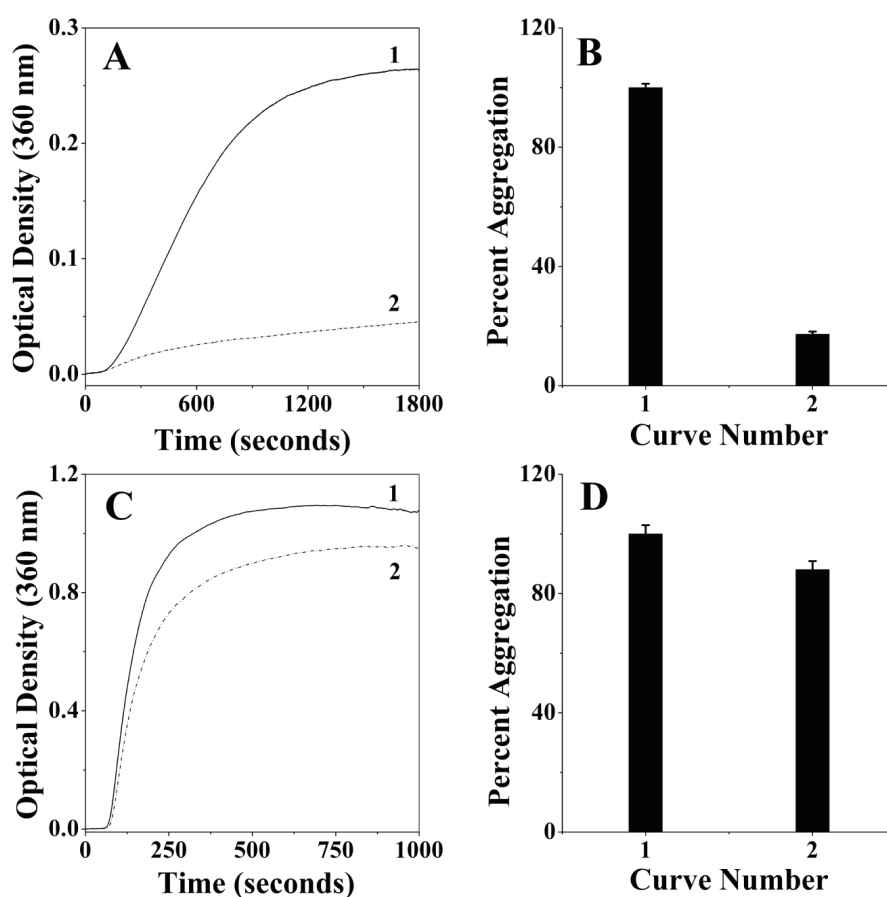


**Fig. 3.9:  Effect of High ionic strength on chaperone-like activity of PDC-109.  A)** Aggregation profile of native ADH at 48 ºC in 10 mM MOPS buffer in the absence (curve 1) and presence of 0.027 mg/mL PDC-109 (curve 2). **B)** Bar diagram representing level of aggregation in 10 mM MOPS buffer.  **C)** Aggregation profile of native ADH at 48 ºC in 10 mM high ionic strength MOPS buffer (containing 50 mM EDTA and 0.5 M NaCl) in the absence (curve 1) and presence of 0.027 mg/mL PDC-109 (curve 2).  **D)** Bar diagram representing level of aggregation in 10 mM high ionic strength MOPS buffer. ADH concentration was 0.2 mg/mL for all the experiments.

ADH which was incubated at 48 ºC in high ionic strength buffer (containing 50 mM EDTA and 0.5 M NaCl) yielded a solution that is significantly more turbid as compared to the sample that was incubated in 10 mM buffer without EDTA and NaCl (Fig 3.9C, curve 1). Addition of PDC-109 (in high ionic strength buffer) to ADH did not significantly decrease the aggregation (curve 2). The relative aggregation of different samples is presented as a bar diagram in Fig. 3.9D.

## 3.4.12. Sequence Alignment of PDC-109 with Other Chaperones and Seminal Plasma Proteins

Comparison of the primary structure of PDC-109 with that of well-established chaperone proteins such as α-synuclein and α-crystallin revealed significant sequence similarity. All the sequences were aligned across their entire length (global alignment) and respective alignment parameters are listed in Table 3.2. Pairwise alignment profile of PDC-109 with α-synuclein, a well known chaperone protein, is shown in Fig. 3.10. It is clear from these data, that PDC-109 shares appreciable sequence homology with other well-known chaperone proteins.

**Table 3.2:** Sequence homology comparison for PDC-109 with different well-known chaperone like proteins.

| Protein | PDB code | Organism | Open gap penalty | Gap extension penalty | % Identity | % Similarity |
|---------|----------|----------|------------------|-----------------------|------------|--------------|
| α-Synuclein | 1XQ8 | *Homo sapiens* | 5 | 0.6 | 20.5 | 35.1 |
| α-Crystallin | AAB33370 | *Homo sapiens* | 1 | 0.1 | 21.3 | 31.4 |

```
PDC-109 (1-38)          1                  DQDEGV--STEPTQDGPAE-LPEDEECVFPFVYRNRKHFDC

                                           ...|||  :.|.|:.|.|.||  ..:.:|.|    :|...|..:.
α-Synuclein (1-47)      1  MDVFMKGLSKAKEGVVAAAEKTKQGVAEAAGKTKEGV---LYVGSKTKEG


PDC-109 (39-71)        39  TVHGSLFPWCSLDADY-------VG-----RWKYCAQR--DYAKCV---F

                                           :|||.    .::  |:.        ||     .....||:  :.|..:    .
α-Synuclein (48-92)    48  VVHGV----ATV-AEKTKEQVTNVGGAVVTGVTAVAQKTVEGAGSIAAAT


PDC-109 (72-109)       72  PFIYG---GKKYETCTKIGSMW-MSWCSLSP-N--YD--KDRAWK-YC

                                           .|:..   ||..|...:.|.:.  |     .:.| |  |:  .:.::: |.
α-Synuclein (93-139)   93  GFVKKDQLGKNEEGAPQEGILEDM---PVDPDNEAYEMPSEEGYQDYEPE


PDC-109              110        109

α-Synuclein         140 A      140
```
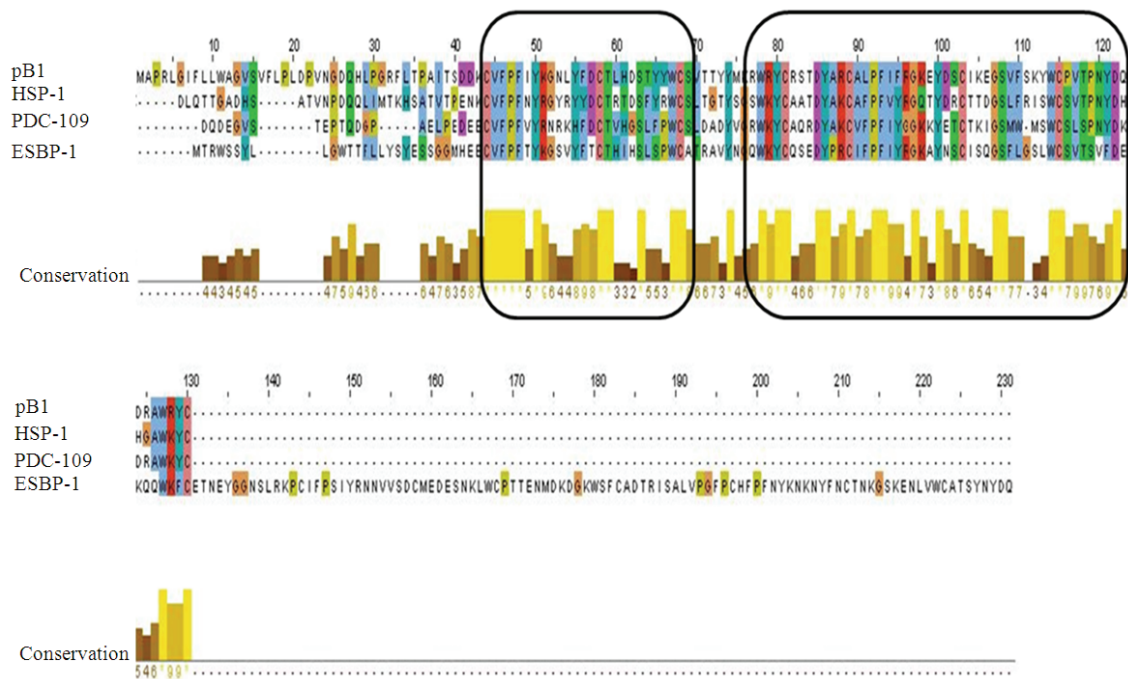
**Fig. 3.10:  Pair-wise alignment of PDC-109 with human α-synuclein.**  Alignment was done using the EMBOSS suite of software with Eblosum40 scoring matrix.

PDC-109 also shares good sequence homology with seminal plasma proteins from other species such as HSP-1 (horse), seminal plasma protein pB1 (*Sus scrofa)* and epididymal sperm binding protein 1 (*Homo sapines*).  All the sequences were aligned across their entire length (global alignment) and respective alignment parameters are mentioned in Table 3.3. Figure 3.11 shows the alignment of PDC-109 with different seminal plasma proteins and the conserved regions are shown in the form of a bar diagram just below the aligned sequences.  These data clearly demonstrate that PDC-109 shares appreciable sequence homology with other seminal plasma proteins.

**Table 3.3:** Results of sequence alignment of PDC-109 with other seminal plasma proteins.

| Seminal plasma protein | PDB code | Organism | Open gap penalty | Gap extension penalty | % Identity | % Similarity |
|---|---|---|---|---|---|---|
| HSP-1 | P81121 | Horse | 5 | 0.2 | 46.4 | 61.6 |
| Epididymal sperm binding protein 1 | NP_071425 | *Homo sapiens* | 5 | 0.2 | 24.3 | 32.6 |
| Seminal plasma protein pB1 | NP_998997 | *Sus scrofa* | 5 | 0.2 | 41.6 | 61.3 |



**Fig. 3.11: Clustal-W2 multiple sequence alignment of PDC-109 with other seminal plasma proteins.** Alignment was done with the primary structures of equine HSP-1, porcine seminal plasma protein pB1 and human epididymal sperm binding protein 1 (ESBP-1). Conserved regions are depicted in a bar diagram, just below the aligned sequences. Regions that are highly conserved have been shown in boxes.

## 3.5. Discussion

Molecular chaperones are a diverse class of proteins which play a crucial role in cell physiology both under normal and stressful conditions, by assisting proper folding of newly synthesized proteins as well as misfolded ones. The presence of chaperone proteins in mammalian seminal plasma has not been established so far; however, several somatic and germline specific molecular chaperones such as calmegin, calnexin etc. have been identified in the male germline (Miller and Al-Harbi, 1992a; Bergeron *et al.*, 1994; Ikawa *et al.*, 1997; Mitchell *et al.*, 2007). The present studies demonstrate that the major protein of bovine seminal plasma, PDC-109 can function as a molecular chaperone. To the best of our knowledge, this is the first study reporting chaperone-like activity of a seminal plasma protein. *In vitro* experiments show functional similarities between PDC-109 and several other well known chaperone proteins such as α-crystallin, spectrin etc.

The results of the present study show that presence of PDC-109 not only provides protection to target proteins under stress conditions but also directs native proteins to a better conformation even under physiological conditions. Aggregation prone proteins such as G6PD may also be present in partially aggregated conformations, even under native conditions. PDC-109 appears to interact with such proteins and assist them to a better, functionally active conformation. This is evident from Fig. 3.1A, where the activity of G6PD in the presence of PDC-109 (at 4 ℃) was observed to be higher than its activity under native conditions, in the absence of PDC-109. CD measurements show that the secondary structure of this protein is largely retained in the presence of PDC-109 even at elevated temperatures, whereas in the absence of PDC-109 the secondary structure is altered significantly (Fig. 3.2). This shows that PDC-109 is able to protect G6PD from thermal unfolding and provides an explanation for the retention of its activity at elevated temperatures in the presence of PDC-109. Natively unfolded

proteins such as α-synuclein have been reported to be good candidates for chaperone like-activity because of the flexibility of their structure, which allows them to interact with other proteins in an effective manner (Kim *et al.*, 2000). PDC-109 also possesses a significant amount of unordered structure (Gasset *et al.*, 1997; Wah *et al.*, 2002), which is consistent with its ability to function as a molecular chaperone.

Results of turbidimetric studies to monitor thermally-induced aggregation of ADH and LDH suggest that PDC-109 functions as a chaperone in a concentration dependent manner, i.e., the chaperone activity increases with increasing concentrations of PDC-109 (Fig. 3.1C and Fig. S3.2). Since isozymes of LDH such as LDH-$C_4$ participate in mammalian sperm capacitation process (O'Flaherty *et al.*, 2002; Duan and Goldberg, 2003), the chaperone-like activity of PDC-109 observed with LDH *in vitro* may be relevant to a similar function under *in vivo* conditions.

AFM experiments provide further strong evidence for the chaperone like activity of PDC-109. To the best of our knowledge, this is the first time that the potential of image processing of AFM data, demonstrating clear-cut differences between aggregated and disaggregated proteins, has been utilized to probe the chaperone like activity of any protein. Both ADH and LDH which were exposed to high temperature form large aggregates as can be judged by larger values of average FFT and were distributed mostly in low frequency domains which means they were spaced apart, hence were distributed inhomogenously (Fig. 3.5E, curve 2). However, protein molecules subjected to similar treatment in the presence of PDC-109 were found to be distributed almost equally in all frequency domains, similar to the native protein molecules (Fig. 3.5E, curves 1 & 3). Uniform distribution of target protein molecules which have been subjected to heat treatment in the presence of PDC-109 is also evident from the lesser entropy values observed for such samples, whereas higher entropy values obtained with aggregated proteins suggest their random distribution (Table 3.1). The present study also explores the potential of PDC-109 to prevent the fibrillation of amyloid prone

proteins such as insulin. This can be of promising significance because some of the proteins of the seminal plasma have been identified to be prone to amyloidogenesis (Pitkänen *et al.*, 1983; Münch *et al.*, 2007).

Experiments aimed at investigating the effect of PDC-109 on the refolding of fully denatured target proteins suggest that PDC-109 binds to unfolded substrate proteins and forms stable complexes with them. This prevents their irreversible aggregation, but does not assist their refolding to the native form, i.e., PDC-109 binding results in a *folding arrest* of the target proteins (Fig. 3.7). In this respect, PDC-109 is similar to spectrin and Hsp90 (Yonehara *et al.*, 1996; Chakrabarti *et al.*, 2001). However, unlike these two chaperone proteins, PDC-109 does not assist the refolding of target proteins in the presence of ATP (data not shown). Although this folding arrest of substrate proteins by PDC-109 suggests that it creates a reservoir of folding intermediates of the substrate proteins (Ehrnsperger *et al.*, 1997; Nakamoto and Vigh, 2007), it should be noted that unlike other such proteins (e.g., murine Hsp25, yeast Hsp26 etc.), which cannot prevent inactivation of the substrate proteins, under stress conditions the activity of target proteins in the presence PDC-109 was found to be comparable to that of native form (Fig. 3.1A).

Binding of phosphorylcholine or choline to PDC-109 resulted in a complete inhibition of its chaperone-like activity in a concentration dependent manner (Fig. 3.8, Fig. S3.7 and Fig. S3.8). Since the specific binding of these ligands to the FnII domains of PDC-109 leads to dissociation of the polydisperse aggregates of the protein, resulting in the formation of dimeric species (Gasset *et al.*, 1997), it is likely that the ligand binding site or the aggregation state of the protein is important for the chaperone activity of PDC-109. In order to understand this better, the effect of high ionic strength of the medium – which is known to result in a dissociation of the polydisperse aggregates of PDC-109 (Gasset *et al.*, 1997) – was studied on the chaperone-like activity of the protein. These experiments indicated that the chaperone-like activity of

PDC-109 is reduced significantly in high ionic strength medium (Fig. 3.9), suggesting that the state of aggregation is an important factor for the chaperone-like activity of this protein.
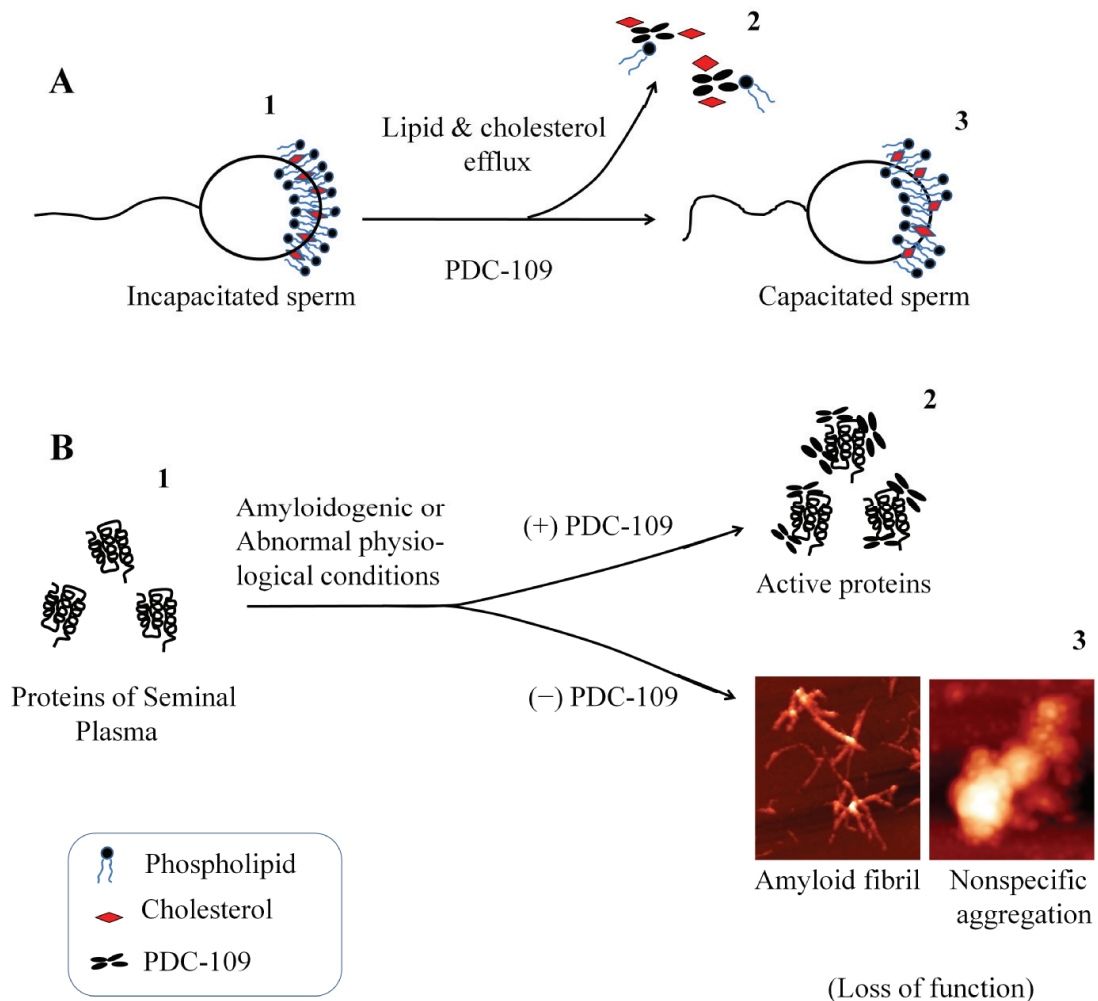


**Fig. 3.12:  A Schematic model for PDC-109 induced sperm capacitation.  A)** PDC-109 induces efflux of cholesterol and choline phospholipids, which is necessary for sperm capacitation.  Epididymal spermatozoa (1), efflux particles made up of PDC-109, cholesterol and choline phospholipids (2), and capacitated sperm (3) are shown. **B)** PDC-109 functions as a molecular chaperone and stabilizes seminal plasma proteins.  Seminal plasma proteins (1), are stabilized in the presence of PDC-109 under stress conditions (2), which in the absence of PDC-109 may form nonspecific aggregates or amyloid fibrils (3).

Pair-wise sequence alignment studies show significant sequence homology and analogy between PDC-109 and other well known chaperone-like proteins (Table 3.2 and Fig. 3.10). These observations are consistent with the present findings, which demonstrate that PDC-109 exhibits chaperone-like activity against a range of target proteins. A search for seminal plasma proteins that are homologous to PDC-109 showed moderate to high homology with proteins from different species such as horse, pig, human etc (Table 3.3 and Fig. 3.11) and indicates that these proteins may also exhibit chaperone-like activity *in vitro*.

On the basis of experimental evidences presented above, a possible mechanism for the involvement of PDC-109 in sperm capacitation process can be proposed. It has been demonstrated by Manjunath and coworkers that PDC-109 induces the efflux of cholesterol and choline phospholipids from sperm membrane, which facilitates sperm capacitation (Thérien *et al.*, 1998; Moreau *et al.*, 1998). The present model suggest that besides inducing phospholipid/cholesterol efflux, PDC-109 directs the aggregated and misfolded proteins of seminal plasma towards a functionally active, folded conformation, which can then participate in fertilization process in a better way. A schematic representation of this hypothesis is shown in Fig. 3.12.

In summary, the results presented in this chapter provide several lines of evidence demonstrating that PDC-109 exhibits chaperone-like activity, which may be relevant to sperm capacitation. Biochemical assays and biophysical investigations have shown that PDC-109 effectively protects a variety of target proteins from denaturation induced by heat, chaotropes and low pH. AFM studies have shown that PDC-109 prevents fibrillation of insulin under amyloidogenic conditions, which is of considerable significance since amyloidogenesis is a serious problem during sperm maturation in certain species. Overall, these results demonstrate that PDC-109 functions as a molecular chaperone, suggesting that it may assist the proper folding of proteins in bovine seminal plasma in vivo.

# Chapter 4

## Correlation of Membrane Binding and Hydrophobicity to the Chaperone-Like Activity of PDC-109
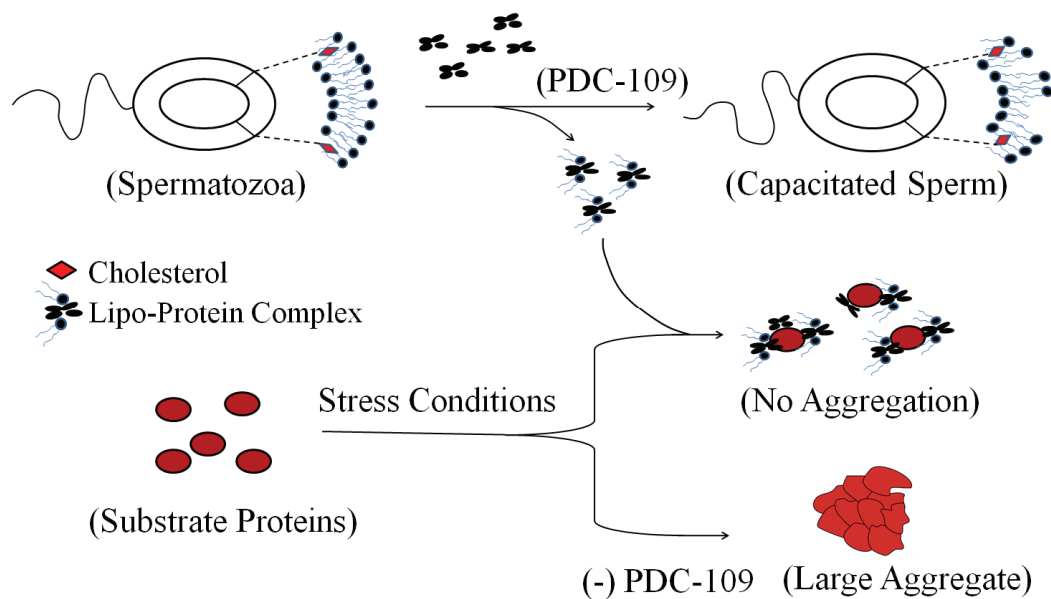
## 4.1. Abstract

The major protein of bovine seminal plasma, PDC-109 binds to choline phospholipids present on the sperm plasma membrane upon ejaculation and plays a crucial role in the subsequent events leading to fertilization. PDC-109 also shares significant similarities with small heat shock proteins and exhibits chaperone-like activity (CLA). Although the polydisperse nature of this protein has been shown to be important for its CLA, knowledge of other factors responsible for such an activity is scarce. Since surface exposure of hydrophobic residues is known to be an important factor which modulates the CLA of chaperone proteins, in the present study the surface hydrophobicity of PDC-109 was probed using bisANS and ANS. Further, effect of phospholipids on the structure and chaperone-like activity of PDC-109 was studied. Presence of DMPC was found to increase the CLA of PDC-109 significantly, which could be due to considerable exposure of hydrophobic regions on the lipid-protein recombinants, which can interact productively with the nonnative structures of the target proteins, resulting in their protection. However, inclusion of DMPG instead of DMPC did not significantly alter the CLA of PDC-109, which could be due to the lower specificity of PDC-109 for DMPG as compared to DMPC. Cholesterol incorporation in DMPC membranes led to a decrease in the CLA of PDC-109-lipid recombinants, which could be attributed to reduced accessibility of hydrophobic surfaces to the substrate protein(s). These results underscore the relevance of phospholipid binding and hydrophobicity to the chaperone-like activity of PDC-109.

## 4.2. Introduction

Although, the studies presented in Chapter 3 demonstrated that PDC-109 exhibits chaperone-like activity (CLA) *in vitro* and established that polydispersity is an important factor for its CLA, a knowledge of other factors responsible for the CLA is scarce.    Several studies suggest the involvement of surface exposed hydrophobic residues on various chaperones, in their association with partially unfolded proteins (Das and Surewicz, 1995; Datta and Rao, 1999; Reddy *et al.*, 2000).    The exposure of hydrophobic regions on the surface of α-crystallin has been attributed to be responsible for enhanced CLA, suggesting the role of hydrophobicity in the chaperone like function of sHSP (Das and Surewicz, 1995; Datta and Rao, 1999; Reddy *et al.*, 2000).    4,4'-Dianilino-1,1'-binaphthyl-5,5'-disulphonic acid (bisANS) and 8-anilinonaphthalene sulphonic acid (ANS) have been widely used to measure the surface hydrophobicity of various proteins.    Binding of PDC-109 and its domain B to phospholipid membranes and partial insertion of sections of the protein, including a segment containing Trp93 into the hydrophobic interior of membranes indicated the presence of hydrophobic stretches in this protein (Ramakrishnan *et al.*, 2001; Greube *et al.*, 2001; Anbazhagan *et al.*, 2008; Damai *et al.*, 2009).    In view of this in the present study we have investigated the binding of bisANS and ANS with PDC-109 using isothermal titration calorimetry and steady state fluorescence spectroscopy, respectively.    Further, the effect ANS binding on the conformation and CLA of PDC-109 was also investigated.    CD and FTIR studies indicate that PDC-109 undergoes significant conformational changes upon membrane binding (Wah *et al.*, 2002; Gasset *et al.*, 2000; Gasset *et al.*, 1997).    Such conformational flexibility may be relevant to the CLA of PDC-109 wherein it interacts with target proteins to protect them against various types of stress (Chapter 3).    Therefore it is of interest to study the possible role of such interactions on the CLA, which was investigated with a number of target proteins such as alcohol dehydrogenase

(ADH), carbonic anhydrase (CA) and lactate dehydrogenase (LDH). Presence of dimyristoylphosphatidylcholine (DMPC) – which is specifically recognized by PDC-109 – resulted in a multifold increase in the CLA of the protein. ANS and bisANS binding to DMPC−PDC-109 mixture revealed enhanced exposure of hydrophobic surfaces, which could be responsible for such a dramatic change in the CLA. Cholesterol which makes lipid membranes in the liquid-crystalline phase more rigid was found to decrease the CLA of PDC-109/DMPC recombinants. Overall, the present results provide a detailed characterization of the hydrophobicity of PDC-109 and demonstrate that phospholipid binding nature of PDC-109 could also be relevant to its chaperone-like activity *in vivo*.

## 4.3. Materials and Method

### 4.3.1. Materials

ANS, bisANS, aldolase, carbonic anhydrase and DEAE Sephadex A-25 were from Sigma (St. Louis, MO). Sephadex G-50 (superfine) was obtained from Pharmacia (Uppsala, Sweden). DMPC, DMPG and cholesterol were purchased from Avanti Polar Lipids (Alabster, AL). LDH, ADH, tris base and other chemicals were purchased from local suppliers and were of the highest purity available. PDC-109 was purified by a combination of gel filtration on Sephadex G-50 and affinity chromatography on DEAE Sephadex A-25 as described in Chapter 2. The purified protein was dialyzed extensively against 50 mM Tris buffer, 0.15 M NaCl, 5 mM EDTA, pH 7.4 (TBS-I) and stored at 4 °C. All experiments were performed in TBS-I unless stated otherwise.

### 4.3.2. Isothermal Titration Calorimetric Study of bisANS Binding to PDC-109

The binding of bisANS to PDC-109 was studied at 30 $^o$C by ITC using a Microcal VP-ITC instrument (MicroCal LLC, Northampton, MA, USA). In a typical experiment, 25 aliquots (5 μL each) of 5 mM bisANS were injected consecutively from the syringe into the calorimeter cell containing 25 μM of PDC-109. To minimize the contribution from heat of dilution to the measured binding enthalpy, the ligand and protein solutions were prepared in the same buffer. Injections were made at intervals of 300 sec, and to ensure proper mixing after each injection, a constant stirring speed of 300 rpm was maintained during the experiment. Control experiments were performed by titrating bisANS into the buffer solution and the resulting heat changes were subtracted from the measured heats of binding. Solutions were degassed under vacuum prior to their use in the calorimetric titrations. The titration data were analyzed by using the *sequential binding model* available in the Origin software provided by MicroCal, which yielded the equilibrium association constant ($K_a$), enthalpy ($\Delta H$), entropy ($\Delta S$) and the stoichiometry of binding, ($n$, which corresponds to the number of bisANS molecules bound per molecule of PDC-109).

### 4.3.3. Fluorescence Studies on ANS Binding to PDC-109

Binding of ANS to PDC-109 was investigated by fluorescence titrations monitoring the fluorescence intensity of the probe. Measurements were performed at 25 $^o$C using a Spex Fluoromax-4 spectrofluorimeter with excitation and emission slits of 2 and 10 nm, respectively. Titrations were performed by adding small aliquots of ANS from a 1 mM stock solution to 2.0 mL of PDC-109 (OD$_{280}$ = 0.05) in the cuvette. Samples were excited at 350 nm and emission spectra were recorded between 400 and 600 nm. All the binding data reported here correspond to the average values obtained from two independent titrations. Fluorescence data were corrected for dilution effects and for fluorescence of free ligand determined in parallel titrations without the protein.

**4.3.4. Effect of ANS Binding on the Conformation and Chaperone-like Activity of PDC-109**

A 6.0 mg/mL solution of PDC-109 was incubated with 10 mM ANS for 30 minutes at ambient temperature. The solution was passed through a Sephadex G-50 column [(10 × 0.5) cm] to remove unbound ANS. Protein concentration in the eluted fractions was determined by Lowry assay (Lowry *et al.*, 1951), whereas the concentration of bound ANS was estimated using its molar absorption coefficient of $5 \times 10^3$ $M^{-1}.cm^{-1}$ at 350 nm. The effect of ANS binding on the secondary structures of PDC-109 was analyzed by CD spectroscopy using a Jasco J-810 spectropolarimeter fitted with a thermostatted cell holder and interfaced to a thermostatic waterbath. Far-UV CD spectra were recorded at 25 °C using a protein concentration of 0.12 mg/mL at a scan rate of 50 nm/min using a 2 mm pathlength quartz cell and a slit width of 2 nm. All spectra were corrected with appropriate buffer blanks and the resulting data are expressed as mean residual ellipticities.

Effect of ANS binding on the CLA of PDC-109 was investigated by the LDH aggregation assay. In a typical experiment, 0.15 mg/mL of LDH was mixed with a fixed concentration (0.05 or 0.075 mg/mL) of native PDC-109 and allowed to stand for 5 minutes at room temperature and then incubated at 48 ºC. Heat induced aggregation of the enzyme was assessed by monitoring the increase in sample turbidity at 360 nm as a function of time. Experiments with ANS bound PDC-109 were performed at similar concentrations as mentioned above and then compared with the activity of the native protein. Effect of ANS alone on the aggregation of the target protein was used as a positive control. Aggregation of native LDH was taken as 100% and the aggregation of other samples was normalized with respect to it.

### 4.3.5. Phospholipid Induced Modulation of the CLA and Tertiary Structure of PDC-109

Unilamellar vesicles of DMPC and DMPG were used in studies aimed at investigating the effect of phospholipids on the CLA of PDC-109. Vesicles were prepared by taking a small amount (~0.5 mg) of the appropriate phospholipid in a glass test tube, dissolving it in ca. 100-200 μL of dichloromethane or dichloromethane/methanol mixture, followed by evaporation of the solvent under a continuous stream of nitrogen gas and vacuum desiccation. The lipid film thus obtained was hydrated with an appropriate volume of TBS-I to give the desired concentration of phospholipid (~1 mM) and then subjected to bath sonication (30 – 60 minutes), which yielded a transparent solution, indicating the formation of unilamellar vesicles. To investigate the effect of phospholipid binding on the protein conformation, PDC-109 (1.0 mg/mL) was incubated with unilamellar vesicles of DMPC or DMPG (final concentration: 0.1 mM) for 5 minutes and then CD spectra were recorded at room temperature on a Jasco J-810 spectropolarimeter.

Chaperone activity was assessed by standard aggregation assays, where heat induced aggregation of target proteins [LDH, ADH and carbonic anhydrase (CA)] was monitored as light scattering, as a function of time. To study the effect of phospholipid binding on the CLA of PDC-109, phospholipids (0-2 μM) were mixed with a fixed concentration of PDC-109 and allowed to bind for 5 minutes. LDH was pre-incubated with the appropriate PDC-109/phospholipid mixture for 5 minutes and then placed in a spectrophotometer cuvette to record the light scattering of the solutions. Aggregation of native LDH was taken as 100% and the aggregation of other samples was normalized with respect to that of the native enzyme. Concentrations of PDC-109, target proteins and the lipids as well as the temperature used in different assays are given in the captions to the figures presenting the results of the experiments.

### 4.3.6. BisANS Binding to PDC-109, Phospholipid Vesicles and PDC-109/Phospholipid Mixtures

Interaction of bisANS with native PDC-109, phospholipid vesicles (DMPC or DMPG) and PDC-109/phospholipid mixtures was investigated at 25 ºC by steady-state fluorescence spectroscopy. Unilamellar vesicles of DMPC and DMPG were prepared by bath sonication as described above. The following samples were prepared: bisANS in buffer; bisANS + PDC-109; bisANS + DMPC; bisANS + DMPG; bisANS + DMPC + PDC-109; bisANS + DMPG + PDC-109. The concentration of PDC-109, phospholipid and bisANS in individual samples were fixed at 0.05 mg/mL, 5 μM and ~12 μM, respectively. For the last two samples, PDC-109 and phospholipid vesicles were mixed and allowed to stand at room temperature for 10 minutes before the addition of bisANS. Fluorescence measurements were performed on a Spex-Fluoromax-4 fluorescence spectrometer. Samples were excited at 385 nm and emission spectra were recorded between 395 and 650 nm. Slit widths of 3 and 5 nm were used for the excitation and emission monochromators, respectively.

### 4.3.7. ANS Binding to PDC-109 and PDC-109/Phosphorylcholine Mixtures

Interaction of ANS with native PDC-109 and PDC-109/PrC mixtures was investigated at 25 ºC by steady-state fluorescence spectroscopy. ANS (50 μM) was added to the following solutions in TBS-I: 10 mM PrC, 0.05 mg/mL PDC-109, and 0.05 mg/mL PDC-109 containing 10 mM PrC. After incubation for 10 minutes, samples were excited at 350 nm and emission spectra were recorded between 450 and 600 nm using a Jobin-Yvon Spex Fluoromax 4 fluorescence spectrometer. Slit widths of 2 and 10 nm were used for the excitation and emission monochromators, respectively.

## 4.3.8. Effect of Cholesterol Incorporation in the Phospholipid Membrane, on the CLA

Unilamellar vesicles of DMPC and DMPC/cholesterol (4:1, mol/mol) were prepared by bath sonication as described above.  CA was used as the target protein and the CLA was monitored by using standard aggregation assays, where heat induced aggregation of the target protein was recorded as light scattering at 360 nm.  In a typical experiment, 0.2 mg/mL of CA was incubated with a fixed concentration of PDC-109 (0.2 mg/mL) for 5 minutes at room temperature and the mixture was then subjected to heat stress by incubating for one hour at 52 ºC.  To investigate the effect of cholesterol incorporation in DMPC vesicles on the CLA of PDC-109, mixtures of DMPC and PDC-109, or DMPC, cholesterol and PDC-109 (containing 5 µM of respective phospholipid and 0.2 mg/mL of PDC-109) were pre-incubated with CA for 5 minutes and then the assay was performed in a similar way as described above.  Aggregation profiles of the two mixtures were compared in order to assess the effect of cholesterol incorporation on the CLA of PDC-109.

## 4.3.9. Effect of DMPC and DMPC/Cholesterol Mixture on the CLA of PDC-109: AFM studies

Carbonic anhydrase was used as a target protein in the AFM studies aimed at investigating the effect of DMPC or DMPC/cholesterol on the CLA of PDC-109. Samples of native CA (0.2 mg/mL) and CA–PDC-109 mixture (1:1 ratio, w/w) were prepared by incubating them at 52 °C in a dry bath for 1 hour.  To probe the effect of DMPC or DMPC/cholesterol binding on the CLA of PDC-109, a mixture containing CA, PDC-109 and DMPC (or DMPC/cholesterol; 4:1, mol/mol) was prepared and incubated at 52 °C for 1 hour.  Here, PDC-109 was first incubated with DMPC or DMPC/cholesterol mixture for 5 minutes and then CA was added to obtain the ternary mixture.  The final concentrations of CA, PDC-109 and DMPC in the above mixture

were 0.2 mg/mL, 0.2 mg/mL and 5 μM, respectively. A 20-30 μL aliquot of the respective sample was carefully deposited on a freshly cleaved mica sheet (1 cm × 1 cm) and allowed to dry for 20-30 minutes, rinsed with HPLC grade water, dried and transferred to the AFM stage. Imaging was performed in Semi-Contact mode using a SOLVER PRO-M atomic force microscope (NT-MDT, Moscow, Russia), equipped with a 10.0 μm bottom scanner. NSG10 cantilevers with Au reflective coating and a nominal spring constant of 11.8 N/m were used for the scanning. Force was kept at the lowest possible value by continuously adjusting the set-point and feed-back gain during imaging.

## 4.4. Results and Discussion

In an earlier study we have demonstrated that PDC-109 exhibits chaperone-like activity and that the polydisperse nature of PDC-109 is critical for its CLA (Sankhala and Swamy, 2010). However, a knowledge of other factors that are important for such an activity, or modulate the CLA, is still lacking. In the studies reported here additional experiments have been carried out to characterize the CLA of PDC-109 using two more target proteins, namely aldolase and carbonic anhydrase. In the studies reported here the effect of phospholipid binding on the CLA of PDC-109 and the role of hydrophobicity in it were also investigated.

### 4.4.1. Isothermal Titration Calorimetric Studies on bisANS Binding to PDC-109

ITC measurements to investigate the binding of bisANS to PDC-109 were carried out at 30 °C and a typical ITC profile is shown in Fig. 4.1. From this figure it can be seen that the binding process is endothermic in nature. The titration data could be best fitted using a *sequential binding model,* which suggests the presence of two types of binding interactions between bisANS and PDC-109 (Fig. 4.1). Thermodynamic parameters obtained from this analysis, listed in Table 4.1, indicate that both the

interactions are endothermic in nature with positive enthalpy changes and large positive entropic contributions, which compensate for the unfavorable enthalpy term and yield a net negative value of free energy ($\Delta G$).  It was observed that the final values of enthalpy and entropy associated with each binding site varied somewhat depending on the input values, although overall both enthalpy and entropy remained positive irrespective of the input data.  Also, the binding constants did not exhibit much variance.  The results obtained with one of the good fits are summarized in Table 4.1, which show that both the binding sites have similar affinity for bisANS.  Variation in the binding parameters depending on the method used for bisANS interaction with other proteins has also been reported (Hawe *et al.*, 2010).  The entropy-favored binding of bis-ANS to PDC-109 suggests the presence of hydrophobic patches on the protein surface, which in turn could be useful in its interaction with the non-native structures of different target proteins, which prevents their aggregation under stress conditions.

**Table 4.1:  Thermodynamic parameters for the interaction of bisANS with PDC-109.**  The values of the parameters were obtained by analyzing the data obtained from isothermal titration calorimetry to a sequential binding model.  Values shown correspond to the averages obtained from two independent titrations and standard deviations are indicated.

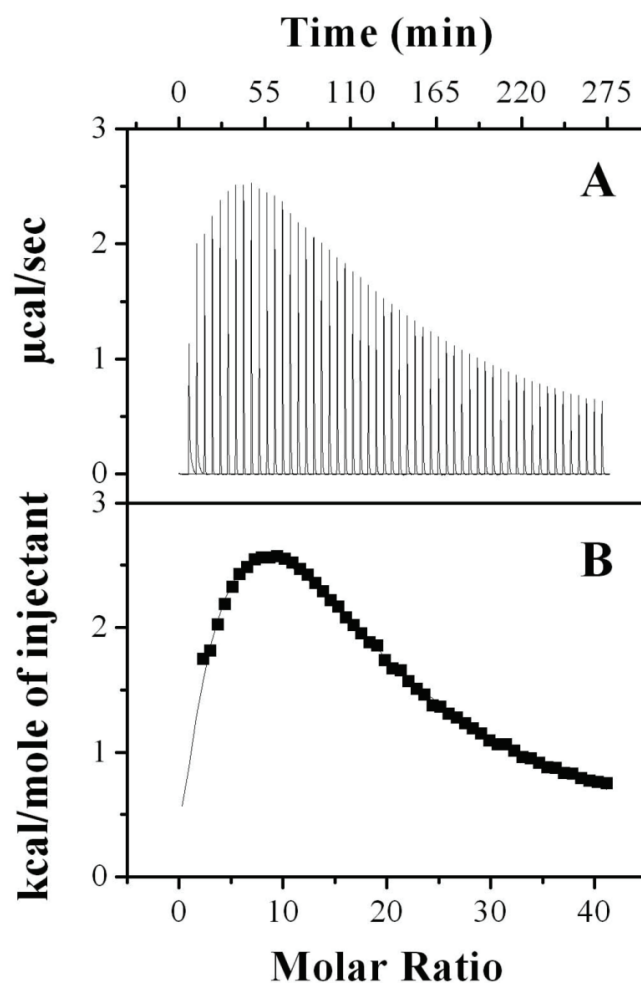| Binding Site | $K_a \times 10^3$ (M$^{-1}$) | $\Delta G$ (kcal.mol$^{-1}$) | $\Delta H$ (kcal.mol$^{-1}$) | $\Delta S$ (cal.mol$^{-1}$.K$^{-1}$) |
|:---:|:---:|:---:|:---:|:---:|
| $n_1$ | $2.57 \pm 0.1$ | $4.71 \pm 0.6$ | $7.8 \pm 1.02$ | 41.3 |
| $n_2$ | $2.53 \pm 0.07$ | $4.65 \pm 0.07$ | $101.4 \pm 1.5$ | 350 |

**Fig. 4.1: Calorimetric titration of bisANS binding to PDC-109.** Raw data for the titration of bisANS with PDC-109 at 30 $^{\circ}$C is shown in the upper panel (**A**) and the integrated heats of binding obtained from the raw data are shown in the lower panel (**B**), after subtracting the heat of dilution. The solid line in the bottom panel represents the best fit of the experimental data to the *sequential binding model* in the MicroCal Origin program. See text for further details.

## 4.4.2. ANS Binding to PDC-109 and Hydropathy Indexing

Fluorescence spectra and binding curve corresponding to the titration of PDC-109 with ANS are given in Figs. 4.2A and B, respectively. It is seen from these two figures that addition of ANS to PDC-109 leads to an increase in the fluorescence intensity of
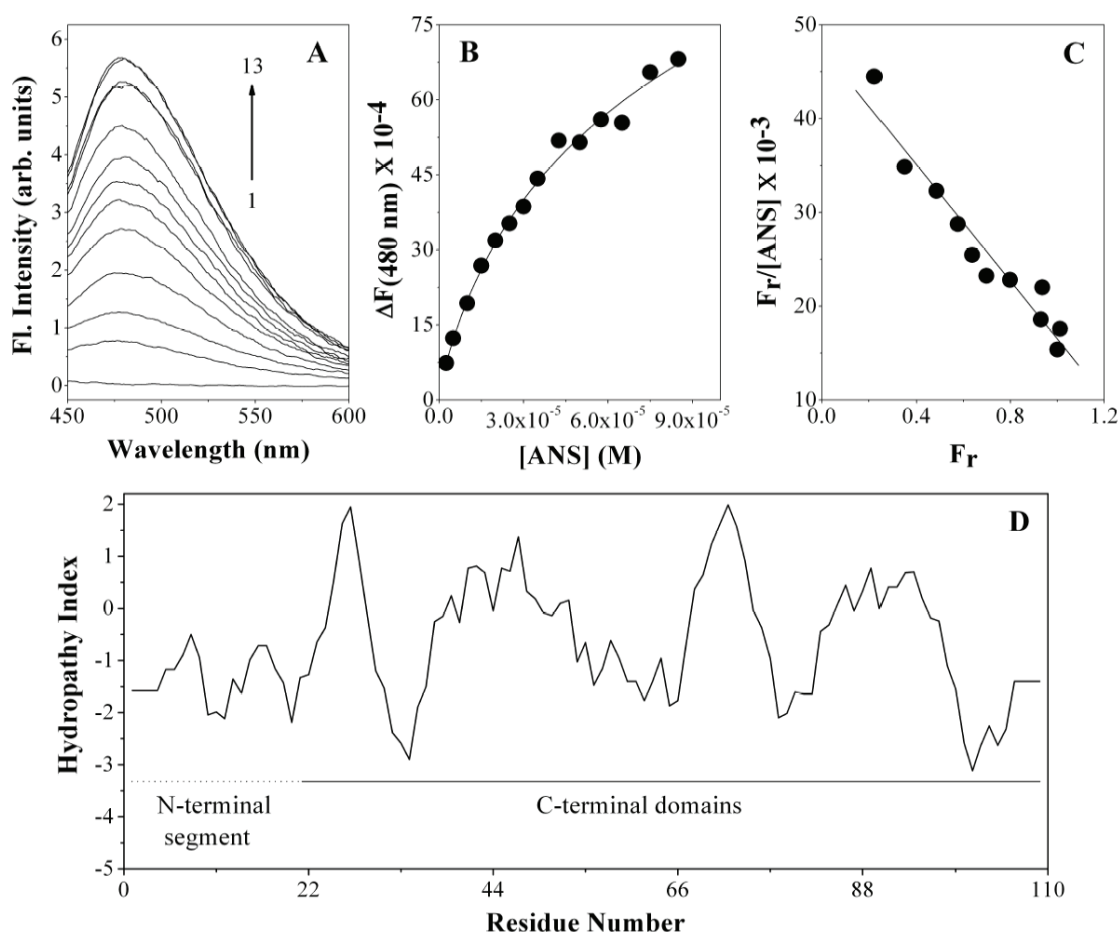
**Fig. 4.2: Fluorescence titration for ANS binding to PDC-109**. **A**) Fluorescence spectra of ANS binding to PDC-109. Spectrum 1 corresponds to PDC-109 alone and spectra 2–13 were recorded in the presence of increasing concentrations of ANS. **B**) Binding curve obtained by plotting change in fluorescence intensity ($\Delta F$) as function of ANS concentration. **C**) Linear Scatchard plot for the binding data. Slope of this plot gives association constant for the interaction and the X-intercept yields the stoichiometry of binding. **D**) Hydropathy plot of PDC-109 according to Kyte and Doolittle (1982) using using a 7-residue window. See text for details.

the probe and the magnitude of the change decreases with increasing ANS concentration, depicting saturation behavior. In these experiments, PDC-109

concentration was kept very low in order to maintain $[ANS]_{bound} \ll [ANS]_{total}$, such that for further analysis of the titration data, $[ANS]_{total}$ could be used as a good approximation of the free ligand concentration (Roberts and Goldstein, 1982; Kavitha *et al.*, 2009). From the titration data the association constant for the binding of ANS to PDC-109 was estimated by Scatchard analysis (Roberts and Goldstein, 1982; Kavitha *et al.*, 2009). From the slope of the Scatchard plot, given in Fig. 4.2C, the association constant, $K_a$ was estimated as $3.09 \times 10^4$ M$^{-1}$, whereas the X-intercept of the plot was obtained as 1.2, indicating that PDC-109 has one binding site for ANS, which is comparable with ANS binding to α-crystallin (Liang and Li, 1991; Sharma *et al.*, 1998). Hydropathy analysis performed according to Kyte and Doolittle (1982) with a sliding window of 7 residues suggests that the sequence corresponding to the two FnII domains of PDC-109 is more hydrophobic than the preceding N-terminal segment (Fig. 4.2D). Although this does not necessarily imply that the FnII domains are directly responsible for the CLA, it is possible that interaction of apolar residues of these domains with target proteins may be relevant to the CLA of PDC-109.

### 4.4.3. Effect of ANS Binding on the CLA and Secondary Structure of PDC-109

Aggregation assays aimed at investigating the effect of ANS binding on the CLA of PDC-109 are shown in Fig. 4.3A. Incubation of LDH at 48 ºC results in a rapid increase in the turbidity of the sample with time in the initial stages, which slows down afterwards (curve 1). A PDC-109 to LDH ratio (w/w) of 1:3 led to a 5% reduction in the extent of aggregation at 60 minutes (curve 3), whereas aggregation decreased further to 50% when the PDC-109/LDH ratio (w/w) was increased to 1:2 (curve 5). ANS binding did not lead to any significant change in the CLA at a PDC-109−ANS:LDH ratio of 1:3 (curve 4), although a slight increase in the CLA (about 10%) was observed, as compared to the native PDC-109, when the ratio was increased to 1:2 (curve 6). The protein fractions eluted from the gel filtration column showed a

molar ratio of 1:1 for PDC-109 and bound ANS.  ANS alone had a negligible effect on the aggregation of target protein at the concentrations mentioned above (curve 2).  A bar diagram, indicating the percent aggregation of LDH under different conditions is shown in Fig. 4.3B.  Far UV CD spectra, shown in Fig. 4.3C, indicate that the secondary structure of PDC-109 in the presence of ANS (dotted line) is nearly identical to that of the native protein (solid line), suggesting that ANS binding does not result in any significant changes in the conformation of the protein.  This could be one reason why ANS binding does not have any noticeable effect on the CLA of PDC-109.  Similar results were observed using ADH as the target protein and the results obtained are shown in Fig. S4.1*.
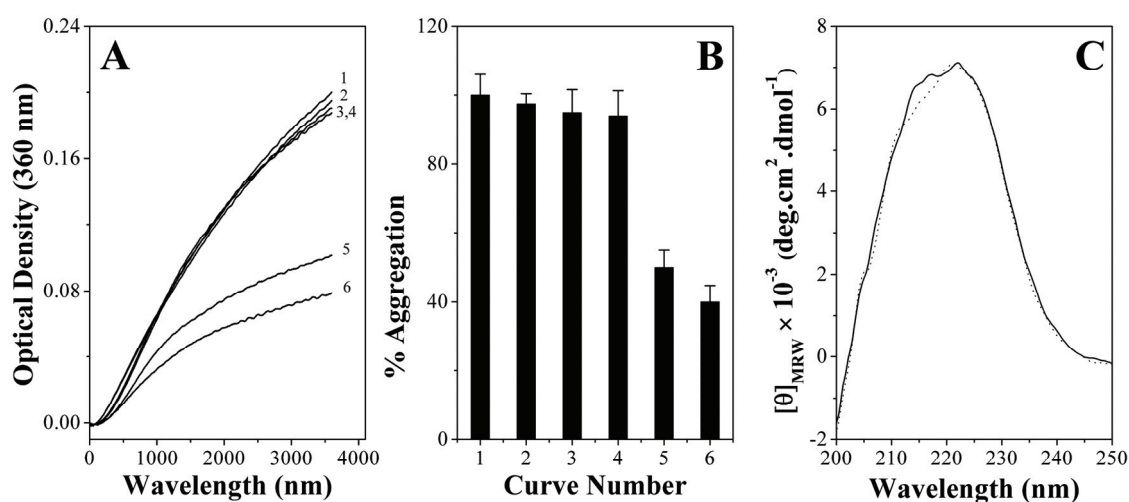


**Fig. 4.3:  Effect of ANS binding on the CLA and secondary structure of PDC-109**.  **A**) Prevention of aggregation of LDH (0.15 mg/mL) by PDC-109.   Aggregation profiles shown correspond to the following samples incubated at 48 °C: (1) LDH, (2) LDH + 6 μM ANS, (3) LDH + 0.05 mg/mL PDC-109, (4) LDH + 0.05 mg/mL (ANS−PDC-109), (5) LDH + 0.075 mg/mL of PDC-109 and (6) LDH + 0.075 mg/mL of (ANS−PDC-109).  **B)** Bar diagram representing percent aggregation of LDH under different conditions as shown in panel (**A**).  **C**) Far UV CD spectra of PDC-109 in the absence (solid line) and presence (dotted line) of ANS at room temperature.

*\* Supporting information is given in electronic format in a CD enclosed with the thesis.*

### 4.4.4. Phospholipid Induced Modulation of the CLA of PDC-109 and Alterations in its Tertiary Structure

Results of aggregation assays to investigate the effect of phospholipid binding on the CLA of PDC-109 are shown in Fig. 4.4. LDH, which is an aggregation-prone enzyme, was used as the target protein. Upon incubation at 48 ºC, turbidity of the sample containing LDH increases rapidly with time initially, but slows down with further incubation (curve 1, Fig. 4.4A). In the presence of PDC-109 at a PDC-109:LDH ratio of 3:4, the extent of aggregation of LDH decreased to ~29% with respect to that of the native enzyme (curve 3). Pre-incubation of PDC-109 with 0.5 μM DMPC (unilamellar vesicles) resulted in a significant decrease in the aggregation and at the same PDC-109:LDH ratio, only 6% aggregation was observed as compared to that of the native enzyme, whereas no aggregation was seen when PDC-109 was pre-incubated with 2 μM of DMPC (curves 4 & 5). On the other hand, inclusion of DMPG vesicles (0.1 and 0.5 μM) in the solution did not yield any alteration in CLA (curves 2 & 3, Fig. 4.4C), which was comparable to the CLA of PDC-109 alone (curve 4). The concentrations of LDH and PDC-109 used for this experiment are mentioned in the figure caption (Fig. 4.4C). Neither DMPC nor DMPG affected the aggregation profiles of target protein significantly at the above concentrations in the absence of PDC-109 (curve 2, Fig. 4.4A and curve 5, Fig. 4.4C). Similar results were obtained in experiments performed using CA and ADH as target proteins (see Figs. S4.2 and S4.3). The near-UV CD spectra of PDC-109 obtained in the presence of these two phospholipids show considerable differences, when compared with that of native PDC-109 (Fig. 4.4E), indicating that the protein tertiary structure is altered upon phospholipid binding, which is consistent with earlier reports (Gasset *et al.*, 1997 and 2000).

Dramatic change in the CLA of PDC-109, in the presence of DMPC can be explained in two different ways. One is the structural changes in PDC-109, induced by

its interaction with DMPC, which can modulate the CLA.  Results of our CD studies are in agreement with this (Fig. 4.4E).  The other explanation is based on PDC-109 induced partial solubilization of the vesicles and formation of lipid-protein particles of various sizes, which could modulate the overall hydrophobicity of the environment, which may alter the CLA.  Our parallel ITC studies on the binding of PDC-109 to DMPC model membranes showed that the interaction is characterized by a large positive heat capacity change ($\Delta C_p$) which suggested that large hydrophobic surfaces are exposed to water upon binding of PDC-109 to DMPC membranes (Anbazhagan, 2005).  Increase in the hydrophobicity upon interaction of PDC-109 with DMPC vesicles, was also probed by studying ANS and bisANS binding as discussed below.  As shown above, another phospholipid, i.e., phosphatidylglycerol, had only a marginal influence on the CLA of PDC-109 (Fig. 4.4C), which could be attributed to the low affinity of its binding to PDC-109 as compared to phosphatidylcholine.

PDC-109 has been reported to play an important role in priming the spermatozoa for fertilization by a membrane remodeling process (Desnoyers and Manjunath, 1992) and it has been demonstrated in Chapter 3 that PDC-109 can also function as a molecular chaperone which could be of physiological significance during fertilization (Sankhala and Swamy, 2010).  The present results establish a correlation between the membrane

---

**Fig. 4.4:  Effect of phospholipid binding on the CLA and tertiary structure of PDC-109**.  **A**) Effect of DMPC on the prevention of aggregation of LDH by PDC-109.  Aggregation profiles shown correspond to the following samples incubated at 48 °C: (1) LDH alone, (2) LDH +2 μM of DMPC, (3) LDH + PDC-109, (4) LDH + PDC-109 + DMPC (0.5 μM) and (5) LDH + PDC-109 + DMPC (2 μM).  In these experiments LDH and PDC-109 were used at a concentration of 0.1 and 0.075 mg/mL, respectively.  **B**) Bar diagram representing percent aggregation of LDH for different samples shown in panel (**A**) at 60 minutes.  **C**) Effect of DMPG on the prevention of aggregation of LDH by PDC-109.  Aggregation profiles shown correspond to the following samples incubated at 48 °C: (1) LDH alone, (2) LDH + PDC-109 + DMPG (0.1 μM), (3) LDH + PDC-109 + DMPG (0.5 μM), (4) LDH + PDC-109 and (5) LDH + DMPG (0.5 μM).  In these experiment LDH and PDC-109 were used at a concentration of 0.12 and 0.05 mg/mL, respectively.  **D**) Bar diagram for the data shown in (**C**).  **E**) Near UV CD spectra of PDC-109 under native conditions (solid line), in the presence of DMPC (dashed line) and DMPG (dotted line).
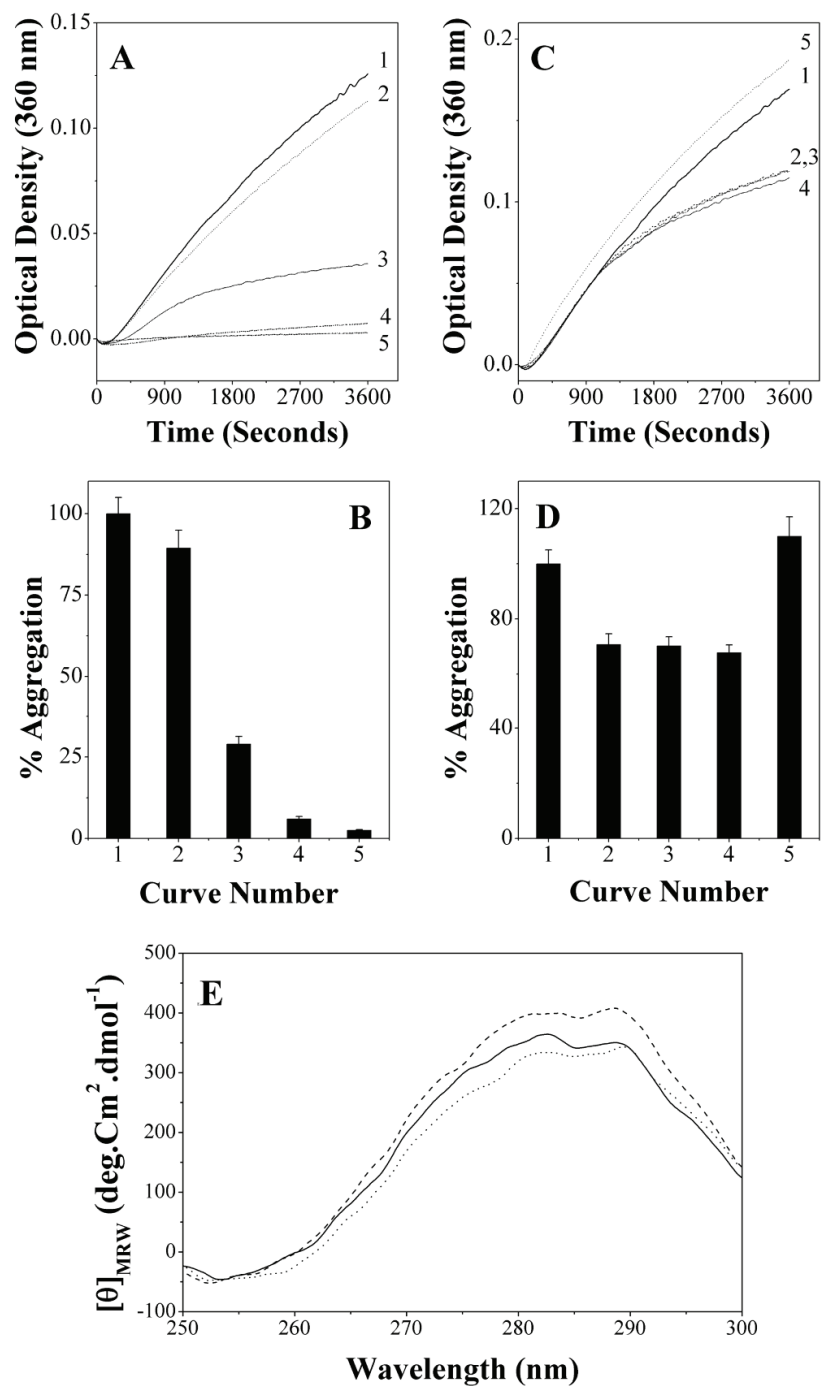
binding and chaperone-like activity of PDC-109, and therefore are of considerable relevance for the better understanding of the role of PDC-109 in fertilization.

## 4.4.5. Enhanced Surface Hydrophobicity Upon Interaction of PDC-109 with Phosphatidylcholine Membrane

BisANS is a fluorescent probe that is being used extensively for identifying and characterizing hydrophobic regions of proteins and other biomolecules. Upon binding to such sites it displays enhanced fluorescence intensity (Manček-Keber and Jerala, 2006). Therefore, the extent of enhancement in its fluorescence intensity could be correlated to increased exposure of hydrophobic residues or surfaces. Fluorescence spectra corresponding to bisANS alone and in the presence of PDC-109, DMPC, DMPG, and mixtures of PDC-109 with DMPC and DMPG are shown in Fig. 4.5A. Fluorescence enhancement upon bisANS binding to DMPG vesicles (dash-dot line), was comparable to that of the control sample (buffer + bisANS, solid thin line), whereas a 11.3-fold enhancement was observed upon binding to DMPC (dash line), which is comparable to the fluorescence enhancement observed upon binding to native PDC-109 (dot line). Fluorescence enhancement upon bisANS binding to DMPG−PDC-109 mixture was slightly higher than that observed for binding to native PDC-109 (dash dot dot line), whereas it was nearly 1.5-fold higher as compared to the enhancement observed for binding to native PDC-109 and 16.4-fold higher than control (buffer + bisANS), in the case of DMPC−PDC-109 complex (solid thick line). A bar diagram indicating the relative fluorescence intensity of bisANS in various samples is shown in Fig. 4.5B.

Dramatic increase in the fluorescence intensity of bisANS, upon binding to DMPC−PDC-109 mixture indicates increased exposure of hydrophobic surfaces. Since PDC-109 binds to choline phospholipids with high affinity, which leads to membrane disruption and formation of lipid/protein complexes, the above results indicate that

these lipid/protein recombinants have a higher degree of surface hydrophobicity. The increased hydrophobicity of these recombinants may be important for their better interaction with partially unfolded target proteins as compared to PDC-109 alone and prevention of their aggregation. This interpretation is consistent with the enhanced chaperone-like activity of DMPC−PDC-109 mixtures as compared to PDC-109 alone (Figs. 4.4A, S4.2A and S4.3A). PDC-109 has a significantly lower affinity for
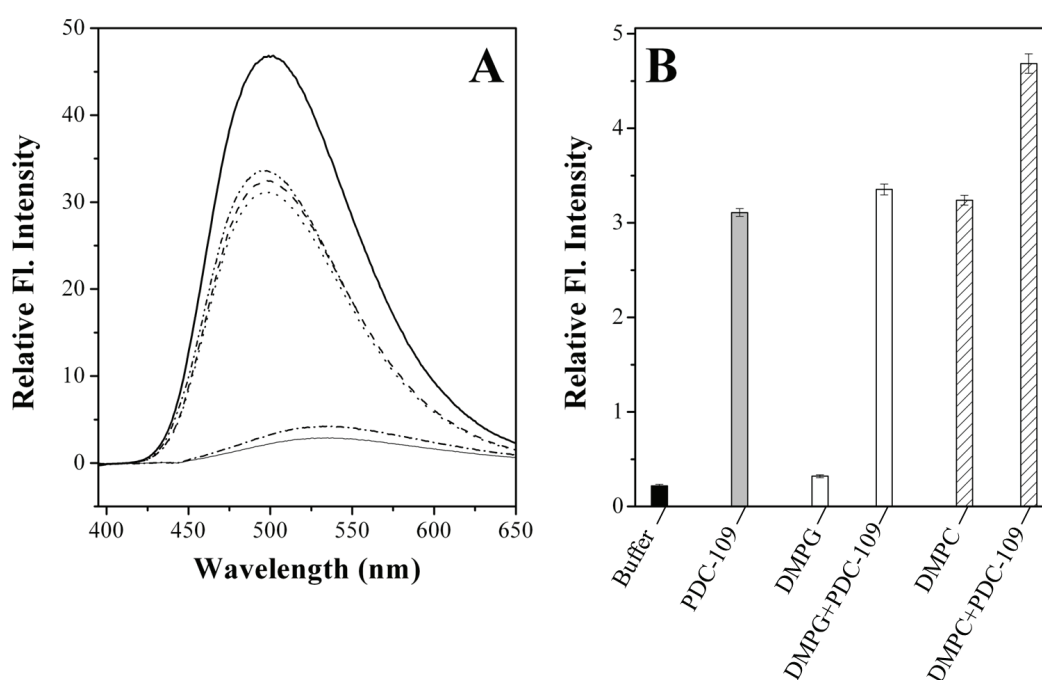


**Fig.4.5: Binding of bisANS to phospholipids, PDC-109 and phospholipid−PDC-109 mixtures**. (**A**) Fluorescence spectra shown correspond to: bisANS in buffer (solid thin line), DMPG (5 μM, dash-dot line), PDC-109 (0.05 mg/mL, dotted line), DMPC (5 μM, dashed line), DMPG−PDC-109 mixture (dash-dot-dot line) and DMPC−PDC-109 mixture (solid thick line). The final concentration of bisANS in each of the sample is 12.2 μM . Relative fluorescence intensity of different samples is shown in the form of a bar diagram in panel (**B**).

phosphatidylglycerol as compared to phosphatidylcholine (Thomas *et al.*, 2003) and hence its binding to DMPG membranes may not expose the interior hydrophobic regions of this lipid to the same extent as is observed upon its binding to DMPC

membranes.  The lack of significant change in the fluorescence intensity of bisANS (dash dot dot line, Figs. 4.5A) as well as in the CLA of the protein (Figs. 4.4C, S4.2C and S4.3C) in the presence of DMPG-PDC-109 mixture, are consistent with the above interpretation.   Similar results were also obtained for ANS binding to the samples described above and the results obtained are shown in Fig. S4.4.

### 4.4.6. Modulation of Surface Hydrophobicity of PDC-109 by PrC Binding

Fluorescence spectra corresponding to ANS in buffer containing PrC and in the presence of PDC-109 and mixtures of PDC-109 with PrC are shown in Fig. 4.6A.
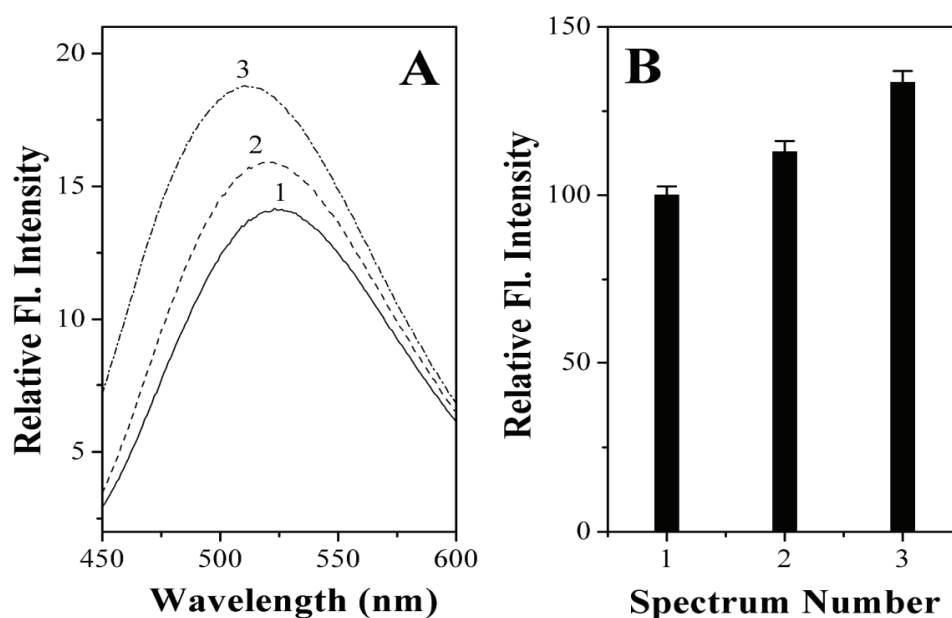


**Fig.4.6:  ANS Binding to PrC and PrC−PDC-109 mixtures**. **A**) Fluorescence spectra of ANS in TBS-1 under different conditions.  1) with PrC; 2) with PDC-109 + PrC; 3) with PDC-109. Concentrations of different components used were: ANS, 50 μM; PDC-109, 0.05 mg/mL; PrC, 10 mM. **B**) Relative fluorescence intensity of different samples shown in **A**.

Fluorescence intensity of ANS in buffer containing PrC (solid line) was considered as 100% and relative intensity of other samples was normalized with respect to it.

Intensity of ANS increased by ~33% in the presence of PDC-109 (dash dot line), whereas prior incubation of PDC-109 with PrC showed only 13% increase in the ANS fluorescence (dash line).   A bar diagram indicating the relative fluorescence enhancement of ANS in various samples is shown in Fig. 4.6B.   These observations indicated that PrC binding leads to a significant decrease in the surface hydrophobicity of the protein (see Supporting Information for details).   In chapter 3 the dramatic decrease in the CLA of PDC-109 upon PrC binding was attributed to the dissociation of the polydisperse aggregates of the protein.   The present results indicated that in addition to the polydispersity, surface hydrophobicity is also important for the CLA of PDC-109.

### 4.4.7. Cholesterol Incorporation into Phospholipid Vesicles Modulates the CLA

As discussed above, incubation of PDC-109 with DMPC unilamellar vesicles leads to a dramatic alteration in the aggregation behavior of various target proteins (Fig. 4.4A, S4.2A and S4.3A).   In order to investigate the effect of cholesterol, similar experiments were carried out with samples containing 25 mol% cholesterol in DMPC unilamellar vesicles and the results obtained are shown in Fig. 4.7.   Incubation of CA at 52 °C results in a rapid increase in the turbidity which reaches a maximum and slows down with time (curve 1, Fig. 4.7A).   The extent of aggregation of CA at the end point of assay (60 minutes) was considered as 100% and the aggregation of other samples was normalized with respect to this.   Prior incubation of CA with PDC-109 led to about 15% reduction in the aggregation (curve 2), whereas pre-incubation of CA with DMPC−PDC-109 mixture resulted in a complete inhibition of aggregation (curve 4).   However, pre-incubation with DMPC/cholesterol−PDC-109 mixture yielded only 45% inhibition of CA aggregation (curve 3), indicating that cholesterol incorporation into DMPC vesicles has a negative impact on the CLA of PDC-109/DMPC recombinants (Figs. 4.4A, S4.2A and S4.3A).   However, it must be noted that DMPC/cholesterol-

PDC-109 recombinants exhibited higher CLA than PDC-109 alone. Similar results were obtained when LDH was used as target protein (see Fig. S4.5).

Upon binding to phospholipid membranes, PDC-109 removes lipid molecules from the outer leaflet (Thérien *et al.*, 1998; Moreau *et al.*, 1998; Tannert *et al.*, 2007), leading to membrane disruption. The fluorescence studies of bisANS and ANS binding to DMPC–PDC-109 mixtures suggest that the surface hydrophobicity of the PDC-109/DMPC recombinants is significantly higher as compared to that of PDC-109 alone (Figs. 4.5 and S4.4). It is known that the interaction of PDC-109 with membranes
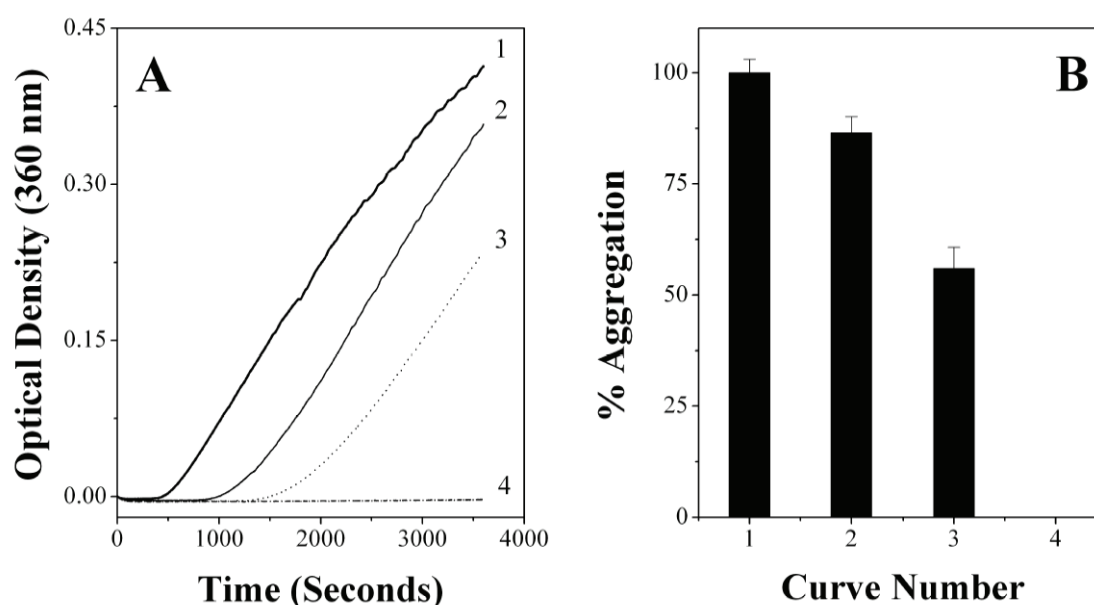


**Fig. 4.7: Effect of cholesterol incorporation into phospholipid membrane on the CLA of PDC-109.** (**A**) Prevention of aggregation of CA. Aggregation profiles shown correspond to the following samples incubated at 52 °C: (1) CA at 52 °C, (2) CA + PDC-109, (3) CA + PDC-109 + DMPC/cholesterol and (4) CA + PDC-109 + DMPC. Concentrations of both CA and PDC-109 were 0.2 mg/mL. **B**) Bar diagram representing percent aggregation of CA under different conditions as shown in panel (**A**).

containing phosphatidylcholine results in the formation of lipid/protein particles with high curvature (Ramakrishnan *et al.*, 2001). In such highly curved aggregates of lipids,

the hydrophobic regions of the lipids will be more exposed than in normal lipid bilayers. Also, conformational changes in the protein resulting from lipid binding (Gasset *et al.*, 2000) may also lead to increased exposure of hydrophobic regions of the protein. Most probably these additional hydrophobic surfaces interact with the non-native structures of aggregation prone proteins, resulting in their protection under stress conditions. On the other hand, interaction of PDC-109 with DMPC vesicles containing 25 mol% cholesterol could not extend similar protection to the target proteins (Figs. 4.7A and S4.5). Since cholesterol is known to provide rigidity to the membranes, PDC-109 binding cannot induce complete disruption of such vesicles (Gasset *et al.*, 2000; Thomas *et al.*, 2003; Damai *et al.*, 2010). This interaction therefore cannot lead to the exposure of the hydrophobic surfaces to the same extent as is achieved by the interaction of PDC-109 with membranes containing only phosphatidylcholine. The CLA of PDC-109 in the presence of DMPC/cholesterol mixture is therefore relatively less as compared to that of PDC-109/DMPC recombinant. It is also possible that direct interaction of cholesterol with the CRAC domain of PDC-109 may alter the CLA of the latter (Scolari *et al.*, 2010).

## 4.4.8. Modulation of the CLA of PDC-109 by DMPC or DMPC/Cholesterol Mixture: AFM Studies

The effect of DMPC or DMPC/cholesterol binding on the CLA of PDC-109 was also studied using AFM, essentially as described in Chapter 3. AFM images of CA, obtained after incubation at 52 ºC indicate that this enzyme forms very large aggregates of several microns in size upon such treatment (Fig. 4.8A). However, when CA was incubated at the same temperature in the presence of PDC-109, considerably smaller aggregates were formed under similar conditions (Fig. 4.8C).
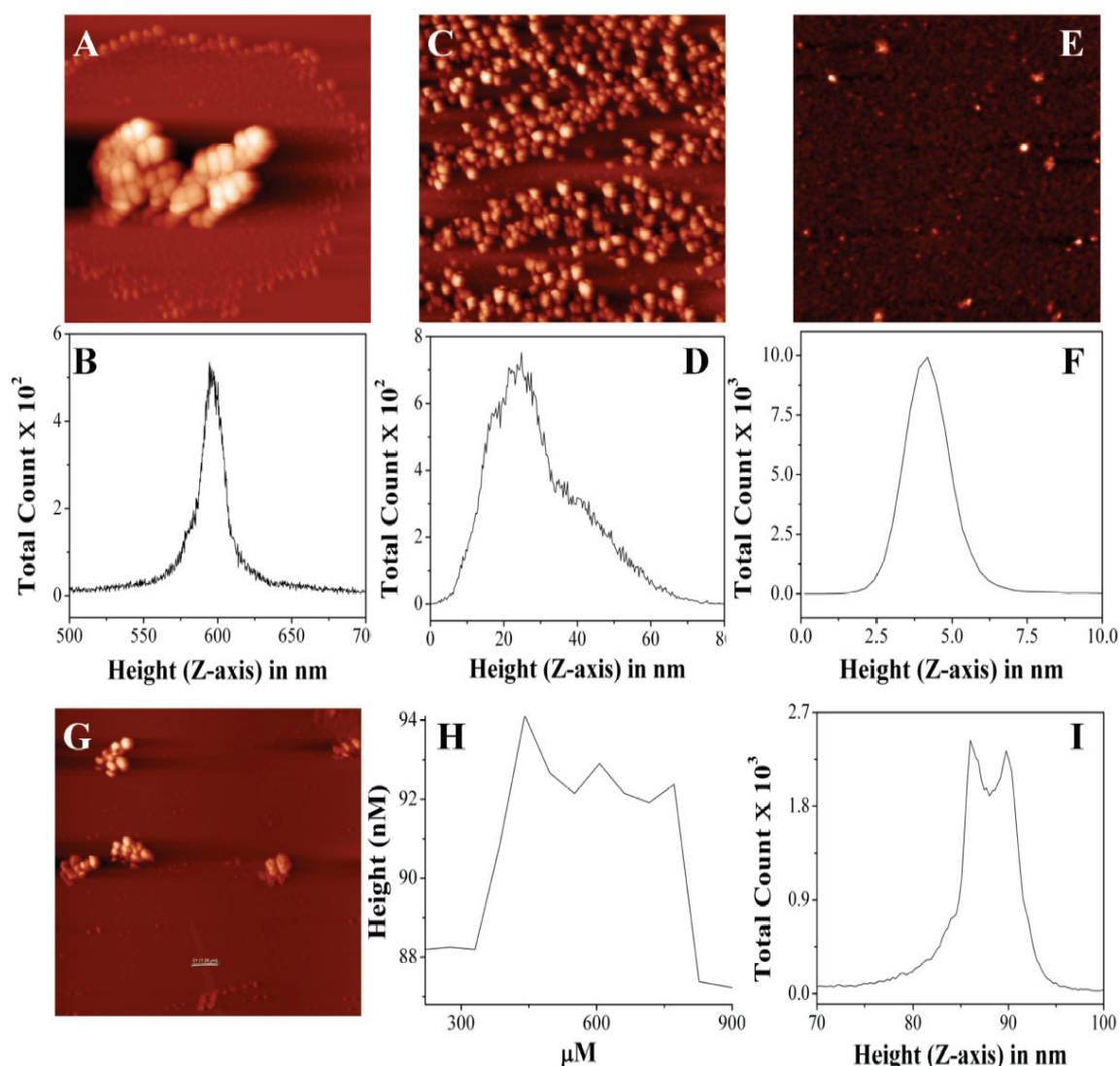
**Fig. 4.8: AFM studies on the modulation of CLA of PDC-109 by cholesterol incorporation into DMPC membranes.** The ability of cholesterol to modulate the chaperone-like activity of PDC-109/DMPC recombinants was investigated by AFM using carbonic anhydrase as the target protein. (**A**) AFM image of CA upon incubation at 52 °C (14 × 14 µm). (**B**) Distribution density histogram for the image shown in (**A**). (**C**) AFM image of CA upon incubation at 52 °C in the presence of PDC-109 (5 × 5 µm). (**D**) Distribution density histogram for the image shown in (**C**). (**E**) AFM image of CA upon incubation at 52 °C in the presence of DMPC−PDC-109 (6 × 6 µm). (**F**) Distribution density histogram for the image shown in (**E**). (**G**) AFM image of CA upon incubation at 52 °C in the presence of DMPC/cholesterol−PDC-109 (14 × 14 µm). (**H**) Height profile corresponding to the bar shown in image (**G**). (**I**) Distribution density histogram for the image shown in (**G**).

Distribution density histogram shows a size distribution in the range of 550–650 nm for CA alone (at 52 ºC), which shifted to 10–60 nm in the presence of PDC-109 (Fig. 4.8B and D). This shows that although PDC-109 prevents the aggregation of CA but is not as efficient as it is against LDH and ADH (Chapter 3). Interestingly, PDC-109 pre-incubated with DMPC prevented the aggregation of CA significantly and the size distribution was observed to be <10 nm (Fig. 4.8E and F). This is consistent with our turbidimetric studies where inclusion of DMPC with PDC-109 resulted in multifold enhancement of its CLA (Figs. 4.4A, S4.2A and S4.3A). On the other hand, pre-incubation of PDC-109 with DMPC vesicles containing 25 mol% cholesterol did not prevent the aggregation of CA as efficiently as DMPC alone (Fig. 4.8G). As discussed above, the enhanced CLA upon interaction of PDC-109 with DMPC vesicles appears to be due to the increased exposure of hydrophobic surface upon such interaction. The presence of a small membrane segment in Fig. 4.8G is consistent with the ability of cholesterol to stabilize choline phospholipid membranes against PDC-109-induced disruption, due to which the exposure of hydrophobic surfaces is decreased. This, in turn, would result in a decrease in the CLA of PDC-109/DMPC recombinants in the presence of cholesterol. These observations demonstrate that the lipid/protein recombinants, formed by the interaction of PDC-109 with phospholipid membranes, exhibit higher CLA and prevent the aggregation of substrate proteins more efficiently than PDC-109 alone. This is schematically illustrated in Fig. 4.9.

In summary, the present *in vitro* studies demonstrate that the lipid/protein complexes formed by the high-affinity binding of PDC-109 to membranes containing choline phospholipids exhibit a higher chaperone-like activity than PDC-109 alone. The lipid/protein recombinants possess a higher surface hydrophobicity as compared to native PDC-109, which could be responsible for their better interaction with partially unfolded proteins and prevention of their aggregation under stress conditions. Cholesterol incorporation resulted in a decrease in the CLA of the PDC-109/DMPC
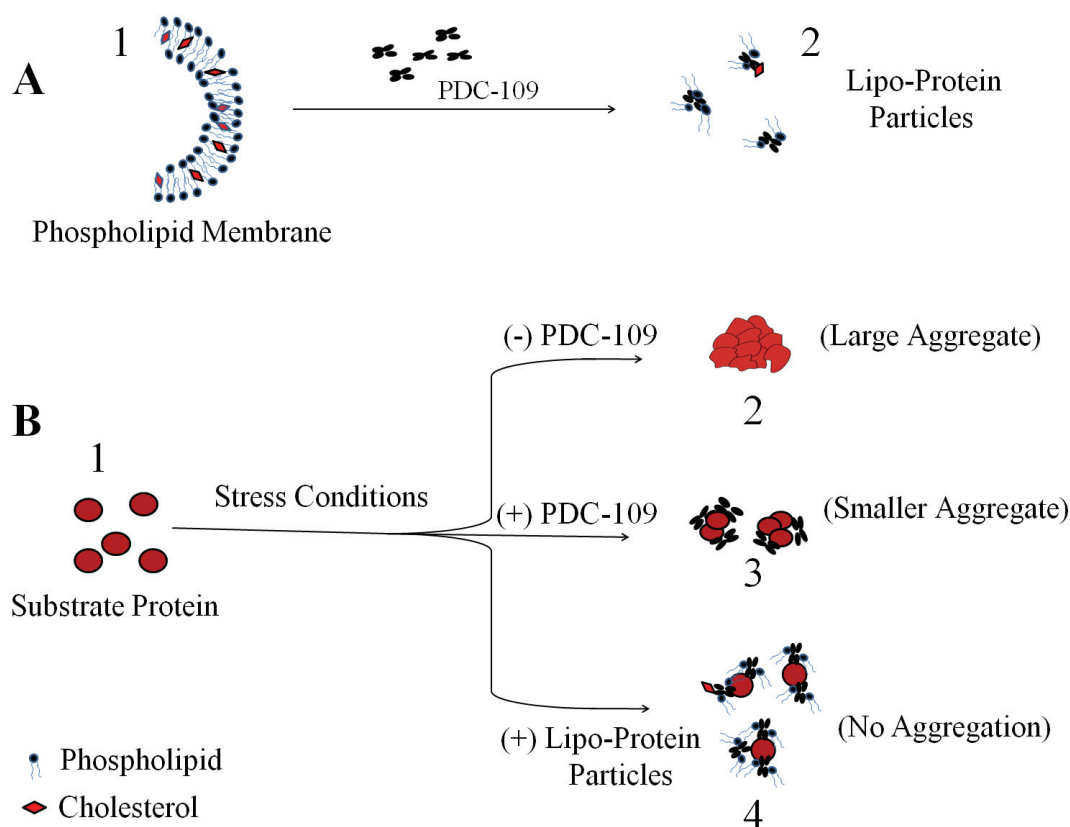
**Fig. 4.9: A schematic model for the functional role of PDC-109 in sperm capacitation.** **A**) PDC-109 binding induces cholesterol and choline phospholipids efflux, which is a necessary step for sperm capacitation. Phospholipid membrane (1) and efflux particles made up of PDC-109, cholesterol and choline phospholipids (2), are shown. **B**) PDC-109 functions as a molecular chaperone and stabilizes substrate proteins. Substrate proteins (1), are aggregated under stress conditions (2), which in the presence of PDC-109 (3) or lipid/protein particles (4) are stabilized efficiently.

recombinants, which could be attributed to membrane rigidification, or to the direct interaction of cholesterol with the CRAC domain of PDC-109. However, the CLA of lipid/protein complexes was always higher than that of PDC-109 alone. ANS binding to PDC-109 in the presence of PrC suggests that in addition to polydispersity, hydrophobicity is also an important factor for the CLA of PDC-109. The present study

could also be important to understand the functional significance of membrane/protein interaction for the other chaperonins such as spectrin and Hsp12 (Bhattacharyya *et al.*, 2004; Welker *et al.*, 2010).

Overall the results presented here shed further light on the CLA of PDC-109 and demonstrate that hydrophobicity plays an important role in this activity.

# Chapter 5

# Biophysical Investigations on the Interaction of PDC-109 with Heparin
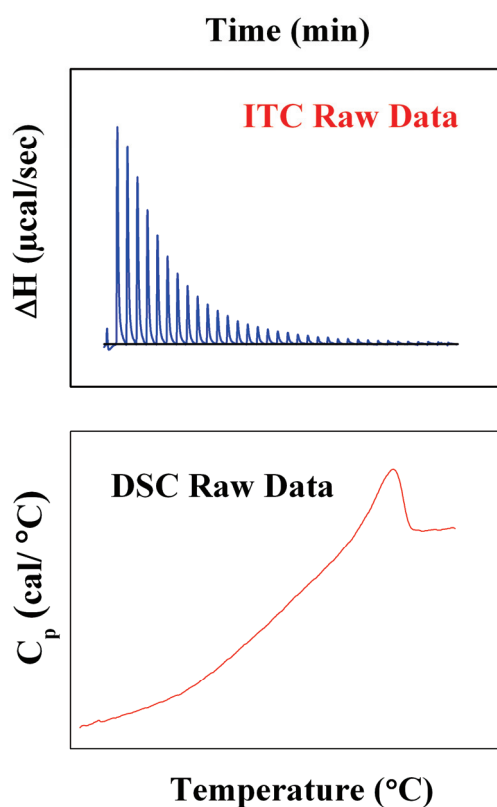
**Time (min)**



ITC Raw Data

ΔH (μcal/sec)

DSC Raw Data

C$_p$ (cal/°C)

**Temperature (°C)**

## 5.1. Abstract

The interaction of PDC-109 with heparin has been investigated employing various biophysical approaches. Isothermal titration calorimetric studies yielded the association constant, and changes in enthalpy and entropy for the interaction at 25 $^{o}$C (pH 7.4) as 1.85 ($\pm \times$1.2) $10^5$ $M^{-1}$, 20.8 ($\pm$0.6) kcal.$M^{-1}$ and 93.7 cal.$M^{-1}$.$K^{-1}$, respectively, whereas differential scanning calorimetric studies provided information on the changes induced by heparin binding in the oligomeric status and thermal stability of PDC-109. The affinity of PDC-109 for heparin decreases with increase in pH and ionic strength, consistent with the involvement of electrostatic forces. CD results show that PDC-109 retains its conformational features up to 70-75 ℃ in the presence of heparin, whereas the native protein unfolds at about 55 ℃. Atomic force microscopic studies indicated the formation of large oligomeric structures upon binding of PDC-109 to heparin, most likely due to the association of several protein molecules with each heparin molecule. This indicates that heparin increases the local density of the protein, which in turn could enhance sperm capacitation. The present results assume significance in view of the involvement of heparin in sperm capacitation and its interaction with PDC-109.

## 5.2. Introduction

Besides binding to the phospholipid membranes (Chapter 1), PDC-109 also interacts with a variety of other ligands including apolipoproteins A1 and A2, several types of collagens and heparin (Manjunath *et al.*, 1987; Chandonnet *et al.*, 1990; Manjunath *et al.*, 2002; Majunath *et al.*, 1989). Heparin and other glycosaminoglycans (GAGs) are components of follicular and oviductal fluids, which play an important role in sperm capacitation (Parrish *et al.*, 1989; Lane *et al.*, 1999). The interaction of BSP proteins with heparin has been exploited in their purification by affinity chromatography (Manjunath *et al.*, 1987). Affinity chromatographic experiments have shown that while polydisperse PDC-109 binds heparin, the monomeric form does not display heparin binding ability (Calvete *et al.*, 1999). In addition, proteolytic digestion and chemical modification studies indicated that lysine and arginine residues are important for heparin binding, indicating that the PDC-109/heparin association is mediated predominantly by electrostatic interactions (Calvete *et al.*, 1999). It has been reported that incubation with heparin increases the fertilizing ability of bovine spermatozoa (Parrish *et al.*, 1985; 1986a). It is also known that incubation of spermatozoa with BSP proteins results in an increased acrosomal reaction (Thérien *et al.*, 1995), whereas obstruction of heparin binding to the BSP proteins with specific antibodies results in a significant decrease (Lane *et al.*, 1999). Taken together, these studies suggest that heparin/BSP interactions are important for the sperm capacitation process, although a molecular level understanding of the role of heparin in BSP-protein induced sperm capacitation remains unclear. It is therefore important to investigate the interaction of PDC-109 and other BSP proteins with heparin.

In the present study, the energetics and mechanism of PDC-109 binding to heparin have been investigated using isothermal titration calorimetry (ITC) and differential scanning calorimetry (DSC), which have been used widely to characterize protein-

carbohydrate interactions (Evans *et al.*, 1992; Surolia *et al.*, 1996; Krupakar *et al.*, 1999; Ziegler and Seelig, 2004). ITC studies indicate the presence of multiple binding sites on heparin for PDC-109. The PDC-109/heparin interaction is associated with a close compensation of enthalpy and entropy, although the latter appears to be a dominant driving force for the interaction. Changes in pH and ionic strength affect the heparin/PDC-109 interaction significantly, with the affinity decreasing at higher pH and ionic strength. Analysis of the DSC data shed further light on the interacting species, binding affinities and thermal stability of PDC-109, upon its interaction with heparin. Both ITC and DSC results indicate the formation of oligomeric structures upon PDC-109/heparin interaction, which was further confirmed using AFM. The fact that one heparin molecule can bind to multiple protein molecules indicates that heparin binding increases the local density of the protein, which could be of significant importance during sperm capacitation. CD studies were in good agreement with DSC results and suggest that heparin binding results in a thermal stabilization of PDC-109. The present observations are of significant interest in view of the crucial role played by heparin in sperm capacitation and acrosome reaction.

## 5.3. Materials and Methods

### 5.3.1. Materials

Phosphorylcholine chloride ($Ca^{2+}$ salt), Tris base and heparin (MW 3000 and 6000) were obtained from Sigma (St. Louis, MO, USA). Sephadex G-50 (superfine) and DEAE Sephadex A-25 were purchased from Pharmacia (Uppsala, Sweden). All other chemicals used were of analytical grade and were obtained from local suppliers. PDC-109 was purified from bovine seminal plasma and characterized as reported in Chapter 2.

**5.3.2. Effect of pH and Ionic Strength on the Interaction of PDC-109 with Heparin**

PDC-109 was taken in sufficiently high concentration and dialyzed against buffers of the desired pH. Tris buffered saline containing 50 mM Tris, 150 mM NaCl, 5 mM EDTA and 0.02% sodium azide at different pH (7.4-9.0) was used as the buffering system. PDC-109 from the stock solution was diluted to a desired final working concentration of 200 μM. Calorimetric titrations were performed using a VP-ITC microcalorimeter from MicroCal (Northampton, MA, USA). The solutions were degassed under vacuum before using in order to prevent bubbling. Binding of heparin to PDC-109 was investigated at 25 °C as follows. Typically, 20-40 consecutive injections of 5 μL aliquots of heparin (1 mM) were injected from the syringe into the calorimeter cell of 1.445 mL filled with the protein solution. Successive additions were separated by 240 s intervals to allow the endothermic peak resulting from the reaction to return to the baseline. To ensure proper mixing after each injection, a constant stirring speed of 300 rpm was maintained during the experiment. To minimize the contribution to the binding heat from dilution, the protein and heparin solutions were prepared in the same buffer. Control experiments were performed by titrating heparin solution into a buffer and the resulting heat changes were subtracted from the measured heats of binding. The first injection is often inaccurate, therefore a 2 μL injection was added first and the resultant data point was deleted before analyzing the remaining data using the Origin ITC data analysis software. In order to probe the effect of ionic strength of the medium on PDC-109/heparin interaction, two different samples of the protein were freshly dialyzed against 50 mM tris buffer (pH 7.4, without salt) and TBS-I, (pH 7.4, containing 150 mM NaCl) respectively at 4 °C. The protein was then diluted with the appropriate buffer to yield a final concentration of 200 μM. Heparin (1 mM) was also dissolved in the above buffers and titrations were performed at 20 °C.

### 5.3.3. Differential Scanning Calorimetry

DSC measurements were performed on a MicroCal VP DSC differential scanning calorimeter (MicroCal LLC, Northampton, MA, USA). PDC-109 solution in TBS-I, at a concentration of 0.6 mg/mL was heated from 10 to 90 °C at a scan rate of 30°/hour under a constant pressure of 22.9 psi. The contribution of the protein to the calorimetrically measured heat capacity was determined by subtracting buffer-buffer base line from the sample data prior to analysis. Data were analyzed by the Origin software provided by MicroCal. Experiments aimed at investigating the effect of heparin binding on the thermal stability of PDC-109 were carried out under similar conditions and the data obtained were analyzed using the '*non two-state mode of fitting*' in the MicroCal Origin software. The binding affinity of heparin to PDC-109, at the thermal transition point, was analyzed according to equation (1) (Schellman, 1975).

$$K_b(T_c) = [\exp\{(T_c\text{-}T_m)\Delta H_c/n\mathrm{R}T_cT_m\} - 1] \,/\, [\mathrm{L}] \qquad (1)$$

where $K_b(T_c)$ is the binding constant at the reference temperature, $\Delta H_c$ is the calorimetric enthalpy of the heparin-protein complex, $T_c$ is the denaturation temperature in the presence of heparin, $T_m$ is the denaturation temperature in the absence of heparin, R is the universal gas constant, [L] is the ligand concentration and $n$ is the number of binding sites on the protein.

### 5.3.4. Atomic Force Microscopy

Appropriate aliquots were drawn from a freshly dialyzed sample of PDC-109 (1 mg/mL) in TBS-I buffer and a 5 mM solution of heparin in the same buffer and mixed to yield a 1.0 mL solution containing 0.4 mg/mL of the protein and 0.5 mM heparin. After a 30-minute incubation, a 20 µL aliquot from the above mixture was deposited on a freshly cleaved mica sheet, allowed to bind for ~30 minutes, and the unbound material

was washed off with HPLC grade distilled water and samples were transferred to AFM stage for imaging, essentially as described earlier (Sankhala and Swamy, 2010). PDC-109 and heparin at the concentrations indicated above were independently used as controls.

### 5.3.5. Circular Dichroism Spectroscopy

Circular dichroism spectra were recorded on a JASCO J-810 spectropolarimeter fitted with a thermostatted cell holder and interfaced to a thermostatic waterbath. Samples were taken in a 0.2 cm path length quartz cell. The effect of temperature on the conformation of PDC-109 was probed in two different ways. First, PDC-109 was preincubated with a fixed concentration of heparin and ellipticities were recorded as a function of wavelength at fixed temperatures between 30 and 80 $^{\circ}$C. Concentrations of PDC-109 and heparin used for the far- and near-UV spectra are mentioned in the respective figure captions. Each spectrum reported was the average of 20 consecutive scans from which buffer scans, recorded under the same conditions, were subtracted. The observed ellipticities were converted to mean residue ellipticities (MRE).

In the second type of experiments, PDC-109 was preincubated with different concentrations of heparin and ellipticities were recorded at fixed wavelengths (221 nm in the far UV region and 289 nm in the near UV region) as a function of temperature. The temperature was increased from 25 to 90 °C at a scan rate of 1°/min. To investigate the effect of heparin binding on the conformational stability of the protein, PDC-109 was incubated with a fixed concentration of heparin, before recording the CD spectra.

## 5.4. Results and Discussion

### 5.4.1. Effect of pH and Ionic Strength on the Interaction of PDC-109 with Heparin

The effect of pH and ionic strength on the thermodynamic parameters associated with the interaction of PDC-109 with heparin was studied using ITC.  Measurements were performed only in the narrow pH range of 7.4 – 9.0 since the protein tended to precipitate at low pH and heparin does not show any observable affinity for the protein at pH 9.0 and above.  ITC profiles for the interaction of heparin with PDC-109 at different pH are shown in Fig. 5.1.  At pH 7.4 addition of 1 mM heparin to 200 µM PDC-109 solution initially yielded large endothermic heats of binding and the magnitude of the endothermic peaks decreased with subsequent injections (Fig. 5.1A), showing saturation of the binding sites at high heparin concentrations.  However, with increasing pH fewer binding sites are saturated by heparin (Figs. 5.1B and C), indicating decreased affinity of heparin with increase in the pH.  Data from the above experiments could be best fitted by a nonlinear least squares method to '*one set of sites*' binding model among the various models available in the Origin ITC data analysis software.  Values of $K_a$, $n$, $\Delta H$, $\Delta S$ and free energy of binding ($\Delta G$) characterizing the heparin-PDC-109 interaction at various temperatures, obtained from this analysis, are listed in Table 5.1.  These data are in good agreement with the above interpretation and show that the affinity of heparin binding to PDC-109 decreases with increasing pH and no more binding is observed at pH $\geq$9.0.  The binding of heparin to PDC-109 has been reported to involve primarily electrostatic interactions (Calvete *et al.*, 1999).  Heparin is a highly-sulfated glycosaminoglycan and bears a large negative charge density on it, whereas PDC-109 is an acidic protein with an isoelectric point (pI) of ~5.0.  When pH of the medium is increased, PDC-109 becomes progressively more negatively charged, which is also clear from the surface charge plot shown in Fig. 5.1D.  At high pH both PDC-109 and heparin will be highly negatively charged and due to the electrostatic
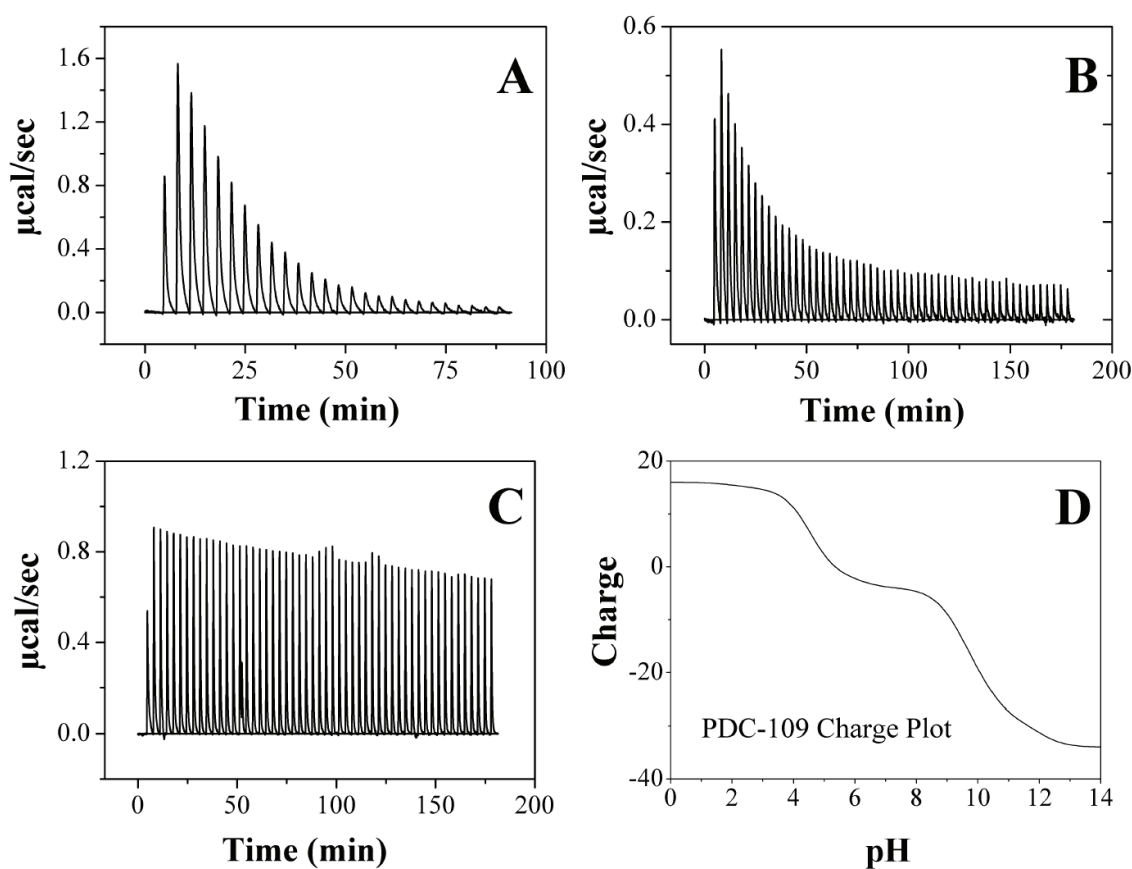
**Fig. 5.1: Effect of pH on heparin binding to PDC-109.** ITC profiles for the titration of 0.25 mM PDC-109 with 1 mM heparin at pH 7.4 (**A**), 8.0 (**B**) and 9.0 (**C**).  T = 25 °C. For all the experiments 50 mM tris buffer containing 150 mM NaCl and 5 mM EDTA was used and the pH was adjusted to the desired value with hydrochloric acid.  **D**) pH dependence of the surface charge of PDC-109, obtained using "*protein charge analysis*" tool of CLCbio (www.clcbio.com).

repulsion between them the binding is expected to be significantly weakened, if not completely abrogated, indicating that the interaction is predominantly mediated by electrostatic forces.  ITC experiments aimed at investigating the effect of ionic strength of the medium on the PDC-109/heparin interaction yielded a binding affinity of $1.14 \times 10^6$ M$^{-1}$ in 50 mM tris buffer (Fig. 5.2), which decreased to $1.4 \times 10^5$ M$^{-1}$ upon inclusion

of 150 mM NaCl in the buffer (Tris.HCl buffer). The decrease in the affinity further confirms the electrostatic nature of the PDC-109/heparin interaction.



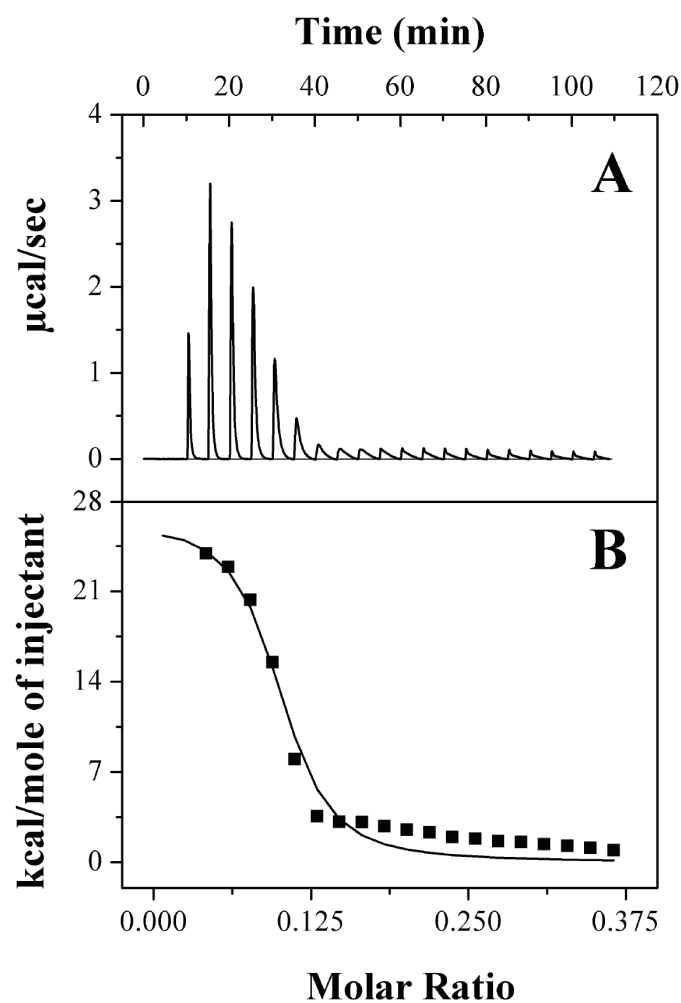**Fig. 5.2: ITC studies of heparin binding with PDC-109 in 50 mM tris buffer without salt**. **A**) Raw data for the titration of 0.2 mM PDC-109 with 1 mM heparin. (**B**) Integrated heats of binding obtained from the raw data shown in panel **B**, after subtracting the heat of dilution. The solid line represents the best curve fit to the experimental data, using the '*one set of sites model*' from Microcal Origin. T = 20 °C.

The results presented in Table 5.1 indicate that the PDC-109/heparin interaction is stabilized by entropy of binding, with negative enthalpic contribution. The positive value of $\Delta S$ for the binding of PDC-109 to heparin indicates that during the binding

**Table 5.1:** Thermodynamic parameters obtained by isothermal titration calorimetry for the binding of PDC-109 to heparin.

| S.No. | pH | Buffer | Temp. (K) | $n$ | $K_a \times 10^{-4}$ (M$^{-1}$) | $-\Delta G$ (kcal.mol$^{-1}$) | $\Delta H$ (kcal.mol$^{-1}$) | $\Delta S$ (cal.mol$^{-1}$.K$^{-1}$) |
|---|---|---|---|---|---|---|---|---|
| 1. | 7.4 | TBS-I | 298 | 0.095 ($\pm$ 0.002) | 18.5 ($\pm$ 1.2) | 7.12 ($\pm$ 0.6) | 20.8 ($\pm$ 0.60) | 93.7 |
| 2. | 8.0 | TBS-I | 298 | 0.095 ($\pm$ 0) | 03.0 ($\pm$ 0.23) | 6.08 ($\pm$ 0.5) | 18.95 ($\pm$ 0.50) | 84 |
| 3. | 9.0 | TBS-I | 298 | – | – | – | – | – |
| 4. | 7.4 | TBS-I | 293 | 0.090 ($\pm$ 0.003) | 14.5 ($\pm$ 0.98) | 6.9 ($\pm$ 0.6) | 17.13 ($\pm$ 0.6) | 82.1 |
| 5. | 7.4 | Tris HCl* | 293 | 0.096 ($\pm$ 0.00) | 114.0 ($\pm$ 0.3) | 7.9 ($\pm$ 1.09) | 26.6 ($\pm$ 1.09) | 118 |

*Tris.HCl: 50 mM tris.HCl buffer without NaCl and EDTA (pH 7.4).

process water molecules are expelled from the interface of PDC-109 – heparin complex. Values of the stoichiometry ($n$), which corresponds to the number of heparin molecules that interact with each molecule of PDC-109, are found to range between 0.09 to 0.096. As these values are fractional, it would be more convenient to take the inverse of this value which gives the stoichiometry of interaction as 10 to 11 moles of PDC-109 per mole of heparin ($M_r$ ~6000). The above result indicates the presence of multiple binding sites on heparin for the protein molecules, which is consistent with the results obtained with other heparin binding proteins such as antithrombin III, heparin binding growth-associated molecule (HB-GAM), HIV-1 TAT protein etc (Tyler-Cross, 1994; Fath *et al.*, 1999; Ziegler and Seelig, 2004). Since PDC-109 exists as a polydisperse

aggregate in the absence of choline containing ligands (Gasset *et al.*, 1997), it would be difficult to get a precise estimate of the number of sites on the heparin molecule for PDC-109. The average molecular weight of heparin used in this study is ca. 6000, indicating that each heparin molecule on an average contains about 20 monosaccharide units. Therefore it is possible that each molecule of heparin can in principle offer a number of binding sites for interaction with PDC-109. This was further confirmed by using a lower molecular weight heparin (~3000 dalton) for the binding titrations. The results obtained demonstrate that only 3-4 molecules of PDC-109 bind to a single molecule of heparin ($M_r$ 3000 dalton), which is considerably lesser than that obtained above for the binding of PDC-109 to heparin ($M_w$ 6000 dalton) under similar experimental conditions. This indicates that the larger heparin molecule presents more binding sites for interaction with PDC-109.

## 5.4.2. Thermal Denaturation of PDC-109 in the Absence and Presence of Heparin: DSC Studies

The thermal stability of PDC-109 in the presence of different concentrations of heparin was studied using high-sensitivity DSC. Thermograms corresponding to PDC-109 alone and in the presence of various concentrations of heparin, corrected for buffer base line are shown in Fig. 5.3. The data shown in these thermograms could be best fitted to a non-two-state model. Native PDC-109 was reported to exhibit two transitions at about 310 and 328 K, which were attributed to dissociation of the oligomeric protein (into monomers) and unfolding of the monomer, respectively (Gasset *et al.*, 1997). The present results show that the calorimetric scans (in the presence of heparin) consist of six entities melting at different temperatures (Fig. 5.3). Values of the calorimetric enthalpy to van't Hoff enthalpy ratio ($\Delta H_c/\Delta H_v$) corresponding to these transitions are given in Table 5.2, which shed light on the oligomeric status of the protein (Surolia *et al.*, 1997). The $\Delta H_c/\Delta H_v$ ratios for the 1$^{st}$

transition (in the presence of varying concentrations of heparin) was observed to be in the range of 0.27 – 0.6, indicating the presence of small oligomeric aggregates. The transition temperature for the dissociation of these oligomeric species was observed to be about 306 K, which matches well with the temperature at which the PDC-109 oligomers dissociate (Gasset *et al.*, 1997). For the 2$^{nd}$ transition, $\Delta H_c/\Delta H_v$ ratios and
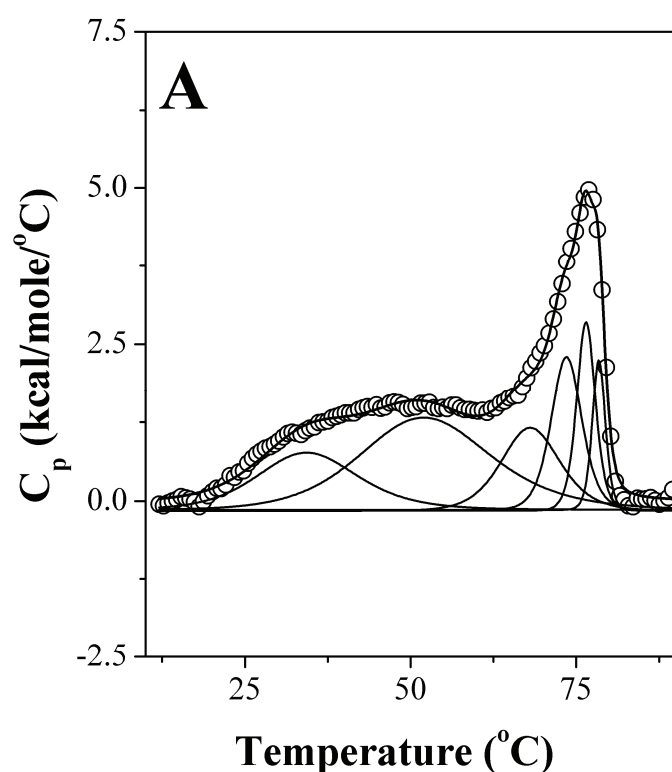


**Fig.5.3:  DSC studies on the effect of heparin binding on the thermal stability of PDC-109.** DSC thermogram of PDC-109/heparin complex is shown as open circles (O) and the best fit of DSC data to the *non-two-state transition model* is shown as a solid thick line ( — ). The data could be fitted assuming 6 transitions and corresponding thermogram profiles are shown as thin lines (−).

transition temperatures were observed as ~1 and ~325.5 K, respectively, which are consistent with the unfolding of PDC-109 monomers (Gasset *et al.*, 1997). The $\Delta H_c/\Delta H_v$ ratios for the remaining transitions (3$^{rd}$–6$^{th}$) were observed to be in the range

of 0.19 to 0.013 (Table 5.2), indicating the presence of large oligomeric structures. Since each PDC-109 monomer shares ~0.1 binding site for one molecule of heparin (Fig. 5.1), these oligomers, to a large extent, must consist of heparin–PDC-109 complexes with several molecules of the protein bound to a single heparin molecule.
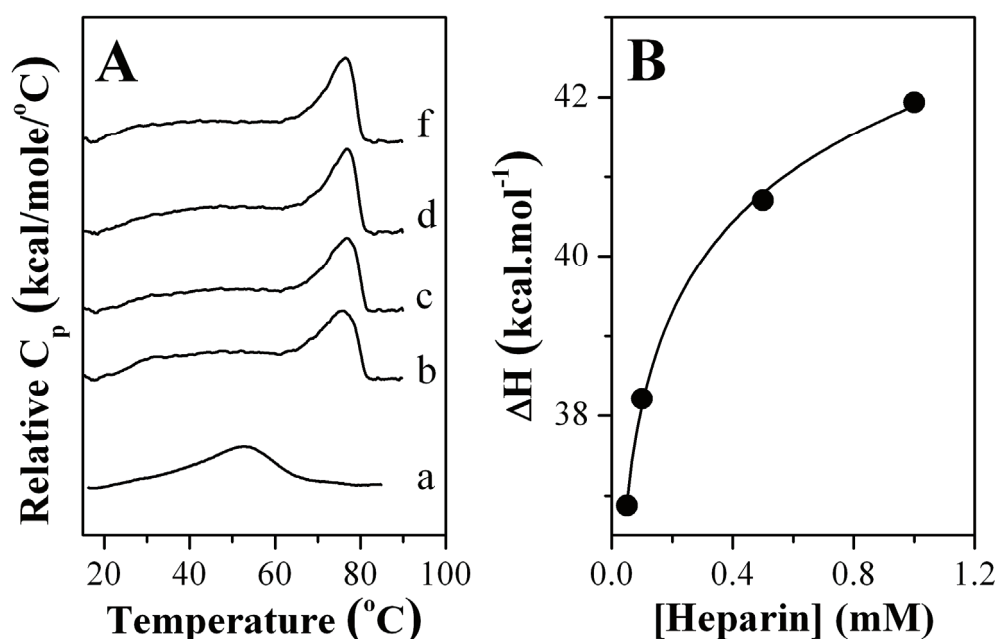


**Fig.5.4: Effect of heparin binding on the thermal stability of PDC-109. A**) Calorimetric profiles of PDC-109 in TBS-I with increasing concentrations of heparin: 0 mM (a), 0.05 mM (b), 0.1 mM (c), 0.5 mM (d) and 1 mM (e). (**B**) A plot of total change in enthalpy obtained from the DSC thermograms of PDC-109–heparin complexes ($\Delta H_T$) have been plotted as a function of heparin concentration.

The transition temperatures observed for such oligomeric states are in the range of 339 K to 352 K (Fig. 5.4A), indicating that heparin–PDC-109 complexes form stable structures, which maintain their integrity even at higher temperatures. Total enthalpy change ($\Delta H_T$) for all these transitions of the heparin–PDC-109 complexes was calculated by adding the enthalpy values of each heparin−PDC-109 complex. A plot of $\Delta H_T$ with respect to increasing concentration of heparin is shown in Fig. 5.4B. The increase in $\Delta H_T$ with increasing heparin concentration indicates that heparin binding

stabilizes the structure of PDC-109, which was further confirmed by CD spectroscopy (see below).

The binding affinities between PDC-109 and heparin at denaturing temperatures were calculated using Schellman's equation (Schellman, 1975) and the data obtained

**Table 5.2:** Thermodynamic parameters obtained from DSC measurements on the thermal transitions of PDC-109 in the presence and absence of heparin. The errors were less than 0.02% for $T_m$ and less than 10% for $\Delta H_c$ and $\Delta H_v$.

| [Heparin] (mM) | $T_{m1}$ (K) | $\Delta H_{c1}$ /$\Delta H_{v1}$ | $T_{m2}$ (K) | $\Delta H_{c2}$ /$\Delta H_{v2}$ | $T_{m3}$ (K) | $\Delta H_{c3}$ /$\Delta H_{v3}$ | $T_{m4}$ (K) | $\Delta H_{c4}$ /$\Delta H_{v4}$ | $T_{m5}$ (K) | $\Delta H_{c5}$ /$\Delta H_{v5}$ | $T_{m6}$ (K) | $\Delta H_{c6}$ /$\Delta H_{v6}$ |
|---|---|---|---|---|---|---|---|---|---|---|---|---|
| 0 | 313.0 | 0.40 | 326.5 | 0.8 | – | – | – | – | – | – | – | – |
| 0.05 | 307.5 | 0.55 | 326.5 | 1.2 | 341.3 | 0.17 | 346.2 | 0.09 | 349.3 | 0.045 | 351.7 | 0.013 |
| 0.1 | 306.6 | 0.3 | 325.3 | 1.1 | 341.9 | 0.18 | 346.9 | 0.09 | 349.9 | 0.042 | 351.9 | 0.013 |
| 0.5 | 307.6 | 0.47 | 325.5 | 1.2 | 341.2 | 0.19 | 346.5 | 0.095 | 349.5 | 0.043 | 351.5 | 0.015 |
| 1.0 | 305.9 | 0.63 | 325.0 | 1.0 | 339.0 | 0.15 | 344.7 | 0.10 | 348.3 | 0.07 | 350.7 | 0.03 |

**Table 5.3:** Association constants corresponding to different PDC-109/heparin oligomeric species.

| [Heparin] (mM) | $T_{m1}$ (K) | $K_1$ (M$^{-1}$) | $T_{m2}$ (K) | $K_2$ (M$^{-1}$) | $T_{m3}$ (K) | $K_3$ (M$^{-1}$) | $T_{m4}$ (K) | $K_4$ (M$^{-1}$) |
|---|---|---|---|---|---|---|---|---|
| 0.5 | 341.2 | 72.5 | 346.5 | 130 | 349.5 | 166 | 351.5 | 103 |
| 1.0 | 339.0 | 210 | 344.7 | 300 | 348.3 | 250 | 350.7 | 144 |

are shown in Table 5.3. Since this method does not provide accurate values at lower ligand concentrations (Brandts and Lin, 1990), the binding affinities were calculated at 1 and 0.5 mM concentration of heparin only. The observed affinities are significantly lower than those measured by calorimetric titrations performed between 14 and 30 $^{\circ}$C, indicating that the affinity of interaction decreases at higher temperatures.

### 5.4.3. Heparin Induced Oligomerization of PDC-109

AFM images of PDC-109 in the absence and presence of heparin are shown in Fig. 5.5. Being a polydisperse protein, native PDC-109 shows an average size distribution in the range of 1-4 nm, although a few oligomeric structures ranging from 20-150 nm can be observed at various places (Figs. 5.5A and B).



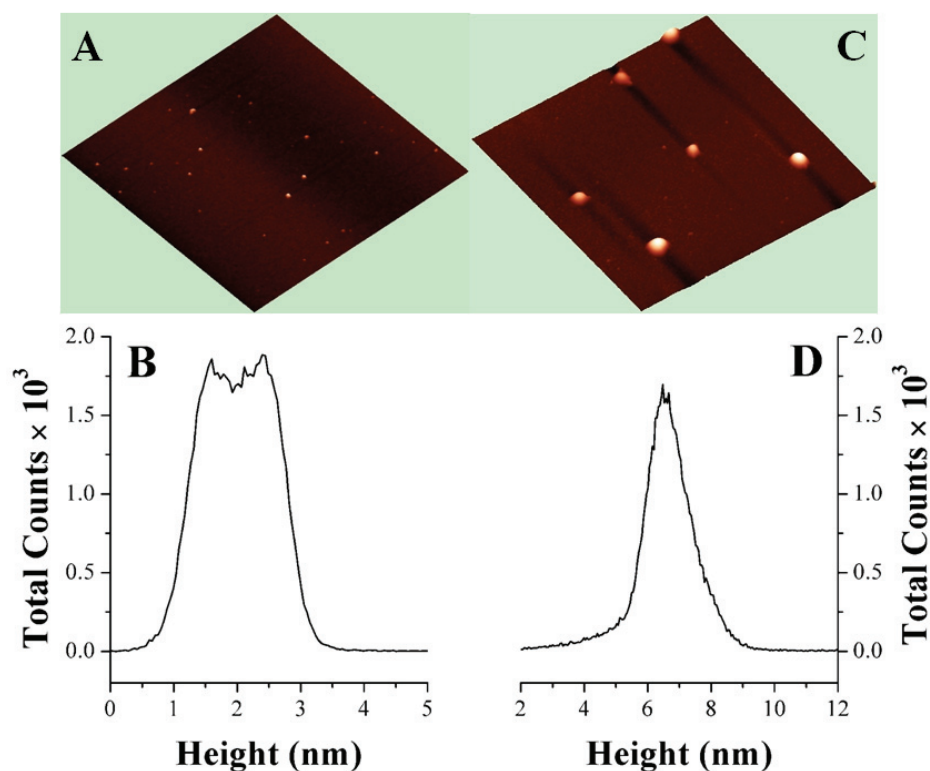**Fig.5.5: AFM studies on PDC-109/heparin interaction. A**) AFM image of native PDC-109 in air (5 × 5 μm). **B**) Histogram corresponding to the image shown in panel **A**. **C**) AFM image of PDC-109 upon interaction with heparin (5 × 5 μm). **D**) Histogram corresponding to the image shown in panel **C**.

PDC-109 which was preincubated with heparin showed an average size distribution in the range of 4-10 nm with frequent occurrence of larger oligomeric structures (50-300 nm) (Figs. 5.5C and D).  These observations suggest that binding of heparin to PDC-109 results in the formation of larger oligomeric structures, which is in good agreement with the results of ITC and DSC studies, discussed above.

### 5.4.4. Heparin Binding Increases the thermal Stability of PDC-109

Heparin was previously shown to stabilize protein and peptide conformers in solution and to impart thermal and chemical stability to peptide-heparin complexes (Evans *et al.*, 1992; Soler-Ferran *et al.*, 1992).  The present DSC results clearly suggest that heparin stabilizes PDC-109 against thermal unfolding (Fig. 5.3).  In order to probe the effect of heparin binding on the conformation of PDC-109 and monitor changes in it at different temperatures, we recorded CD spectra of PDC-109 in the absence and in the presence of heparin (Figs. 5.6 and 5.7).  The near-UV CD spectrum of PDC-109 is characterized by a broad positive band with two discrete maxima at 282 nm and 289 nm, whereas the far-UV spectrum is characterized by a major positive band with a maximum at 223 nm and a shoulder at about 215 nm, consistent with previous reports (Gasset *et al.*, 1997; Anbazhagan and Swamy, 2005).  Upon heparin binding the intensity of the near- and far-UV CD spectra decreased considerably (Figs. 5.6B and 5.7B), indicating heparin induced conformational changes in the protein structure.  Both the near and far-UV spectra of the free protein undergo a reduction in overall intensity as the temperature is increased upto 50 $^{\circ}$C.  Above 50 $^{\circ}$C significant loss was observed in the secondary and tertiary structures of the protein and above 60 $^{\circ}$C no dichroic behavior was observed with the native protein (Figs. 5.6A and 5.7A), whereas significant amounts of both secondary and tertiary structures could be seen even at 70 $^{\circ}$C in the presence of heparin (Figs. 5.6B and 5.7B).  The protein denatured rapidly above 70 $^{\circ}$C.

**Fig.5.6: Effect of heparin binding on the thermal stability of PDC-109.** Near-UV CD spectra of PDC-109 at various temperatures in the absence (**A**) and presence (**B**) of 1 mM heparin. Arrow represents the direction of increase in the temperature. The temperatures used are: (1) 25 $^{\circ}$C, (2) 30 $^{\circ}$C, (3) 35 $^{\circ}$C, (4) 40 $^{\circ}$C, (5) 50 $^{\circ}$C, (6) 55 $^{\circ}$C, (7) 60 $^{\circ}$C, (8) 70 $^{\circ}$C and (9) 80 $^{\circ}$C. Thermal scans of the protein in the absence and presence of varying concentrations of heparin, at a fixed wavelength of 289 nm (near-UV) are shown in panel (**C**) and (**D**). The concentrations of heparin used are: (1) 0.03 mM, (2) 0.05 mM, (3) 0.2 mM and (4) 0.5 mM.
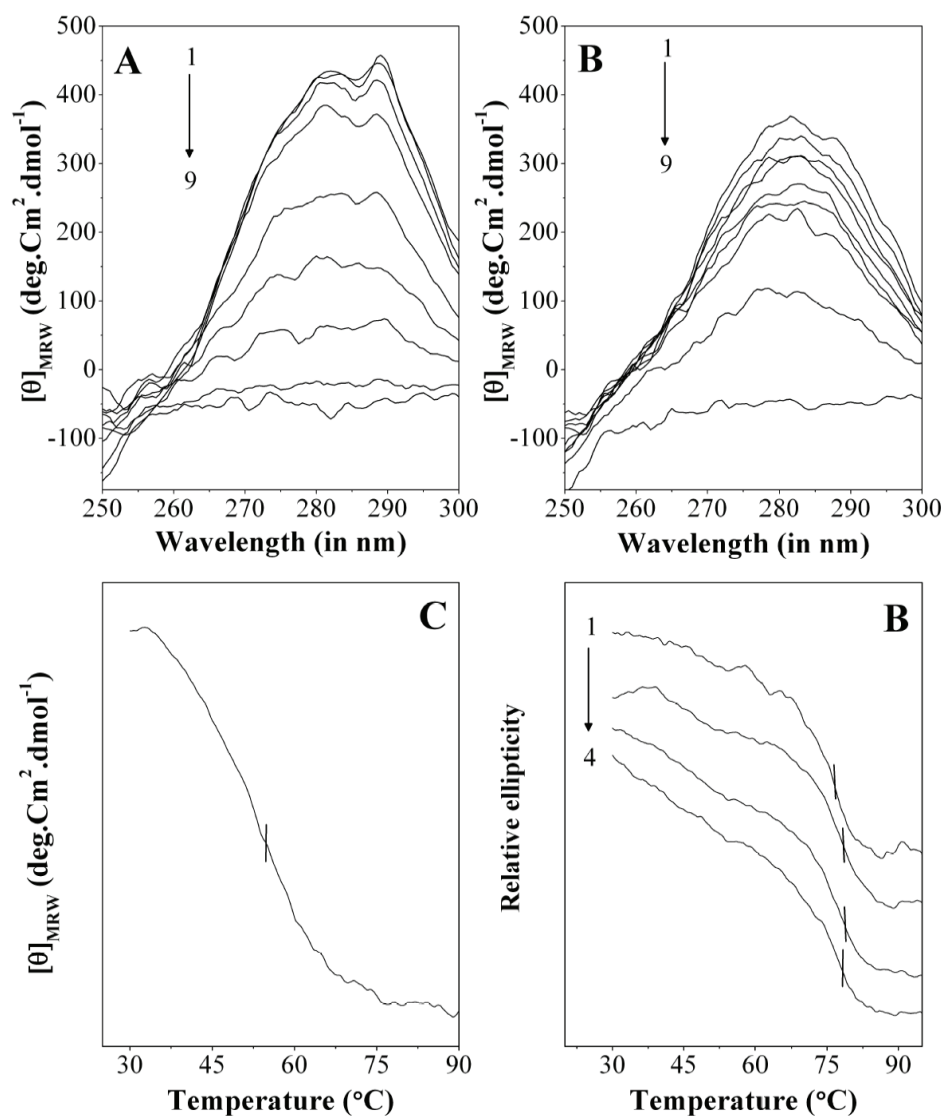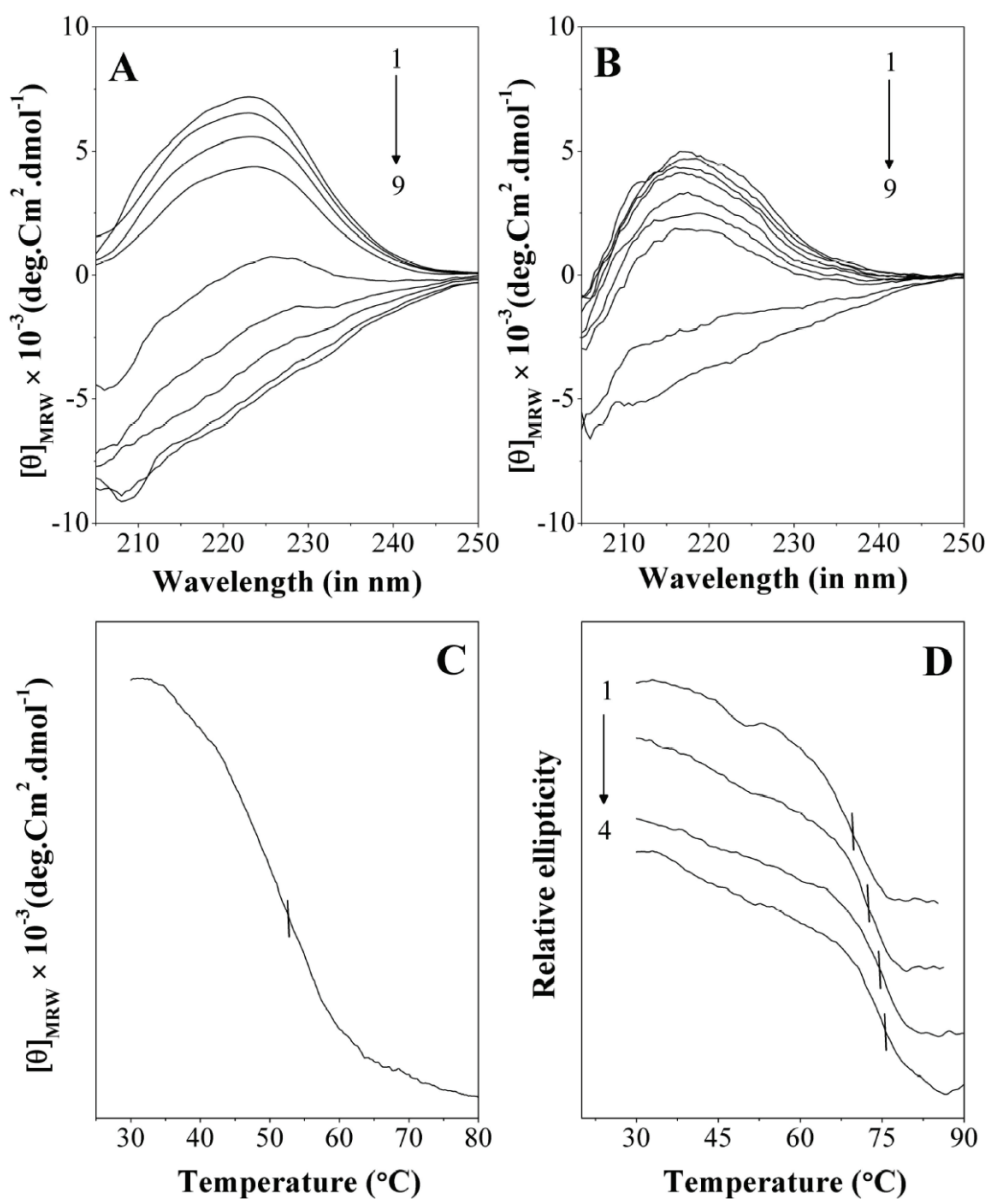
**Fig. 5.7:  Effect of heparin binding on the thermal stability of PDC-109**. Far-UV CD spectra of PDC-109 at various temperatures in the absence and presence of heparin (0.2 mM) are shown in **A** and **B**, respectively.  Arrow represents the direction of increase in the temperature.  The temperatures used are: (1) 25 $^{\circ}$C, (2) 30 $^{\circ}$C, (3) 35 $^{\circ}$C, (4) 40 $^{\circ}$C, (5) 50 $^{\circ}$C, (6) 55 $^{\circ}$C, (7) 60 $^{\circ}$C, (8) 70 $^{\circ}$C and (9) 80 $^{\circ}$C.  Thermal scans of the protein in the absence and presence of varying concentrations of heparin, at a fixed wavelength of 289 nm (near-UV) as a function of temperature, are shown in panel (**C**) and (**D**).  The concentrations of heparin used are:  (1) 3.0 µM, (2) 5 µM, (3) 10 µM and (4) 20 µM.

In order to investigate the relation between the thermal stability of PDC-109 and heparin concentration, CD spectral intensities were recorded at a fixed wavelength corresponding to the maximum intensity as a function of temperature.  The temperature dependence of CD signal intensity at 289 nm (near-UV) and 223 nm (far-UV), gave sigmoidal curves centered at ~55 °C, corresponding to the mid-point of the unfolding transition of the protein (Figs. 5.6C and 5.7C).  With increasing concentrations of heparin the transition midpoint shifted towards higher temperatures (70 to 78 ºC) (Figs. 5.6D and 5.7D).  Changes in the transition midpoints of near and far-UV spectral intensities were plotted against heparin concentration (Figs. 5.8A and B), which clearly show that heparin stabilizes both the secondary and tertiary structures of PDC-109 in a concentration dependent manner.
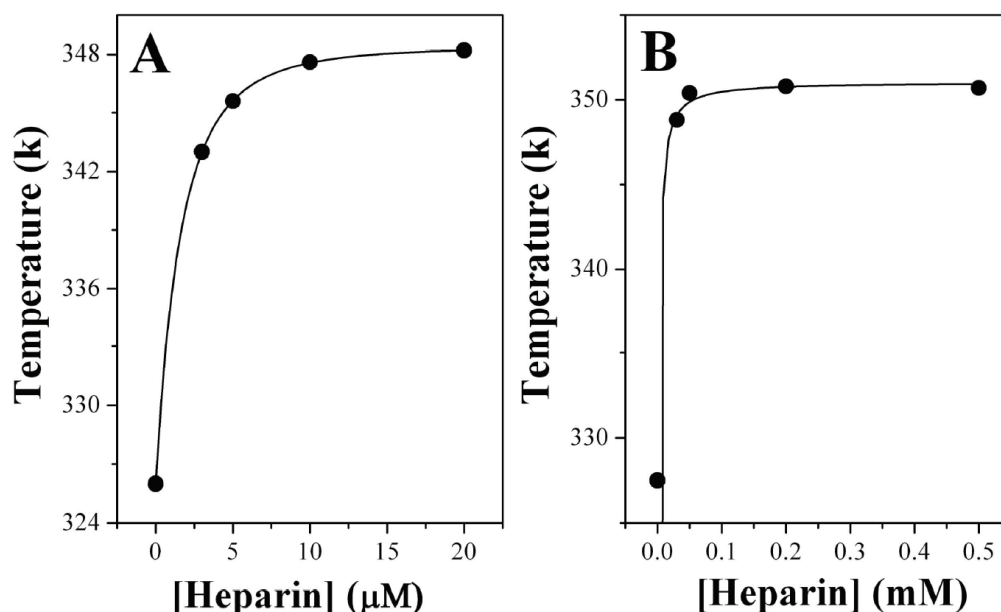


**Fig.5.8:  Heparin induced stabilization of PDC-109.**  Plots of transition temperatures obtained from the far and near-UV CD spectra obtained in the presence of different concentrations of heparin (see Fig. 5.7C & D and Fig. 5.6C & D) are given in **A** and **B**, respectively.

## 5.5. A Working Model

Our ITC and DSC results demonstrate that several molecules of PDC-109 can simultaneously bind to a single molecule of heparin, resulting in the formation of large oligomeric structures. This indicates that binding to heparin increases the local density of PDC-109, which is in good agreement with results obtained with other heparin binding proteins (Ziegler and Seelig, 2004). Increased local density of the protein should enhance its functional activity and this is consistent with the fact that sperm incubated in-vitro with heparin display higher fertilizing capacity than sperm incubated without heparin (Parrish *et al.*, 1985; 1986a; Thérien *et al.*, 1995). In the female genital tract when seminal plasma comes in contact with oviductal fluid, PDC-109 interacts with heparin with a subsequent increase in its local concentration, which can capacitate the sperm more effectively than native PDC-109.

In summary, the energetics of interaction of PDC-109 with heparin has been investigated by isothermal titration calorimetry and differential scanning calorimetry. ITC results suggest that ~11.0 molecules of PDC-109 can bind to a single molecule of heparin and this interaction is predominantly driven by a large positive entropic contribution. A decrease in the heparin/PDC-109 affinity with increasing pH/ionic strength indicates that the heparin/PDC-109 interaction is governed by electrostatic forces. Results of DSC studies suggest the presence of four types of PDC-109/heparin oligomeric clusters, which maintain their integrity even at elevated temperatures (>70 ºC). Both DSC and CD studies suggest that the structure of PDC-109 is stabilized by heparin in a concentration dependent manner. Overall the present studies explore the energetics of the heparin/PDC-109 interaction and shed light on the molecular level details of this interaction, which plays a vital role in sperm capacitation.

# Chapter 6

## General Discussion and Conclusions

## 6.1. General Discussion and Conclusions

The work embodied in this thesis "*Biochemical and Biophysical Investigations on the Ligand Binding and Chaperone-like Activities of PDC-109*" presents results from investigations on several aspects related to the involvement of PDC-109 in sperm capacitation or fertilization.  PDC-109 is the major protein of bovine seminal plasma, which has been reported to participate in sperm capacitation by inducing the efflux of phospholipids and cholesterol from the outer membrane of spermatozoa (Thérien *et al.,* 1998; Moreau *et al.,* 1998).  Although the interaction of PDC-109 with phospholipids has been investigated by various research groups, a knowledge of the thermodynamic forces governing this interaction is scarce.  Also, direct evidence showing PDC-109-induced membrane disruption is lacking. *Chapter 2* presents some new aspects related to PDC-109/phospholipid interactions and also provides direct and conclusive evidences for the earlier observations. Isothermal titration calorimetric experiments, aimed at investigating the thermodynamic parameters for the interaction of PDC-109 with DMPC and DMPG vesicles, indicate that both the interactions are endothermic in nature and are driven predominantly by entropic forces.  These results are in contrast to the interaction of PDC-109 with POPC (1-palmitoyl-2-oleoyl-sn-glycero-3-phosphocholine) membranes, which shows endothermic behavior at low temperature and exothermic at higher temperatures (Lassiseraye *et al.,* 2008).  This difference in the nature of interaction could be attributed to the different phase structures of the lipids used in the two studies.  The experiments with POPC membranes were carried out in the liquid crystalline state, whereas in the present study DMPC vesicles are used in their gel phase.  The results obtained suggest that PDC-109 binds to DMPC vesicles more strongly than DMPG, which is in good agreement with the earlier reports (Thomas *et al.*, 2003; Swamy, 2004).  Experiments aimed at investigating

the effect of pH on the interaction of PDC-109 with phospholipids suggest that PDC-109/DMPG interaction is more susceptible to the pH variation than PDC-109/DMPC interaction.  The affinity of PDC-109 with DMPC increases with pH, which is physiologically relevant in view of the basic nature of seminal plasma.

AFM experiments suggest that PDC-109 disrupts supported bilayers of choline phospholipids in a concentration dependent manner and that cholesterol provides partial stabilization to the membrane against the action of PDC-109.  Overall, these results support a model in which interaction of PDC-109 with cell plasma membranes and model membranes containing choline phospholipids results in their destabilization, leading to the formation of small lipid/protein particles (Deanoyers and Manjunath, 1992; Moreau and Manjunath, 1999; Gasset *et al.*, 2000; Ramkrishnan *et al.*, 2001).  This process is strongly dependent on the lipid composition, wherein the presence of choline phospholipids at high concentration leads to destabilization of the membrane whereas the ability of PDC-109 to disrupt membranes containing other phospholipids such as phosphatidylglycerol is significantly lower and incorporation of cholesterol affords a partial protection to the lamellar structure of the membrane. These results are in agreement with the earlier reports (Gasset *et al.*, 2000; Ramkrishnan *et al.*, 2001).

In the studies reported in *Chapter 3* various biophysical and biochemical approaches have been employed to demonstrat that PDC-109 can function as a molecular chaperone.  To the best of the author's knowledge this is the first study reporting the chaperone-like activity of any seminal plasma protein in animal kingdom.  The high abundance, polydisperse nature and reversibility of thermal unfolding of PDC-109 suggest significant similarities to chaperone-like proteins such as spectrin, α-crystallin and α-synuclein.  In view of this, a series of aggregation and activity assays have been performed using a number of target proteins such as ADH, LDH, β-crystallin, insulin, GST and G6PD.  The results

obtained clearly demonstrated that PDC-109 functions as a molecular chaperone *in vitro*. Interestingly, the results of the present study showed that presence of PDC-109 not only provides protection to target proteins under stress conditions but also directs native proteins to a better conformation even under physiological conditions. This is evident from G6PD activity assay, where the activity of G6PD in the presence of PDC-109 (at 4 ºC) was observed to be higher than its activity under native conditions, in the absence of PDC-109. These observations suggest that PDC-109 may prevent the proteins of seminal plasma to undergo denaturation both under stressful and physiological conditions, which could be of significant importance in fertilization. Studies aimed at investigating the effect of PDC-109 on the refolding of completely denatured target proteins suggest that PDC-109 prevents their irreversible aggregation, but does not assist their refolding to the native form, indicating that it creates a reservoir of folding intermediates of the substrate proteins (Ehrnsperger *et al.*, 1997; Nakamoto and Vigh, 2007). The substrate proteins of such reservoirs could be directed to a functionally active conformation by the protein alone or with the help of other chaperones upon arrival of favorable conditions.

It is known that PDC-109 exists as polydisperse aggregates under native conditions, which are dissociated to yield dimers or monomers in the presence of phoshoryl choline or high salt concentrations (Gasset *et al.*, 1997). These conditions have been utilized in the present study to probe the role of polydispersity in the chaperone-like activity of PDC-109. The results obtained clearly suggested that dissociation of oligomeric structures leads to the loss of CLA of PDC-109. ANS binding experiments, which are used to probe the hydrophobic surfaces, suggest that hydrophobicity of PDC-109 is decreased in the presence of phosphorylcholine (*Chapter 4*). This suggests that hydrophobicity also could be responsible for the CLA of PDC-109 because surface exposure of hydrophobic

residues have been reported to be important for the CLA of several other chaperone-like proteins (Das and Surewicz, 1995; Datta and Rao, 1999).

Since PDC-109 binds to phospholipid membranes and facilitates their disruption, it is of interest to study the possible role of such interactions on the CLA. In view of this experiments have been carried out with a number of target proteins such as ADH, LDH and carbonic anhydrase. The results obtained suggested that presence of DMPC – which is specifically recognized by PDC-109 – resulted in a multifold increase in the CLA of the protein, whereas interaction of PDC-109 with DMPG did not yield any significant alteration in the CLA (*Chapter 4*). There could be two possible explanations for the above findings. One is the conformational changes in PDC-109, induced by its interaction with DMPC, which can modulate the CLA and CD studies are in agreement with it. The other explanation is based on PDC-109 induced partial solubilization of the vesicles and formation of lipid-protein particles of various sizes. These lipid/protein recombinants may have large exposed hydrophobic surfaces, which may alter the CLA. This was further elucidated by hydrophobic ligand binding experiments. ANS and bisANS binding to PDC-109−phospholipid mixture revealed an enhanced exposure of hydrophobic surfaces for DMPC/PDC-109 complexes (as compared to native PDC-109), whereas no significant alteration was observed for the DMPG/PDC-109 complexes. ITC studies from our laboratory are also in support of the above conclusion and show that binding of PDC-109 to DMPC model membranes results in a large positive heat capacity change ($\Delta C_p$), which suggested that large hydrophobic surfaces are exposed to water upon binding of PDC-109 to DMPC membranes (Anbhazagan, 2005). Binding of DMPG had only a marginal influence on the CLA of PDC-109, which could be attributed to its low affinity for PDC-109 as compared to DMPC.

Since cholesterol is known to provide rigidity to membranes, it is of interest to probe the effect of cholesterol incorporation into phospholipid vesicles, on the CLA. Results of experiments carried out using DMPC vesicles containg 25 mol% cholesterol clearly suggest that the CLA of DMPC/Cholesterol−PDC-109 mixture was lower than that of DMPC-PDC-109 recombinants. Since PDC-109 cannot disrupt the DMPC/cholesterol membranes as efficiently as it does with DMPC vesicles, the extent of the exposed hydrophobic surfaces in them will be lesser than upon interaction of PDC-109 with membranes made up of DMPC alone. The CLA of PDC-109 in the presence of DMPC/cholesterol mixture is therefore relatively less as compared to that of PDC-109/DMPC recombinant. The results of AFM studies (*Chapter 2*) are in good agreement with above explanation. The observation of CLA by PDC-109 in the presence of phospholipids also mimics the *in vivo* environment where PDC-109 binds to the outer leaflet of the sperm plasma membrane, which makes the experiments of this study physiologically relevant.

Another important aspect related to the involvement of PDC-109 in sperm capacitation is its interaction with glycosaminoglycans (e.g. heparin), which have been reported to increase the sperm capacitation (Thérien *et al.*, 1995). However a molecular level understanding of the role of heparin in BSP induced sperm capacitation is not clear. In view of this, the interaction of PDC-109 with heparin has been investigated using various biophysical techniques (*Chapter 5*). Thermodynamics of PDC-109/heparin interaction was studied using ITC and DSC. The results obtained suggest that this interaction is endothermic in nature and is predominantly driven by entropic contributions. This interaction was observed to be sensitive to the pH and ionic strength of the medium, with the affinity decreasing at higher pH and ionic strength. Heparin is a negatively charged glycosaminoglycan, whereas PDC-109 is an acidic protein with an isoelectric point (pI) of ~5.0. When pH of the medium is increased, PDC-109 becomes increasingly

negatively charged and due to electrostatic repulsion affinity is weakened significantly. These observations are in good agreement with the earlier reports (Calvete *et al.*, 1999). ITC and DSC results demonstrated that several molecules of PDC-109 can simultaneously bind to a single molecule of heparin, resulting in the formation of large oligomeric structures. This indicates that binding to heparin increases the local density of PDC-109, which is in good agreement with results obtained with other heparin binding proteins (Ziegler and Seelig, 2004). Increased local density of the protein should enhance its functional activity and this is consistent with the observation that sperm incubated *in vitro* with heparin display higher fertilizing capacity than sperm incubated without heparin (Parrish *et al.*, 1985; Parrish *et al.*, 1986a; Thérien *et al.*, 1995). Based on the above results it is proposed that in female genital tract when seminal plasma comes in contact with oviductal fluid, PDC-109 interacts with heparin with a subsequent increase in its local concentration. PDC-109, with increased local population, can capacitate the sperm in a more effective manner rather than functioning alone.

## 6.2. Future Prospects

This study explores a new functional aspect of PDC-109, i.e. chaperone-like activity, which could be of significant relevance in the process of fertilization. The sequence alignment of PDC-109 with the seminal plasma proteins from other species shows considerable sequence homology (*Chapter 3*), which indicates that chaperone-like proteins are likely to exist in other mammalian species as well. These proteins can be investigated further to characterize their putative chaperone-like activity. In the present study, the chaperone-like activity has been correlated to phospholipid binding and it has been shown that the CLA of PDC-109 increases quite significantly upon binding to DMPC membranes. Since many chaperones such as Hsp 12, spectrin, have been shown to interact with phospholipid

membranes (Welker *et al.*, 2010; Bhattacharyya *et al.*, 2004), the effect of membrane binding on their CLA could be investigated which will unfold a new area of research in chaperone biology.

# References
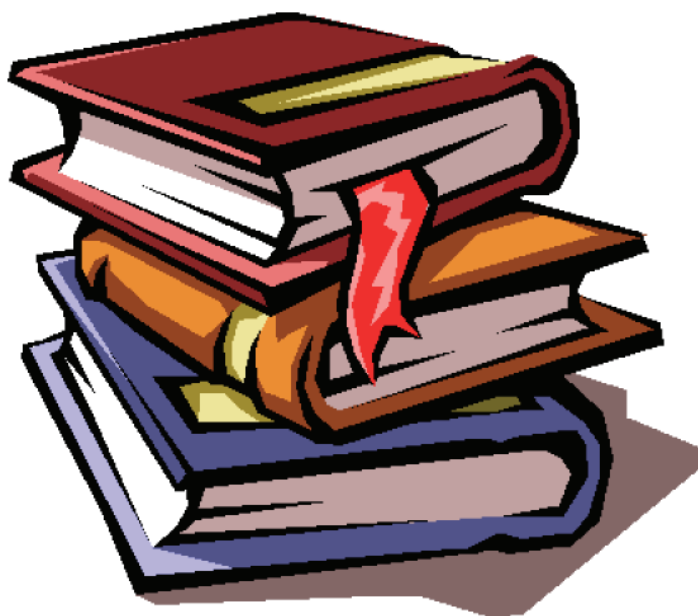
150  *References…*

# REFERENCES

Abbott, E. J. and Firestone, F. A. (1933) in Specifying surface quality. *Mechanical Engineering 55*, 569–572.

Anbazhagan, V. (2005) Biophysical investigations on the interaction of the major bovine seminal plasma protein, PDC-109 with model membranes. Doctoral Thesis, University of Hyderabad.

Anbazhagan, V. and Swamy, M. J. (2005) Thermodynamics of phosphorylcholine and lysophosphatidylcholine binding to the major protein of bovine seminal plasma, PDC-109. *FEBS Lett. 579*, 2933−2938.

Anbazhagan, V., Damai, R. S., Paul, A. and Swamy, M. J. (2008) Interaction of the major protein from bovine seminal plasma, PDC-109 with phospholipid membranes and soluble ligands investigated by fluorescence approaches. *Biochim. Biophys. Acta 1784*, 891−899.

Arnoult, C., Zeng, Y. and Florman, H. M. (1996) ZP3-dependent activation of sperm cation channels regulates acrosomal secretions during mammalian fertilization. *J. Cell Biol. 134*, 637−645.

Auluck, P. K., Chan, H. Y., Trojanowski, J. Q., Lee, V. M. and Bonini, N. M. (2002) Chaperone suppression of α-synuclein toxicity in a Drosophila model for Parkinson's disease. *Science 295*, 865–868.

Austin, C. R. (1952) The capacitation of the mammalian sperm. *Nature (Lond), 170*, 326.

Baker, M. E. (1985) The PDC-109 protein from bovine seminal plasma is similar to the gelatin-binding domain of bovine fibronectin and a kringle domain of human tissue-type plasminogen activator. *Biochem. Biophys. Res. Commun. 130*, 1010–1014.

Barrel, J. M., Broadley, S. A., Schaffar, G. and Hartl, F. U. (2004) Roles of molecular chaperones in protein misfolding diseases. *Semin Cell Dev. Biol. 15*, 17–29.

Bergeron, J. J., Brenner, M. B., Thomas, D. Y. and Williams, D. B. (1994) Calnexin: a membrane-bound chaperone of the endoplasmic reticulum. *Trends Biochem. Sci. 19*, 124–128.

Bergeron, A., Villemure, M., Lazure, C. and Manjunath, P. (2005) Isolation and characterization of the major proteins of ram seminal plasma. *Mol. Reprod. Dev. 71*, 461−470.

Berke, S. J. S. and Paulson, H. L. (2003) Protein aggregation and the ubiquitin proteasome pathway: gaining the upper hand on neurodegeneration. *Curr. Opin. Genet. Dev. 13*, 253–261.

Bhattacharyya, M., Ray, S., Bhattacharya, S. and Chakrabarti, A. (2004) Chaperone activity and prodan binding at the self-associating domain of erythroid spectrin. *J. Biol. Chem. 53,* 55080–55088.

Bleil, J. D. and Wasserman, P. M. (1983) Sperm-egg interaction in the mouse: sequence of events and induction of the acrosome reaction by a zona pellucida glycoprotein. *Dev. Biol. 95*, 317−324.

Bochkareva, E. S., Lissin, N. M., Flynn, G. C., Rothman, J. E. and Girshovich, A. S. (1992) Positive cooperativity in the functioning of molecular chaperone GroEL. *J. Biol. Chem. 267*, 6796−6800.

Boisvert, M., Bergeron, A., Lazure, C. and Manjunath, P. (2004) Isolation and characterization of gelatin-binding bison seminal vesicle secretory proteins. *Biol. Reprod. 70*, 656−661.

Borkovich, K. A., Farrelly, F. W., Finkelstein, D. B., Taulien, J. and Lindquist, S. (1989) Hsp82 is an essential protein that is required in higher concentrations for growth of cells at higher temperatures. *Mol. Cell Biol. 9*, 3919–3930.

Brandts, J. F. and Lin, L-N. (1990) Study of strong to ultralight protein interactions using differential scanning calorimetry. *Biochemistry 29*, 6927−6940.

Calvete, J. J., Raida, M., Sanz, L., Wempe, F., Scheit, K. H., Romer, A. and Töpfer-Petersen, E. (1994) Localization and structural characterization of an oligosaccharide O-linked to bovine PDC-109. Quantitation of the glycoprotein in

seminal plasma and on the surface of ejaculated and capacitated spermatozoa. *FEBS Lett. 350,* 203−206.

Calvete, J. J., Mann, K., Schafer, W., Sanz, L., Reinert, M., Nessau, S., Raida, M. and Topfer-Petersen, E. (1995) Amino acid sequence of HSP-1, a major protein of stallion seminal plasma: effect of glycosylation on its heparin- and gelatin-binding capabilities. *Biochem. J. 310,* 615−622.

Calvete, J. J., Paloma, F. V., Sanz, L. and Romero, A. (1996) A procedure for the large-scale isolation of major bovine seminal plasma proteins. *Protein Expr. Purif. 8,* 48−56.

Calvete, J. J., Raida, M., Gentzel, M., Urbanke, C., Sanz, L. and Topfer-Petersen, E. (1997) Isolation and characterization of heparin and phosphorylcholine binding proteins of boar and stallion seminal plasma. Primary structure of porcine pB1. *FEBS Lett. 407,* 201−206.

Calvete, J. J., Campanero-Rhodes, M. A., Raida, M. and Sanz, L. (1999) Characterization of the conformational and quaternary structure-dependent heparin-binding region of bovine seminal plasma protein PDC-109. *FEBS Lett. 444,* 260−264.

Chakrabarti, A., Bhattacharya, S., Ray, S. and Bhattacharya, M. (2001) Binding of a denatured heme protein and ATP to erythroid spectrin. *Biochem. Biophys. Res. Commun. 282,* 1189–1193.

Chandonnet, L., Roberts, K. D., Chapdelaine, A. and Manjunath, P. (1990) Identification of heparin-binding proteins in bovine seminal plasma. *Mol. Reprod. Dev. 26,* 313–318.

Chang, M. C. (1951) Fertilizing capacity of spermatozoa deposited into the fallopian tubes. *Nature 168,* 697−698.

Chaudhuri, T. K. and Paul, S. (2006) Protein-misfolding diseases and chaperone-based therapeutic approaches. *FEBS J. 273,* 1331−1349.

Chernoff, Y. O., Lindquist, S. L., Ono, B., Inge-Vechtomov, S. G. and Liebman, S. W. (1995) Role of the chaperone protein Hsp104 in propagation of the yeast prion-like factor [psi+]. *Science 268,* 880–884.

154 *References…*

Clermont, Y., Oko, R. and Hermo, L. (1993) Cell biology of mammalian spermiogenesis. In: *Cell and Molecular Biology of the Testis* (Eds: Desjardans, C. and Ewing, J.), Oxford University Press, New York, pp. 332−376.

Cohen, F. E. and Kelly, J. W. (2003) Therapeutic approaches to protein misfolding diseases. *Nature 426*, 905–909.

Cyr, D. M. (1995) Cooperation of the molecular chaperone Ydj1 with specific Hsp70 homologs to suppress protein aggregation. *FEBS Lett. 359*, 129–132.

Damai, R. S., Anbazhagan, V., Rao, K. B. and Swamy, M. J. (2009) Fluorescence studies on the interaction of choline-binding domain B of the major bovine seminal plasma protein, PDC-109 with phospholipid membranes. *Biochim. Biophys. Acta 1794*, 1725−1733.

Damai, R. S., Sankhala, R. S., Anbazhagan, V. and Swamy, M. J. (2010) $^{31}$P-NMR and AFM studies on the destabilization of cell and model membranes by the major bovine seminal plasma protein, PDC-109. *IUBMB Life 62*, 841−851.

Das, K. P. and Surewicz, W. K. (1995) On the substrate specificity of α-crystallin as a molecular chaperone. *Biochem. J. 311*, 367−370.

Datta, S. A. and Rao, C. M. (1999) Differential temperature-dependent chaperone-like activity of αA- and αB-crystallin homoaggregates. *J. Biol. Chem. 274*, 34773−34778.

De Crouy-Chanel, A., Kohiyama, M. and Richarme, G. (1995) A novel function of *Escherichia coli* chaperone DnaJ. Protein-disulfide isomerase. *J. Biol. Chem. 270*, 22669–22672.

De Krester, D. M. and Kerr, J. B. (1994) The cytology of the testis. In: *Physiology of Reproduction* (Eds: Knobil, E and Neill, J.), Raven Press, New York, pp. 117−290.

Denis, M. and Gustafsson, J. (1989) The Mr approximately 90,000 heat shock protein: an important modulator of ligand and DNA-binding properties of the glucocorticoid receptor. *Cancer Res. 49*, 2275s–2281s.

Desnoyers, L. and Manjunath, P. (1992) Major proteins of bovine seminal plasma exhibit novel interactions with phospholipids. *J. Biol. Chem. 267*, 10149–10155.

Dobson, C. M. (1999) Protein misfolding, evolution and disease. *Trends Biochem. Sci. 24*, 329–332.

Dobson, C. M. and Karplus, M. (1999) The fundamentals of protein folding: bringing togother theory and experiment. *Curr. Opin. Struct. Biol. 9*, 92−101.

Duan, C. and Goldberg, E. (2003) Inhibition of lactate dehydrogenase C4 (LDH-C4) blocks capacitation of mouse sperm in vitro. *Cytogenet. Genome. Res. 103*, 352–359.

Ehrnsperger, M., Gräber, S., Gaestel, M. and Buchner, J. (1997) Binding of non-native protein to Hsp25 during heat shock creates a reservoir of folding intermediates for refolding. *EMBO J. 16*, 221–229.

Ehrnsperger, M., Gaestel, M. and Buchner, J. (1998) Structure and function of small heat-shock proteins. In: *Molecular Chaperones in the Life Cycle of Proteins* (Eds: Fink, A. L. and Goto, Y.), Dekker, New York, pp. 533–575.

El. Feninat, F., Elouatik, S., Ellis, T. H., Sacher, E. and Stangel, I. (2001) Quantitative assessment of surface roughness as measured by AFM: application to polished human dentin. *Appl. Surf. Sci. 183*, 205–215.

Ellis, R. J. (1987) Proteins as molecular chaperones. *Nature 328*, 378−379.

Ellis, R. J. and van der Vies, S. M. (1991) Molecular chaperones. *Annu. Rev. Biochem. 60,* 321−347.

Esch, F. S., Ling, N. C., Bohlen, P., Ying, S. Y. and Guillemin, R. (1983) Primary structure of PDC-109, a major protein constituent of bovine seminal plasma. *Biochem. Biophys. Res. Commun. 113*, 861–867.

Evans, D. L., Marshall, C. J., Christey, P. B. and Carrell, P. W. (1992) Heparin binding site, conformational change, and activation of antithrombin. *Biochemistry 31*, 12629–12642.

Fath, M., VanderNoot, V., Kilpeläinen, I., Kinnunen, T., Rauvala, H. and Linhardt, R. J. (1999) Interaction of soluble and surface-bound heparin binding growth-associated molecule with heparin. *FEBS Lett. 454*, 105−108.

Fayet, O., Ziegelhoffer, T. and Georgopoulos, C. (1989) The GroES and GroEL heat shock gene products of *Escherichia coli* are essential for bacterial growth at all temperatures. *J. Bacteriol. 171*, 813–818.

Fink, A. L. (1999) Chaperone mediated protein folding. *Physiol. Rev. 79*, 425–442.

Florman, H. M., Arnoult, C., Kazan, I. G., Li, C. and O'Toole, C. M. B. (1998) A perspective on the control of mammalian fertilization by egg-activated ion channels in sperm: a tale of two channels. *Biol. Reprod. 59*, 12−16.

Forloni, G., Terreni, L. and Bertani, I. (2002) Protein misfolding in Alzheimer's and Parkinson's disease: genetics and molecular mechanisms. *Neurobiol. Aging 23*, 957–976.

Fraser, L. R. (1995) Cellular biology of capacitation and acrosome reaction. *Hum. Reprod. Suppl. 10*, 22−30.

Freeman, B. C. and Morimoto, R. I. (1996) The human cytosolic molecular chaperones Hsp90, Hsp70 (Hsc70) and Hdj-1 have distinct roles in recognition of a non-native protein and protein refolding. *EMBO J. 15*, 2969–2979.

Games, D., Adams, D. and Alessandrini, R. (1995) Alzheimer-type neuropathology in transgenic mice overexpressing V717F β-amyloid precursor protein. *Nature 373*, 523–527.

Gasset, M., Saiz, J. L., Sanz, L., Gentzel, M., Töpfer-Petersen, E. and Calvete, J. J. (1997) Conformational features and thermal stability of bovine seminal plasma protein PDC-109 oligomers and phosphorylcholine-bound complexes. *Eur. J. Biochem. 250*, 735–744.

Gasset, M., Magdaleno, L. and Calvete, J. J. (2000) Biophysical study of the perturbation of model membrane structure caused by seminal plasma protein PDC-109. *Arch. Biochem. Biophys. 374*, 241−247.

Georgopoulos, C. P., Hendrix, R. W., Casjens, S. R. and Kaiser, A. D. (1973) Host participation in bacteriophage lambda head assembly. *J. Mol. Bid. 76*, 45−60.

Gething, M. J. and Sambrook, J. (1992) Protein folding in the cell. *Nature 355*, 33–45.

Glover, J. R., Schirmer, E. C., Singer, M. A. and Lindquist, S. L. (1998) Hsp104. In: *Molecular Chaperones in the Life Cycle of Proteins*. (Eds: Fink, A. L. and Goto, Y.), Dekker, New York, pp. 193–224.

Goloubinoff, P., Mogk, A., Peres Ben Zvi, A., Tomoyasu, T. and Bukau, B. (1999) Sequential mechanism of solubilization and refolding of stable protein aggregates by a bichaperone network. *Proc. Natl. Acad. Sci. USA 96*, 13732–13737.

Grandbois, M., Clausen-Schaumann, H. and Gaub, H. (1998) Atomic force microscope imaging of phospholipid bilayer degradation by Phospholipase-A$_2$. *Biophys. J. 74*, 2398−2404.

Gray, T. E. and Fersht, A. R. (1991) Cooperativity in ATP hydrolysis by GroEL is increased by GroES. *FEBS Lett. 292*, 254−258.

Greube, A., Müller, K., Töpfer-Petersen, E., Herrmann, A. and Müller, P. (2001) Influence of the bovine seminal plasma protein PDC-109 on the physical state of membrane. *Biochemistry 40*, 8326–8334.

Guraya, S. S. (1965) Histochemical studies on spermateleosis in sheep, goat and buffalo. *Cellule 65*, 367−378.

Habig, W. H., Pabst, M. J. and Jakoby, W. B. (1974) Glutathione-S-transferase: the first enzymatic step in mercapturic acid formation. *J. Biol. Chem. 249*, 7130–7139.

Harper, M. J. K. (1994) Gamete and zygote transport. In: *Physiology of Reproduction* (Eds: Knobil, E. and Neill, J. D.), Raven Press, New York, pp. 123–187.

Harrison, R. A. P. (1996) Capacitation mechanisms, and the role of capacitation as seen in eutherian mammals. *Reprod. Fertil. Dev. 8*, 581–596.

Hartl, F. U. (1996) Molecular chaperones in cellular protein folding. *Nature 381*, 571–579.

Hartl, F. U. and Hayer-Hartl, M. (2002) Molecular chaperones in the cytosol: from nascent chain to folded protein. *Science 295*,1852−1858.

Hawe, A., Rispens, T., Herron, J. N. and Jiskoot, W. (2010) Probing bis-ANS binding sites of different affinity on aggregated IgG by steady-state fluorescence, time-resolved fluorescence and isothermal titration calorimetry. *J. Pharm. Sci.* published online (doi: 10.1002/jps.22368).

Hendershot, L., Wei, J., Gaut, J., Melnick, J., Aviel, S. and Argon, Y. (1996) Inhibition of immunoglobulin folding and secretion by dominant negative BiP ATPase mutants. *Proc. Natl. Acad. Sci. USA 93*, 5269–5274.

Hendrix, R. W. (1979) Purification and properties of GroE, a host protein involved in bacteriophage assembly. *J. Mol. Biol. 129*, 375−392.

Hightower, L. E. and Hendershot, L. M. (1997) Molecular chaperones and the heat shock response at Cold Spring Harbor. *Cell Stress Chaperones 2*, 1–11.

Hill, R. B., Flanagan, J. M. and Prestegard, J. H. (1995) $^1$H and $^{15}$N magnetic resonance assignments, secondary structure, and tertiary fold of *Escherichia coli* DnaJ (1–78). *Biochemistry 34*, 5587–5596.

Höhfeld, J., Cyr, D. M. and Patterson, C. (2001) From the cradle to the grave: molecular chaperones that may choose between folding and degradation. *EMBO rep. 10*, 885−890.

Hohn, T., Hohn, B., Engel, A., Wurtz, M. and Smith, P. R. (1979) Isolation and characterization of the host protein GroE involved in bacteriophage lambda assembly. *J. Mol. Biol. 129*, 359−373.

Hooper, N. M. (2001) Could inhibition of the proteasome cause mad cow disease? *Trends Biotechnol. 21*, 144–145.

Horwitz, J. (1992) Alpha-crystallin can function as a molecular chaperone. *Proc. Natl. Acad. Sci. USA 89*, 10449–10453.

Ignotz, G., Lo, M. C., Perez, C. L., Gwathmey, T. M. and Suarez, S. S. (2001) Characterization of a fucose binding protein from bull sperm and seminal plasma that may be responsible for formation of oviductal sperm reservoir. *Biol. Reprod. 64*, 1806−1811.

Ikawa, M., Wada, I., Kominami, K., Watanabe, D., Toshimori, K., Nishimune, Y. and Okabe, M. (1997) The putative chaperone calmegin is required for sperm fertility. *Nature 387*, 607–611.

Kavitha, M., Sultan, N. A. M. and Swamy, M. J. (2009) Fluorescence studies on the interaction of hydrophobic ligands with *Momordica charantia* (bitter gourd) seed lectin. *J. Photochem. Photobiol. B: Biol. 94*, 59−64.

Kerem, B., Rommens, J. M., Buchanan, J. A., Markiewicz, D., Cox, T. K., Chakravarti, A., Buchwald, M. and Tsui, L. C. (1989) Identification of the cystic fibrosis gene: genetic analysis. *Science 245*, 1073–1080.

Kim, H. J., Choi, M. Y., Kim, H. J. and Llians, M. (2010) Conformational dynamics and ligand binding in the multi-domain protein PDC109. *PLoS ONE 5*, e9180.

Kim, T. D., Paik, S. R., Yang, C. H. and Kim, J. (2000) Structural changes in α-synuclein affect its chaperone like activity in vitro. *Protein Sci. 9*, 2489–2496.

Kopito, R. R. (1999) Biosynthesis and degradation of the CFTR. *Physiol. Rev. 79*, S167–S173.

Kopito, R. R. (2000) Aggresomes, inclusion bodies and protein aggregation. *Trends Cell Biol. 10*, 524–530.

Kumar, M. S., Reddy, P. Y., Sreedhar, B. and Reddy, G. B. (2005) αB-Crystallin assisted reactivation of glucose-6-phosphate dehydrogenase upon refolding. *Biochem. J. 391*, 335−341.

Krupakar, J., Swaminathan, C. P., Das, P. K., Surolia, A. and Podder, S. K. (1999) Calorimetric studies on the stability of the ribosome-inactivating protein abrin II : effects of pH and ligand binding. *Biochem. J. 338*, 273−279.

Kyte, J. and Doolittle, R. F. J. (1982) A simple method for displaying the hydropathic character of a protein. *J. Mol. Biol. 157*, 105−132.

Laemmli, U. K. (1970) Cleavage of structural proteins during assembly of bacteriophage T4. *Nature 227*, 680−685.

Lane, M-E., Thérien, I., Moreau, R. and Manjunath, P. (1999) Heparin and high-density lipoprotein mediate bovine sperm capacitation by different mechanisms. *Biol. Reprod. 60*, 169−175.

Langer, T., Lu, C., Echols, H., Flanagan, J., Hayer, M. K. and Hartl, F. U. (1992a) Successive action of DnaK, DnaT and GroEL along the pathway of chaperone-mediated protein folding. *Nature 356*, 683−689.

Langer, T., Pfeifer, G., Martin, J., Baumeister, W. and Hartl, F. U. (1992b) Chaperonin-mediated protein folding: GroES binds to one end of the GroEL cylinder, which accommodates the protein substrate within its central cavity. *EMBO J. 11*, 4757−4765.

Laskey, R. A., Honda, B. M., Mills, A. D. and Finch, J. T. (1978) Nucleosomes are assembled by an acidic protein which binds histones and transfers them to DNA. *Nature 275*, 416–20.

Lassiseraye, D., Courtemanche, L., Bergeron, A., Manjunath, P. and Lafleur, M. (2008) Binding of bovine seminal plasma protein BSP-A1/A2 to model membranes: Lipid specificity and effect of the temperature. *Biochim. Biophys. Acta 1778*, 502−513.

Laufen, T., Zuber, U., Buchberger, A. and Bukau, B. (1998) DnaJ proteins In: *Molecular Chaperones in the Life Cycle of Proteins* (Eds: Fink, A. L. and Goto, Y.), Dekker, New York, pp. 241–274.

Lee, D. H., Sherman, M. Y. and Goldberg, A. L. (1996) Involvement of the molecular chaperone Ydj1 in the ubiquitin-dependent degradation of short-lived and abnormal proteins in *Saccharomyces cerevisiae*. *Mol. Cell. Biol. 16*, 4773–4781.

Lee, G. J., Roseman, A. M., Saibil, H. R. and Vierling, E. (1997) A small heat shock protein stably binds heat-denatured model substrates and can maintain a substrate in a folding-competent state. *EMBO J. 16*, 659–671.

Liang, J. N. and Li, X. Y. (1991) Interaction and aggregation of lens crystallins. *Exp. Eye Res. 53*, 61–66.

Liberda, J., Kraus, M., Ryslava, H., Vlaskova, M., Jonakova, V. and Ticha, M. (2001) D-fructose binding proteins in bull seminal plasma. Isolation and characterization. *Folia Biol. (Praha) 47*, 113−119.

Lievano, A., Santi, C. M., Serrano, J., Trevano, C. L., Bellve, A. R., Hernandez-Cruz, A. and Dorszon, A. (1996) A T-type $Ca^{2+}$ channels and $\alpha_{1E}$ expression in spermatogenic cells and their possible relevance to the sperm acrosome reactions. *FEBS Lett. 388*, 150−154.

Lindquist, S. and Craig, E. A. (1988) The heat-shock proteins. *Annu. Rev. Genet. 22*, 631–677.

Lis, L. J., McAlister, M., Fuller, N., Rand R. P. and Parsegian, V. A. (1982) Interactions between neutral phospholipid bilayer membranes. *Biophys. J. 37*, 657−665.

Lowry, O. H., Rosebrough, N. J., Farr, A. L. and Randall, R. J. (1951) Protein measurement with the Folin phenol reagent. *J. Biol. Chem. 193*, 265–273.

Manček-Keber, M. and Jerala, R. (2006) Structural similarity between the hydrophobic fluorescent probe and lipid A as a ligand of MD-2. *FASEB J. 20*, 1836−1842.

Manjunath, P. and Sairam, M. R. (1987) Purification and biochemical characterization of three major acidic proteins (BSP-A1, BSP-A2 and BSP-A3) from bovine seminal plasma. *Biochem. J. 241*, 685−692.

Manjunath, P., Sairam, M. R. and Uma, J. (1987) Purification of four gelatin-binding proteins from bovine seminal plasma by affinity chromatography. *Biosci. Rep. 7*, 231−238.

Manjunath, P., Marcel, Y. L., Uma, J., Seidah, N. G., Chretien, M. and Chapdelaine, A. (1989) Apolipoprotein A-I binds to a family of bovine seminal plasma proteins. *J. Biol. Chem. 264*, 16853−16857.

Manjunath, P., Nauc, V., Bergeron, A. and Menard, M. (2002) Major proteins of bovine seminal plasma bind to the low density lipoprotein fraction of hen's egg yolk. *Biol. Reprod. 67*, 1250−1258.

Mann, T. (1954) The Biochemistry of Semen. John Wiley & Sons, New York, 223pp.

Martin, J., Langer, T., Boteva, R., Schramel, A., Horwich, A. L. and Hartl, F-U. (1991) Chaperonin-mediated protein folding at the surface of GroEL through a 'molten globule'-like intermediate. *Nature 352*, 36−42.

Martin, J. B. (1996) Pathogenesis of neurodegenerative disorders: the role of dynamic mutations. *Neuroreport 20*, 1–7.

Mendoza, J. A., Rogers, E., Lorimer, G. H. and Horowitz, P. M. (1991) Chaperonins facilitate the *in vitro* folding of monomeric mitochondrial rhodanese. *J. Biol. Chem. 266*, 13044−13049.

Michelin, K., Wajner, A., Goulart Lda, S., Fachel, A. A., Pereira, M. L., de Mello, A. S., Souza, F. T., Pires, R. F., Giugliani, R. and Coelho, J. C. (2004) Biochemical study on β-glucosidase in individuals with Gaucher's disease and normal subjects. *Clin. Chim. Acta 343*, 145–153.

Milhiet, P-E., Gubellini, F., Berquand, A., Dosset, P., Rigaud, J-L., Grimellec, C. L. and Lévy, D. (2006) High-resolution AFM of membrane proteins directly incorporated at high density in planar lipid bilayer. *Biophys. J. 91*, 3268−3275.

Miller, D., Brough, S. and Al-Harbi, O. (1992a) Characterization and cellular distribution of human spermatozoal heat shock proteins. *Hum. Reprod. 7*, 637–645.

Minami, Y., Hohfeld, J., Ohtsuka, K. and Hartl, F. U. (1996) Regulation of the heat-shock protein 70 reaction cycle by the mammalian DnaJ homolog, Hsp40. *J. Biol. Chem. 271*, 19617–19624.

Minton, A. P. (2000) Implications of macromolecular crowding for protein assembly. *Curr. Opin. Struct. Biol. 10*, 34−39.

Mitchell, L. A., Nixon, B. and Aitken, R. J. (2007) Analysis of chaperone proteins associated with human spermatozoa during capacitation. *Mol. Hum. Reprod. 13*, 605–613.

Mogk, A., Tomoyasu, T., Goloubinoff, P., Rudiger, S., Roder, D., Langen, H. and Bukau, B. (1999) Identification of thermolabile Escherichia coli proteins: prevention and reservation of aggregation by DnaK and ClpB. *EMBO J. 18*, 6934–6949.

Moreau, R., Thérien, I., Lazure, C. and Manjunath, P. (1998) Type II domains of BSP-A1/-A2 proteins: binding properties, lipid efflux and sperm capacitation potential. *Biochem. Biophys. Res. Commun. 246*, 148–154.

Moreau, R. and Manjunath, P. (1999) Characterization of lipid efflux particles generated by seminal phospholipid-binding proteins. *Biochim. Biophys. Acta 1438*, 175–184.

Muchowski, P. J. (2002) Protein misfolding, amyloid formation and neurodegeration: a critical role for molecular chaperones? *Neuron 35*, 9–12.

Müller, P., Erlemann, K-R., Müller, K., Calvete, J. J., Töpfer-Petersen, E., Marienfeld, K. and Herrmann, A. (1998) Biophysical characterization of the interaction of bovine seminal plasma protein PDC-109 with phospholipid vesicles. *Eur. Biophys. J. 27*, 33−41.

Münch, J., Rücker, E., Ständker, L., Adermann, K., Goffinet, C., Schindler, M., Wildum, S., Chinnadurai, R., Rajan, D., Specht, A., Giménez-Gallego, G., Sánchez, P. C., Flower, D. M., Koulov, A., Kelly, J. W., Mothes, W., Grivel, J-C., Margolis, L., Keppler, O. T., Forssmann, W-G. and Kirchhoff, F. (2007) Semen-derived amyloid fibrils drastically enhance HIV infection. *Cell 131*, 1059−1071.

Nakamoto, H. and Vigh, L. (2007) The small heat shock proteins and their clients. *Cell. Mol. Life Sci. 64*, 294–306.

Needleman, S. B. and Wunsch, C. D. (1970) A general method applicable to the search for similarities in the amino acid sequence of two proteins. *J. Mol. Biol. 48*, 443–453.

O'Flaherty, C. M., Beorlegui, N. B. and Beconi, M. T. (2002) Lactate dehydrogenase-C4 is involved in heparin and NADH-dependent sperm capacitation. *Andrologia 34*, 91–97.

Oltersdorf, T., Fritz, L. C. and Schenk, D. B. (1989) The secreted form of the Alzheimer's amyloid precursor protein with the Kunitz domain is protease nexin-II. *Nature 341*, 144–147.

Palleros, D. R., Reid, K. L., Shi, L., Welch, W. J. and Fink, A. L. (1993) ATP-induced protein Hsp70 complex dissociation requires K1 but not ATP hydrolysis. *Nature 365*, 664–666.

Parrish, J. J., Susko-Parrish, J. L. and First, N. L. (1985) Effect of heparin and chondroitin sulfate on the acrosome reaction and fertility of bovine sperm *in vitro*. *Theriogenology 24*, 537–549.

Parrish, J. J., Susko-Parrish, J. L., Leibfried-Rutledge, M. L., Crister, E. S., Eye-Stone, W. H. and First, N. L. (1986a) Bovine *in vitro* fertilization with frozen-thawed semen. *Theriogenology 25*, 591–600.

Parrish, J. J., Susko-Parrish, J. L., Handrow, R. R., Ax, R. L. and First, N. L. (1989) Effect of sulfated glycoconjugates on capacitation and acrosome reaction of bovine and hamster spermatozoa. *Gamete Res. 24*, 403–413.

Parsell, D. A., Kowal, A. S., Singer, M. A. and Lindquist, S. (1994) Protein disaggregation mediated by heat-shock protein Hsp104. *Nature 372*, 475–478.

Patino, M. M., Liu, J. J., Glover, J. R. and Lindquist, S. (1996) Support for the prion hypothesis for inheritance of a phenotypic trait in yeast. *Science 273*, 622–626.

Patrat, C., Serres, C. and Jouannet, P. (2000) The acrosome reaction in human spermatozoa. *Biol. Cell 92*, 255–266.

Pellecchia, M., Szyperski, T., Wall, D., Georgopoulos, C. and Wuthrich, K. (1996) NMR structure of the J-domain and the Gly/Phe-rich region of the *Escherichia coli* DnaJ chaperone. *J. Mol. Biol. 260*, 236–250.

Phillips, D. M. (1975) *Endocrinology*, *Sect 7*. In: *Handbook of Physiology*: (Eds: Hamilton, D. W and Greep, R. O.), Am. Physiol. Soc., Washington DC, pp 405−420.

Pitkänen, P., Westermark, P., Cornwell III, G. G. and Murdoch, W. (1983) Amyloid of the seminal vesicles. A distinctive and common localized form of senile amyloidosis. *Am. J. Pathol. 110*, 64−69.

Premkumar, E. and Bhargava, P. M. (1972) Transcription and translation in bovine spermatozoa. *Nature New Biol. 240*, 139–143.

Premkumar, E. and Bhargava, P. M. (1973) Isolation and characterization of newly synthesized RNA and protein in mature bovine spermatozoa and effect of inhibitors on these syntheses. *Ind. J. Biochem. Biophys. 10*, 239−253.

Prevost, J. L. and Dumas, J. B. A. (1842a) *Ann. Sci. Nat. (paris) 1*, 220.

Prevost, J. L. and Dumas, J. B. A. (1842b) *Ann. Sci. Nat. (paris) 3*, 113.

Prodromou, C., Roe, S. M., Piper, P. W. and Pearl, L. H. (1997) A molecular clamp in the crystal structure of the N-terminal domain of the yeast Hsp90 chaperone. *Nature Struct. Biol. 4*, 477–482.

Prusiner, S. B. (2001) Neurodegenerative diseases and prions. *N. Engl. J. Med. 344*, 1516–1526.

Pushkin, A., Tsuprun, V., Solojeva, N., Shubin, V., Evstigneeva, Z. and Kretovich, W. (1982) High molecular weight pea leaf protein similar to the groE protein of *Escherichia coli*. *Biochim. Biophys. Acta 704*, 379−384.

Qian, Y. Q., Patel, D., Hartl, F. U. and Mccoll, D. J. (1996) Nuclear magnetic resonance solution structure of the human Hsp40 (HDJ-1) J-domain. *J. Mol. Biol. 260*, 224–235.

Qu, J., Susanne, B-K., Holst, O. and Kleinschmidt, J. H. (2009) Binding regions of outer membrane protein A in complexes with the periplasmic chaperone Skp. A site-directed fluorescence study. *Biochemistry 48*, 4926−4936.

Radford, S. E. (2000) Protein folding: progress made and promises ahead. *Trends Biochem. Sci. 25*, 611−618.

Rajaraman, K., Raman, B. and Rao, C. M. (1996) Molten-globule state of carbonic anhydrase binds to the chaperone-like alpha-crystallin. *J. Biol. Chem. 271*, 27595–27600.

Ramakrishnan, M., Anbazhagan, V., Pratap, T. V., Marsh, D. and Swamy, M. J. (2001) Membrane insertion and lipid-protein interactions of bovine seminal plasma protein, PDC-109 investigated by spin label electron spin resonance spectroscopy. *Biophys. J. 81*, 2215–2225.

Rao, P. V., Huang, Q. L., Horwitz, J. and Zigler, J. S. Jr. (1995) Evidence that alpha-crystallin prevents non-specific protein aggregation in the intact eye lens. *Biochim. Biophys. Acta 1245*, 439–447.

Reddy, G. B., Das, K. P., Petrash, J. M. and Surewicz, W. K. (2000) Temperature-dependent chaperone activity and structural properties of human αA- and αB-crystallins. *J. Biol. Chem. 275*, 4565−4570.

Revah, I, Gadella, B. M., Flesch, F. M., Colenbrander, B. and Suarez, S. S. (2000) Physiological state of bull sperm affects fucose and mannose binding properties. *Biol. Reprod. 62*, 1010−1015.

Roberts, D. D. and Goldstein, I. J. (1982) Hydrophobic binding properties of the lectin from lima beans (*Phaseolus lunatus*). *J. Biol. Chem. 257*, 11274–11277.

Sankhala, R. S. and Swamy, M. J. (2010) The major protein of bovine seminal plasma, PDC-109, is a molecular chaperone. *Biochemistry 49*, 3908−3918.

Scheit, K. H., Kemme, M., Aumüller, G., Seitz, J., Hagendorff, G. and Zimmer. M. (1988) The major protein of bull seminal plasma: biosynthesis and biological function. *Biosci. Rep. 8*, 589–608.

Schellman, J. A. (1975) Macromolecular binding. *Biopolymers 14*, 999−1018.

Schmid, D., Baici, A., Gehring, H. and Christen, P. (1994) Kinetics of molecular chaperone action. *Science 263*, 971–973.

Scolari, S., Müller, K., Bittman, R., Herrmann, A. and Müller, P. (2010) Interaction of mammalian seminal plasma protein PDC-109 with cholesterol: implications for a putative CRAC domain. *Biochemistry 49*, 9027−9031.

Seidah, N. G., Manjunath, P., Rochemont, J., Sairam, M. R. and Cheretian, M. (1987) Complete amino acid sequence of BSP-A3 from bovine seminal plasma. Homology to PDC-109 and to the collagen-binding domain of fibronectin. *Biochem. J. 243*, 195−203.

Sharma, K. K., Kaur, H., Kumar, G. S. and Kester, K. (1998) Interaction of 1,1-bis(4-anilino)naphthalene-5,5-disulfonic acid with α-crystallin. *J. Biol. Chem. 273*, 8965–8970.

Shastry, B. S. (2003) Neurodegenerative disorders of protein aggregation. *Neurochem. Int. 43*, 1–7.

Shivaji, S., Scheit, K. H. and Bhargava, P. M. (1990) Proteins of seminal plasma. Wiley, New York, 526pp.

Soler-Ferran, D., Sobel, M. and Harris, R. B. (1992) Design and synthesis of a helix heparin binding peptide. *Biochemistry 31*, 5010–5016.

Spinaci, M., Volpe, S., Bernardini, C., De Ambrogi, M., Tamanini, C., Seren, E. and Galeati, G. (2005) Immunolocalization of heat shock protein 70 (Hsp 70) in boar spermatozoa and its role during fertilization. *Mol. Reprod. Dev. 72*, 534–541.

Suarez, S. S. (1998) The oviductal sperm reservoir in mammals. Mechanisms of formation. *Biol. Reprod. 58*, 1105−1107.

Sun, Y. and MacRae, T. H. (2005) The small heat shock proteins and their role in disease. *FEBS J. 272*, 2613–2627.

Surolia, A., Sharon, N. and Schwarz, F. P. (1996) Thermodynamics of monosaccharide and disaccharide binding to *Erythrina corallodendron* lectin. *J. Bio. Chem. 271*, 17697−17703.

Surolia, A., Swaminathan, C. P., Ramkumar, R. and Podder, S. K. (1997) Unusual structural stability and ligand induced alterations in oligomerization of a galectin. *FEBS Lett. 409*, 417−420.

Swamy, M. J., Marsh, D., Anbazhagan, V. and Ramakrishnan, M. (2002) Effect of cholesterol on the interaction of seminal plasma protein, PDC-109 with phosphatidylcholine membranes. *FEBS Lett. 528*, 230−234.

Swamy, M. J. (2004) Interaction of bovine seminal plasma proteins with model membranes and sperm plasma membranes. *Curr. Sci. 87*, 203−211.

Tannert, A., Kurz, A., Erlemann, K. R., Müller, K., Herrmann, A., Schiller, J., Töpfer-Petersen, E., Manjunath, P. and Müller, P. (2007) The bovine seminal plasma protein PDC-109 extracts phosphorylcholine-containing lipids from the outer membrane leaflet. *Eur. Biophys. J. 36*, 461–475.

Tyler-Cross, R., Sobel, M., Marques, D. and Harris, R. B. (1994) Heparin binding domain peptides of antithrombin III: analysis by isothermal titration calorimetry and circular dichroism spectroscopy. *Protein Sci. 3*, 620−627.

Thérien, I., Bleau, G. and Manjunath, P. (1995) phosphatidylcholine-binding proteins of bovine seminal plasma modulate sperm capacitation of spermatozoa by heparin. *Biol. Reprod. 52*, 1372−1379.

Thérien, I., Moreau, R. and Manjunath, P. (1998) Major proteins of bovine seminal plasma and high-density lipoprotein induce cholesterol efflux from epididymal sperm. *Biol. Reprod. 59*, 768–776.

Thomas, C. J., Anbazhagan, V., Ramakrishnan, M., Sultan, N., Surolia, I. and Swamy, M. J. (2003) Mechanism of membrane binding by the bovine seminal plasma protein, PDC-109. A surface plasmon resonance study. *Biophys. J. 84*, 3037–3044.

Tissieres, A., Mitchell, H. K. and Tracy, U. M. (1974) Protein synthesis in salivary glands of Drosophila melanogaster: relation to chromosome puffs. *J. Mol. Biol. 84*, 389 –398.

van der Vies, S. M., Viitanen, P. V., Gatenby, A. A., Lorimer, G. H. and Jaenicke, R. (1992) Conformational states of ribulosebisphosphate carboxylase and their interaction with chaperonin 60. *Biochemistry 31*, 3635−3644.

Villemure, M., Lazure, C. and Manjunath, P. (2003) Isolation and characterization of gelatin-binding proteins from goat seminal plasma. *Reprod. Biol. Endocrinol. 1*, 39−48.

Visconti, P. E., Bailey, J. L., Moore, G. D., Pan. D., Olds-Clarke, P. and Kopf, G. S. (1995) Capacitation of mouse spermatozoa: correlation between the capacitation state and protein tyrosine phosphorylation. *Development 121*, 1129−1137.

Visconti, P. E., Calantino-Hormer, H., Moore, G. D., Bailey, J. L., Ning, X., Fornes, M. and Kopf, G. S. (1998) The molecular basis of sperm capacitation. *J. Androl. 19*, 242–248.

Von Leeuwenhoek, A. (1679) Observationes de natis è semine genitali animalculis. *Phil. Trans. Roy. Soc. 12*, 1040−1043.

Wah, D. A., Fernández-Tornero, C., Sanz, L., Romero, A., and Calvete, J. J. (2002) Sperm coating mechanism from the 1.8 Å crystal structure of PDC-109-phosphorylcholine complex. *Structure 10*, 505–514.

Wang, H., Duennwald, M. L., Roberts, B. E., Rozeboom, L. M., Zhang, Y. L., Steele, A. D., Krishnan, R., Su, L. J., Griffin, D., Mukhopadhyay, S., Hennessy, E. J., Weigele, P., Blanchard, B. J., King, J., Deniz, A. A., Buchwald, S. L., Ingram, V. M., Lindquist, S. and Shorter, J. (2008) Direct and selective elimination of specific prions and amyloids by 4,5-dianilinophthalimide and analogs. *Proc. Natl. Acad. Sci.* USA *105*, 7159–7164.

Wang, K. and Spector, A. (1994) The chaperone activity of bovine α-crystallin. *J. Biol. Chem. 269*, 13601–13608.

Wang, X., Venable, J., La Pointe, P., Hutt, D., Koulov, A., Coppinger, J., Gurkan, C., Kellner, W., Matteson, J., Plutner, H., Riordan, J. R., Kelly, J. W., Yates, J. R. and Balch, W. E. (2006) Hsp90 cochaperone Aha1 downregulation rescues misfolding of CFTR in cystic fibrosis. *Cell 127*, 803–815.

Ward, C. R. and Kopf, G. S. (1993) Molecular events mediating sperm activation. *Dev. Biol. 104*, 287−296.

Welch, W. J. (2003) Role of quality control pathways in human diseases involving protein misfolding. *Semin Cell Dev. Biol. 15*, 31–38.

Welker, S., Rudolph, B., Frenzel, E., Hagn, F., Liebisch, G., Schmitz, G., Scheuring, J., Kerth, A., Blume, A., Weinkauf, S., Haslbeck, M., Kessler, H. and Buchner, J. (2010) Hsp12 is an intrinsically unstructured stress protein that folds upon membrane association and modulates membrane function. *Mol. Cell 39*, 507–520.

Whitesell, L. and Lindquist S. L. (2005) Hsp90 and the chaperoning of cancer: Normal chaperone biology. *Nat. Rev. Cancer 10*, 761−772.

Xu, Z. H., Horwich, A. L. and Sigler, P. B. (1997) The crystal structure of the asymmetric GroEL–GroES–(ADP)$_7$ chaperonin complex. *Nature 388*, 741−750.

Yanagimachi, R. (1994) Mammalian fertilization. In: *Physiology of Reproduction.* (Eds: Knobil, E. and Neill, J), Raven Press, New York, pp. 189−317.

Yonehara, M., Minami, Y., Kawata, Y., Nagai, J. and Yahara, I. (1996) Heat-indiced chaperone activity of Hsp90. *J. Biol. Chem. 271*, 2641–2645.

Young, J. C., Agashe, V. R., Siegers, K. and Hartl, F. U. (2004) Pathways of chaperone-mediated protein folding in the cytosol. *Nature Rev. Mol. Cell Biol. 5*, 781−791.

Zahn, R., Perrett, S. and Fersht, A. R. (1996) Conformational states bound by the molecular chaperones GroEL and secB: a hidden unfolding (annealing) activity. *J. Mol. Biol. 261*, 43–61.

Ziegler, A. and Seelig, J. (2004) Interaction of the protein transduction domain of HIV-1 TAT with heparan sulfate: binding mechanism and thermodynamic parameters. *Biophys. J. 86*, 254−263.

# Curriculum Vitae

# Rajeshwer Singh Sankhala

School of Chemistry
University of Hyderabad
Hyderabad-500046 (INDIA)
Email: rajeshwer.21@gmail.com

*Rajeshwer Singh Sankhala was born in Khetri (Dist. Jhunjhunu, Rajasthan) on 21ˢᵗ December, 1979.  After completing high school education at Jai Singh higher secondary school (Class VI to XII), Khetri,  he joined Vinodini P. G. college, Khetri, and obtained his B.Sc. degree (Chemistry, Botany and Zoology) in 2002.  He received his M.Sc. degree (Biotechnology) in 2004 from Jiwaji University, Gwalior.  He joined for Ph.D. at School of Chemistry, University of Hyderabad in 2005-06.  He was qualified as JRF (2005) and SRF (2007) by Council of Scientific and Industrial Research, India.  His major research focus was on "Molecular Chaperones", his areas of research interests also include protein/protein and protein/lipid interactions which play crucial role in cell physiology.*

## List of Publications

1. **Sankhala, R. S.** and Swamy, M. J. (2010) The Major Protein of Bovine Seminal Plasma, PDC-109, is a Molecular Chaperone. ***Biochemistry*** 49, 3908−3918.

2. Damai, R. S.\*, **Sankhala, R. S.\***, Anbazhagan, V. and Swamy, M. J. (2010) $^{31}$P-NMR and AFM Studies on the Destabilization of Cell and Model Membranes by the Major Bovine Seminal Plasma Protein, PDC-109. ***IUBMB Life*** 62, 841−851. (**\*Both authors contributed equally**).

3. **Sankhala, R. S.**, Damai, R. S. and Swamy, M. J. (2011) Correlation of Membrane Binding and Hydrophobicity to the Chaperone-Like Activity of PDC-109, the Major Protein of Bovine Seminal Plasma. ***PLoS ONE*** (*In Press*).

4. Anbazhagan, V., **Sankhala, R. S.** and Swamy, M. J. (2011) Thermodynamics of Interaction of the Major Bovine Seminal Plasma Protein, PDC-109 with Phospholipid Membranes. An Isothermal Titration Calorimetric Study. (Submitted for publication).

5. **Sankhala, R. S.**, Damai, R. S., Anbazhagan, V. and Swamy, M. J. (2011) Biophysical Investigations on the Interaction of the Major Bovine Seminal Plasma Protein, PDC-109 with Heparin. (Submitted for publication).

## Conferences and Presentations

1. 8th International Synposium on "Biochemical Roles of Eukaryotic Cell Surface Macromolecules" held at Centre for Cellular & Molecular Biology (CCMB), Hyderabad−500 007, India, Jan. 2008.

2. National Symposium on "Cellular and Molecular Biophysics" organized by Indian Biophysical Society at Centre for Cellular & Molecular Biology, Hyderabad−500 007, India, Jan. 2009.

3. Oral presentation on "The Major Protein of Bovine Seminal Plasma, PDC-109, Is a Molecular Chaperone" in the Chemfest-2010, School of Chemistry, University of Hyderabad, Hyderabad-500046, India, Jan. 2010.